2023

Contrasting seasonal cycling of arsenic in a series of subarctic shield lakes with different morphometric properties

Jeremy Harbinson
Wilfrid Laurier University, harb3960@mylaurier.ca

Contrasting seasonal cycling of arsenic in a series of subarctic shield lakes with different morphometric properties

by

Jeremy Harbinson
Bachelor of Science in Environmental Sciences, University of Guelph, 2018

THESIS

Submitted to the Department of Geography and Environmental Studies
Faculty of Science
in partial fulfilment of the requirements for
Master of Science in Geography
Wilfrid Laurier University
2023

Abstract

The subarctic shield near Yellowknife, Northwest Territories (NWT), is populated with thousands of small lakes (<1.5 km^2) and several large lakes. Historic mining activities in the region have left a legacy of environmental impacts and widespread arsenic (As) contamination in both aquatic and terrestrial environments. In particular, several small subarctic lakes near Yellowknife have been previously documented to be contaminated with high levels of As. Subarctic lakes are characterized by seasonal ice-cover that can persist for more than half of the year, yet little is known about the under-ice spatial and seasonal dynamics of As cycling. The objective of this study is to contrast seasonal changes in As cycling within and among a series of lakes with different basin morphologies during ice-cover and into the ice-free seasons. In this study, a combination of data including water profile sampling, sediment cores, snow and ice measurements, and bathymetric mapping were collected in four lakes from November 2020 to October 2021. Continuous monitoring of lake physical properties (dissolved oxygen, temperature, and light) was conducted via data loggers installed at 1 m depth intervals in each lakes' water column. Detailed profiles of water chemistry were collected monthly at the deepest part of each lake, examining numerous key water chemistry elements with a focus on dissolved and particulate As concentrations. Key results from this study indicated: 1) Distinct seasonal variation in As over the ice-on and open-water periods, 2) The important role of lake mixing regimes in the mobility of As, 3) Field evidence of Fe attenuation of As from the water column. This project contributes important information on the winter cycling of As, which will help to inform our understanding of the chemical recovery of subarctic lakes from As pollution.

Acknowledgements

Supervisor	Dr. Homa Kheyrollah Pour
Co-advisor	Dr. Michael Palmer
Committee	Dr. Michael English
Reader	Dr. Derek Gray
Field Assistants	Niels Wiess, Mason Dominico, Rosy Tutton, Nigel Rouss, Seamus Daly, Mike Palmer, Anna Coles, Jack Panayi, Nora Alsafi, Jaedyn Smith, Isabelle de Grandpre, Jessie Bowser, Bruce Hannah, Alex MacLean, Dr. Michael Palmer (Aurora Research Institute)
ReSEC Research Group	Alex MacLean, Grant Simpson, Alicia Pouw, Gifty Attiah, Arash Rafat, Ida Moalemi, Ariana Mansingh, Ali Reza Shahvaran, Michael Dallosch, Dilshan Kariyawasam, Ethan Lim, Vivian Cao
Laboratory Analysis	Taiga Environmental Laboratory, Queen's University- Analytical Services Unit

Funding: This research was supported by NT Cumulative Impact Monitoring Program (CIMP project #212), Canada Research Chair and Discovery Grant from the Natural Sciences and Engineering Research Council of Canada (NSERC) to H. Kheyrollah Pour, Northern Student Training Program (NSTP) from Polar Knowledge Canada and Cold Regions Research Centre (CRRC) Travel Grant from Wilfrid Laurier University to J. Harbinson.

Land Acknowledgment: This research was conducted on the beautiful traditional lands of the Yellowknives Dene and Métis with neighbouring indigenous communities of Ndilǫ, Behchokǫ̀, Gametì, Łutselk'e, Wekweètì, Whatì, and Dettah. The Chief Drygeese territory is home to Yellowknives Dene First Nation.

Table of Contents

List of Tables

List of Figures

1. Chapter 1: Introduction

The Mackenzie River Basin is the largest watershed in Canada that occupies one-fifth of the country (Wayland, 2003). The basin expands across three provinces and two territories with six sub-basins, one of which is the Great Slave sub-basin. The Great Slave sub-basin contains hundreds of small and large lakes across fourteen major drainage systems (Wayland, 2003). This area is in the Ecoregion of Taiga Shield and is underlain by the Slave Geological Province (Kokelj, 2003). The Taiga Shield is a result of glacial scouring leaving behind formations of numerous lakes and rivers that are often shallow and coarse (Kokelj, 2003). The North Slave region is a geopolitical boundary located north of the eastern arm of Great Slave Lake (*Tinde'e*) and surrounds the City of Yellowknife (Kokelj, 2003). The traditional territory of the Yellowknives Dene and home to the communities of Ndilǫ, Behchokǫ̀, Gametì, Łutselk'e, Wekweètì, Whatì, Dettah and the City of Yellowknife.

The North Slave Region has a long history of legacy anthropogenic impacts from mining development because of the landscape's minerals. Two major mines: Con Mine (1938-2003) and Giant Mine (1948-2001) were operated in and near the City of Yellowknife (Wayland, 2003). Giant Mine was a one of the largest gold mining operations in Canadian history operating for over 50 years, which left behind a legacy of environmental contamination, predominately arsenic (As) from the roasting of arsenopyrite for gold (Keeling & Sandlos, 2012; Wayland, 2003). A total of 237 000 tonnes of arsenic trioxide (As_2O_3) waste was captured and is currently being stored underground (Bromstad *et al.,* 2017; Wrye, 2008). More than 20 000 tonnes of As emissions were not captured onsite and were released atmospherically across the region (Bromstad *et al.,* 2017; Wrye, 2008). The majority of the total As emissions (84%) were released

from Giant Mine in the first decade of operation and prior to 1958 (Bromstad *et al.,* 2017; Wrye, 2008).

An approximate 15 km radius surrounding the vicinity of the mine site became a heavily contaminated environment (Hocking *et al*., 1978; Wayland, 2003). Arsenic levels in lakes near Yellowknife have been well-documented, and concentrations often exceed the Canadian Drinking Water Standard of 10 µg/ L in small lakes (Health Canada, 2006; Health Canada, 2022; Palmer *et al*., 2015; Wagemann *et al.,* 1978). Houben *et al.* (2016) notes that the City of Yellowknife's drinking water is drawn from the Yellowknife River, only 5 km away from historical operations. However, As exceedance in the city's drinking water sources is generally not a concern with a watershed of over 10 000 km^2 instrumented with continuous monitoring programs (Houben *et al.,* 2016). Subarctic lakes in the region are distinctly characterized by ice-cover that could occur for half of the calendar year (Duthie, 1979; Environment Climate Change Canada, 2022; Palmer *et al.*, 2019). Lake ice plays a central role in the chemical and physical properties of small subarctic lakes, yet few studies have explored the geochemical cycling of As in lakes under-ice.

1.1 Arsenic (As)

Arsenic (As) is a metalloid and can exist in both inorganic and organic forms in the environment (Tamaki & Frankenberger, 1992). Arsenic exists in four different oxidation states: arsenite As(+III), arsenate As(+V), zero valent arsenic As(0), and arsine As(-III) (Oremland, 2003; Rahman *et al*., 2012; Tamaki & Frankenberger, 1992). Arsenic occurs naturally in sediments and rock formations throughout the globe (Tamaki & Frankenberger, 1992). However, As can also be related to waste streams from anthropogenic activities like mining, pesticide application, or industrial practices (Chen *et al*., 2015). Arsenic is designated as a chemical of

major public health concern by the World Health Organization (WHO). Acute and chronic illness or poisoning from As can lead to many forms of cancer and health complications (Bissen & Frimmel, 2003). The level of toxicity and bioavailability for As is largely based on its oxidation state or mineral form, although, external factors of biotic and abiotic nature can alter As form (Bissen & Frimmel, 2003). For instance, As can be highly carcinogenic and a neurotoxin toxic when remobilized from a solid to gas phase, exposing a high risk to human or ecosystem health (Chen *et al*., 2015). Arsenic trioxide (As_2O_3) is one of the most bio-accessible and toxic forms of As (Oremland, 2003; Plumlee & Morman, 2011). The current Canadian Drinking Water Standard for As concentration in water is 10 µg/L, previously updated in 2018 from 25 µg/L (MacDonald *et al.,* 2002; Health Canada, 2006; Health Canada, 2022). Freshwater lakes in Canada have naturally occurring As concentrations that are usually less than 2 µg/L (Canadian Public Health Association (CPHA), 1977) and the guideline for protection of aquatic health is 5 µg/L (CCME, 2002). The guideline for As in lake sediment is 5.9 mg/kg under the Canadian Council of Ministers of the Environment (CCME) Interim Freshwater Sediment Quality Guidelines (CCME, 1999; Galloway *et al*., 2015).

The mobility of As in freshwater environments is controlled by changes in redox conditions within the water column and lake sediments (Bissen & Frimmel, 2003; Schroth *et al.,* 2017). The biogeochemical concept of a redox-ladder or redox cascade is fundamental when understanding redox elements like As (Dixit & Hering, 2003). Redox reactions entail multiple electron exchanges that do not occur simultaneously (Dixit & Hering, 2003). Instead, there is an order of operations when it comes to a redox reaction, hence the redox ladder (Dixit & Hering, 2003). Arsenic(V) has a greater ability to be in a more thermodynamically stable state throughout oxic conditions, in comparison to As(III) presence being more prominent in anoxic

and reduced environments (Ng, 2005; Rahman *et al.,* 2012; Wilkin & Ford, 2006). The process of As sequestration by Fe-oxyhydroxides under oxic conditions is well documented in the literature (Couture *et al.,* 2010). Comparatively, in anoxic conditions with an electron benefactor like organic matter (OM), Fe(oxy)hydroxides dissolve and release As (Ng, 2005; Rahman *et al.,* 2012).

Controls on arsenic via adsorption, desorption, precipitation, co-precipitation, diffusion, and remobilization are dependent on the redox potential of an environment (Bissen & Frimmel, 2003). Oxyhydroxides of iron (Fe(III)) and manganese (Mn (III/IV)) are often key in the biogeochemical cycling of As, OM, and sulfur (S) (Bauer & Blodau 2006; Couture *et al.,* 2010; Kneebone *et al.,* 2002; Palmer *et al.,* 2020; Root *et al.,* 2007). Arsenic cycling between sediments and surface waters is controlled by the position of the redoxcline, associated with oxic-anoxic boundaries that can migrate within the sediment and water column (Rahman *et al*., 2012). Concentration gradients of As within lake sediment and overlying waters can cause diffusion of As from an area of high to low concentrations, this is known as Fick's Law of diffusion (Bissen & Frimmel, 2003).

1.2 Within lake cycling of As

Arsenic cycling within a lake occurs through the exchange of As between the lake sediment and water column, which is predominately controlled by redox conditions (Andrade *et al.,* 2010; Bissen & Frimmel, 2003; Martin and Pederson, 2002; Schroth *et al.,* 2017). Redox conditions within a lake are shaped by key physical lake characteristics and processes of water temperature, availability of oxygen, circulation or mixing, and benthic respiration (Aggett & Kriegman, 1988; Dixit & Hering, 2003; Rahman *et al.,* 2012; Schroth *et al.,* 2017).

These physical lake characteristics can establish gradients in the water column like a thermocline, oxic boundary, redoxcline, and chemocline (Aggett & O'Brien 1985; Azcue & Nriagu 1995; Barringer *et al.,* 2011; Hutchinson, 1967; Senn *et al.,* 2007). These gradient boundaries can shift within a lake and create barriers to the cycling of As, influencing As concentrations and mobility (Rahman *et al*., 2012). A thermocline develops at the point of the highest water density difference in a water column due to contrasting temperatures (Gorham & Boyce, 1989; Hutchinson, 1967). This is a part of the thermal stratification process, where water density layers develop in a water column forming the epilimnion, metalimnion, and hypolimnion (Gorham & Boyce, 1989; Hutchinson, 1967). Thus, redox conditions in a lake are largely influenced by mixing regime and thermal stratification occurrence and duration (Aggett & O'Brien 1985; Azcue & Nriagu 1995; Barringer *et al.,* 2011; Senn *et al.,* 2007). These different water density layers can restrict the movement and migration of solutes like As in a water column because of the water density differences make it difficult for different water layers to mix (Gorham & Boyce, 1989; Hollibaugh *et al.,* 2005; Senn *et al.,* 2007; Smedley & Kinniburgh, 2002; Rahman *et al.,* 2012).

The oxic boundary marks the transition between oxic (well oxygenated) and anoxic conditions (oxygen depleted) in a water column (Hutchinson, 1967). This boundary is associated with a redoxcline (Hutchinson, 1967). The reduction of As(V) to As(III) in the water column is often observed after the onset of anoxia (Aggett & Kriegman, 1988). Anoxic conditions in a lake can enable As enrichment through the dissolution and mobilization of As into the hypolimnion from the lake sediment (Andrade *et al.,* 2010: Bennett *et al.,* 2012). The mobilization of As under reducing conditions occurs through the reductive dissolution of iron (oxy)hydroxides releasing As into a dissolved phase (Bennett *et al.,* 2012; Nikolaidis *et al.,* 2004). Typically,

ferrous iron Fe(II) and arsenite As(III) concentrations are well correlated under anoxic conditions in the water-column (Bennett et al. 2012).

The mobilization of As is correlated to that of Fe and manganese (Mn) under reducing conditions in the hypolimnion (Aggett & Kriegman, 1988). The sorption behaviour of As is dependent on its oxidation state and minerology of iron-oxide (Dixit & Hering, 2003). Since iron-oxide is a strong sorbent, As competes with other species like phosphate for surface sites under oxidizing conditions (Dixit & Hering, 2003). If reducing conditions are present and persist, the redox cascade moves towards the reduction of sulfate (SO4) to dissolved sulfide (S(II-)) (Bostick & Fendorf, 2003; O'Day *et al.,* 2004). The coexistence of dissolved sulfide and As(III) can lead to the diffusion of As from lake sediments due to the precipitation of As-sulfides or coprecipitation with Fe-sulfides (Bostick & Fendorf, 2003; O'Day *et al.*, 2004).

The sediment-water boundary is an important interface in lakes for controlling the mobility of As and other redox sensitive elements (Barrett *et al.*, 2018; Petersen *et al.,* 1995; Santschi *et al.,* 1990). Lake sediments can be a main source or sink of legacy As through storage and accumulation of the contaminated metal bounded within layers of the sediment (Barrett *et al.,* 2019). The regional boundary of the sediment water interface (SWI) is significant for the cycling of As in freshwater lakes because of the sediment porewater diffusion of As (Barrett *et al.*, 2018; Santschi *et al.,* 1990). Aquatic organisms within lake sediment are a factor in the speciation, distribution, and cycling of As because aquatic organisms take up, metabolize, store, and release As back into the water column (Aggett & O'Brien 1985; Barrett *et al.,* 2019; Rahman *et al.,* 2012). High bottom water and sediment temperatures, which is more prevalent in shallow lakes can increase biological activity (benthic respiration) and stimulate As mobilization through the oxidation of organic carbon (Barrett *et al*., 2019).

1.3 Ice-covered lakes and seasonal As mobility

Lake ice plays a central role in shaping various characteristics of the physical and chemical processes of a lake system (Bertilsson *et al.,* 2013; Deshpande *et al.,* 2015; Mathias & Barica, 1980). Lake ice prevents the exchange of oxygen between the atmosphere and surface waters (Bertilsson *et al.,* 2013; Deshpande *et al.,* 2015; Leppäranta, 2014; Mathias & Barica, 1980). Ice-cover can lead to the progressive depletion of oxygen and the onset of anoxic conditions in the water column when oxygen demand exceeds the supply (Leppäranta, 2014). Physical characteristics affecting As mobility can shift in a lake during the winter period, as lake ice enables reducing conditions in the lake waters (Golosov *et al.,* 2007). Development of anoxia can be more pronounced especially near the bottom of a lake and within sediments from microbial respiration activity (Bertilsson *et al.,* 2013; Palmer *et al*., 2020). This allows for As to remobilize in the water column raising the concentration of As, which is especially a concern in shallow lakes (Martin & Pedersen, 2002). Shallow lakes (depth < 4 m) in northern latitudes can potentially develop complete water column anoxia due to the long extent of lake ice-cover (max ice thickness = ~ 1 m) during winter (Spliethoff *et al.,* 1995; Palmer *et al.*, 2020).

Ice-covered lakes can also enable the process of cryoconcentration, which can influence As concentrations resulting from lake ice formation (Bergmann *et al.*, 1985; Belzile *et al.*, 2002; Deshpande *et al.*, 2015; Pieters & Lawrence, 2009). Cryoconcentration is the enrichment of solute concentrations due to the development of lake ice exsolving dissolved solutes, which can drive higher concentrations in solutes like As under the ice (Bergmann *et al.*, 1985; Belzile *et al.*, 2002; Deshpande *et al.*, 2015; Palmer *et al.,* 2019; Pieters & Lawrence, 2009). The exsolving process is particularly efficient when freezing rates of ice is slow, but inefficient when it is fast (Bergmann *et al.*, 1985; Belzile *et al.*, 2002; Deshpande *et al.*, 2015; Palmer *et al.,* 2019; Pieters

& Lawrence, 2009). Factors controlling lake ice development is related to the thickness of snow (insulator) and the temperature gradient between the atmosphere and the lake ice/water interface (Bergmann *et al.*, 1985; Belzile *et al.*, 2002; Deshpande *et al.*, 2015; Palmer *et al.,* 2019; Pieters & Lawrence, 2009). Cryoconcentration is also magnified in shallow lakes (depth = < 4 m) as there is an inverse relationship between cryconcentration in a lake and lake depth (Bergmann *et al.*, 1985; Belzile *et al.*, 2002; Deshpande *et al.*, 2015; Palmer *et al.,* 2019; Pieters & Lawrence, 2009).

The spring-melt period of shallow subarctic lakes is an important time of re-oxygenation throughout the water column as lake waters shift from an extended period of anoxic conditions to oxic levels (Bertilsson *et al.,* 2013). The freshet period brings an influx water volume and increase of oxygen which can lead to rapid scavenging of As from the water column via the precipitation of Fe-oxyhydroxides (Joung *et al.,* 2017; Palmer *et al.*, 2020). Reoxygenation of a lake is accelerated as the lake ice ablates and the surface water is exposed to the wind which increases lake mixing (Bertilsson *et al.,* 2013). In terms of open-water conditions in lakes, a mechanism known to influence As concentrations is evapoconcentration (Gibson *et al.,* 1998: Palmer *et al.,* 2019; Spence, 2006). Evapoconcentration occurs when evaporation of water exceeds precipitation inputs and a subsequent decrease in water volume causes an increased in solute concentrations like As (Gibson *et al.,* 1998: Palmer *et al.,* 2019; Spence, 2006). Warming lake sediment temperatures have also been documented to enable increased release of As from the sediment into the overlying water column (Barrett *et al.,* 2019; Nelligan *et al.,* 2019). Sediment temperatures particularly rise over the course of the open-water period and more microbial respiration can occur, which changes the redox conditions through a thinning oxic boundary in the sediment (Barrett *et al.,* 2019; Nelligan *et al.,* 2019). This subsequently triggers

higher As release from the sediments into the overlying waters (Barrett *et al.,* 2019; Nelligan *et al.,* 2019).

Overall, the seasonal mobility of As within a lake system can vary due to a number of factors: changing dissolved oxygen concentrations, physical lake mixing, thermal stratification, redox conditions, and ice-cover (Barret *et al.*, 2018; Hollibaugh *et al.,* 2005; Palmer *et al.,* 2020; Senn *et al*., 2007). There is a need to further our understanding of the seasonal variation in As cycling in small subarctic lakes.

1.4 Research Objectives & Significance

The City of Yellowknife's long history of gold mining left behind a significant legacy of As pollution from roaster stack emissions. The legacy of As pollution across Yellowknife's surrounding landscape and lakes present complexities in ongoing environmental and human health concerns (CPHA, 1977; Galloway *et al.,* 2015; Hutchinson *et al*., 1982; Kerr & Wilson, 2000). Specifically, recent research highlighting surface water As levels in various small lakes near Yellowknife in exceedance of Health Canada's Canadian Drinking Water Standard guidelines of 10 μg/L (Health Canada, 2006; Health Canada, 2022; Palmer *et al.,* 2015). The results from Palmer *et al.* (2015) study instigated the Government of the Northwest Territories Health and Social Services, Public Health to issue ongoing advisories to raise awareness to the public in order to avoid and/or minimize exposure to areas with high levels of As (Government of the Northwest Territories, 2019).

In light of the significant legacy As environmental footprint, many different types and large numbers of research projects have been carried out and continue today. However, only a few studies have examined lake systems in this region during the winter, despite being ice-covered for almost half of the calendar year (Block *et al.,* 2019; Palmer *et al.,* 2019; Palmer *et*

al., 2020). This could be partly due to the logistical challenges of conducting winter fieldwork and previous assumptions that lakes are relatively dormant during the winter (Block *et al.,* 2019). However, some previous research has specifically investigated the mobility and biogeochemistry of As in small subarctic during ice-covered conditions (Palmer *et al.,* 2019; Palmer *et al.,* 2020). Several questions remain unanswered regarding under-ice cycling of As in shallow subarctic lakes.

This study investigated the seasonal changes of As cycling among lakes with different basin morphologies in Yellowknife, Northwest Territories (NWT), Canada. An examination of under-ice cycling of As concentration profiles in subarctic shield lakes was conducted. The results from this study aim to contribute to the understanding of winter cycling of As in small lake systems within the subarctic. Insights from this study will contribute towards evolving information on the chemical recovery of subarctic lakes from As pollution. Furthering the understanding of the biogeochemical cycling of As is critical in the steps toward strengthening the knowledge surrounding the complex chemical and biological recovery of small lake systems.

1.5 Study Area and Environmental Conditions

This study took place on Chief Drygeese territory, the traditional lands of the Yellowknives Dene First Nation. Several of the study lakes are located within or near the capital City of Yellowknife, shown in Figure 1.1 (62˚27'17"N and 114˚22'35"W). The study area resides in the Ecoregion of Taiga Shield High Boreal and the geopolitical boundary of the North Slave, which is part of the Slave Geological Province of the Canadian shield (Ecosystem Classification Group, 2007; Wolfe *et al.,* 2017). The Taiga Shield High Boreal is a low-elevation granitic bedrock plain with an average elevation of 301 m and widespread discontinuous permafrost (Ecosystem Classification Group, 2007; Wolfe *et al.,* 2017).

Weather station data from 1981 to 2010 in Yellowknife, NWT was examined, as information up to present time was not consistently available. Annual air temperatures in Yellowknife from 1981 to 2010 ranged approximately from -40°C to 25°C (Environment Climate Change Canada, 2022). The during 1981 to 2010 the coldest month of the year in Yellowknife was typically January, with a daily average air temperature of -26.8°C (Environment Climate Change Canada, 2022). In contrast, the warmest month of the year during 1981 to 2010 was typically July with a daily average air temperature of 16.8°C (Environment Climate Change Canada, 2022). Climate normals for the region of Yellowknife based on data from 1981 to 2010, on average had 175 days (49%) per year with maximum air temperatures less than or equal to 0°C, and an annual daily average air temperature of -4.7°C (Environment Climate Change Canada, 2022). Further, climate normals from 1981 to 2010 for Yellowknife observed annual snowfall amounts accumulated to 151.8 cm, rainfall of 164.5 mm, and receives 2 264.8 total hours of sunshine annually (Environment Climate Change Canada, 2022).

This study spanned the period from November 16th, 2020, to October 1st, 2021. During this period, the mean air temperature was -4.7°C, an approximate total of 75.2 cm of snow accumulated, and an approximate sum of 183 mm of precipitation had fallen (Table 1.1) (Environment Climate Change Canada, 2022). Lake ice conditions in the Yellowknife region can persist for up to 6 months of the calendar year due to air temperatures being below freezing (0°C), typically from early October into late April annually (Environment Climate Change Canada, 2022). For instance, 44% (154 days) of the study period (347 days) had maximum air temperatures less than or equal to 0°C (Table 1.1; Environment Climate Change Canada, 2022). Specifically in the 2020-2021 calendar year, the first day of consecutive mean air temperatures below 0°C was October 13th, 2020, with a mean temperature of -3.2°C (Environment Climate

Change Canada, 2022). The last day of consecutive mean air temperatures below 0°C during the study was May 3rd, 2021, with a mean air temperature of -2.3°C (Environment Climate Change Canada, 2022). A total period of 202 days observed mean air temperatures less than or equal to 0°C over the 2020-2021 calendar year (Environment Climate Change Canada, 2022).

Three time-period categories were established within the study: 1) Ice-on period (November 2020 - April 2021), 2) Spring ice-off (May 2021 – June 2021), and 3) Open-water period (June 2021 to October 2021). Specific meteorological statistics from the Yellowknife Airport Weather Station (Climate ID: 2204101) for each of these periods are outlined in Table 1.1 below.

Table 1.1 Calculated mean air temperature, total accumulated snow, total precipitation, and percentage of days with max air temperatures </= 0°C of historical weather station data from Yellowknife A (Climate ID: 2204101) located at Yellowknife Airport, YZF (62°27'46.000" N Latitude, 114°26'25.000" W Longitude, 205.7m elevation) during November 16th 2020 to October 1st 2022 extent of the study (Environment Climate Change Canada, 2022).

	Mean Air Temp (°C)	***Total Accumulated Snow (cm)***	***Total Precipitation (mm)***	***% of Days </= 0°C Max Air Temp (%)***
16 November 2020 – 1 October 2021 "Study Period"	-4.7	75.2	183	43
16 November 2020 – 30 April 2021 "Ice-on Period"	-19.2	73.4	38.7	85
1 May – 31 June 2021 "Spring ice-off Period"	8.7	1.8	33.9	2
1 June – 1 October 2021 "Open water Period"	13.1	0	142.2	0

Four small lakes (Handle, Fiddler, Jackfish, and Small Lakes) were selected for this study due to their different physical lake characteristics and distances from historical mining operation sites (Fig. 1.1). Small lakes in the region were shaped by glacial action and as Glacial Lake McConnell retreated depressions left by glacial scaring were initially filled with from Lake

McConnel and ancestral Great Slave Lake from the previous 10 000 years (Wolfe *et al*., 2017).

The physical characteristics of the study lake sites are shown in Table 1.2.

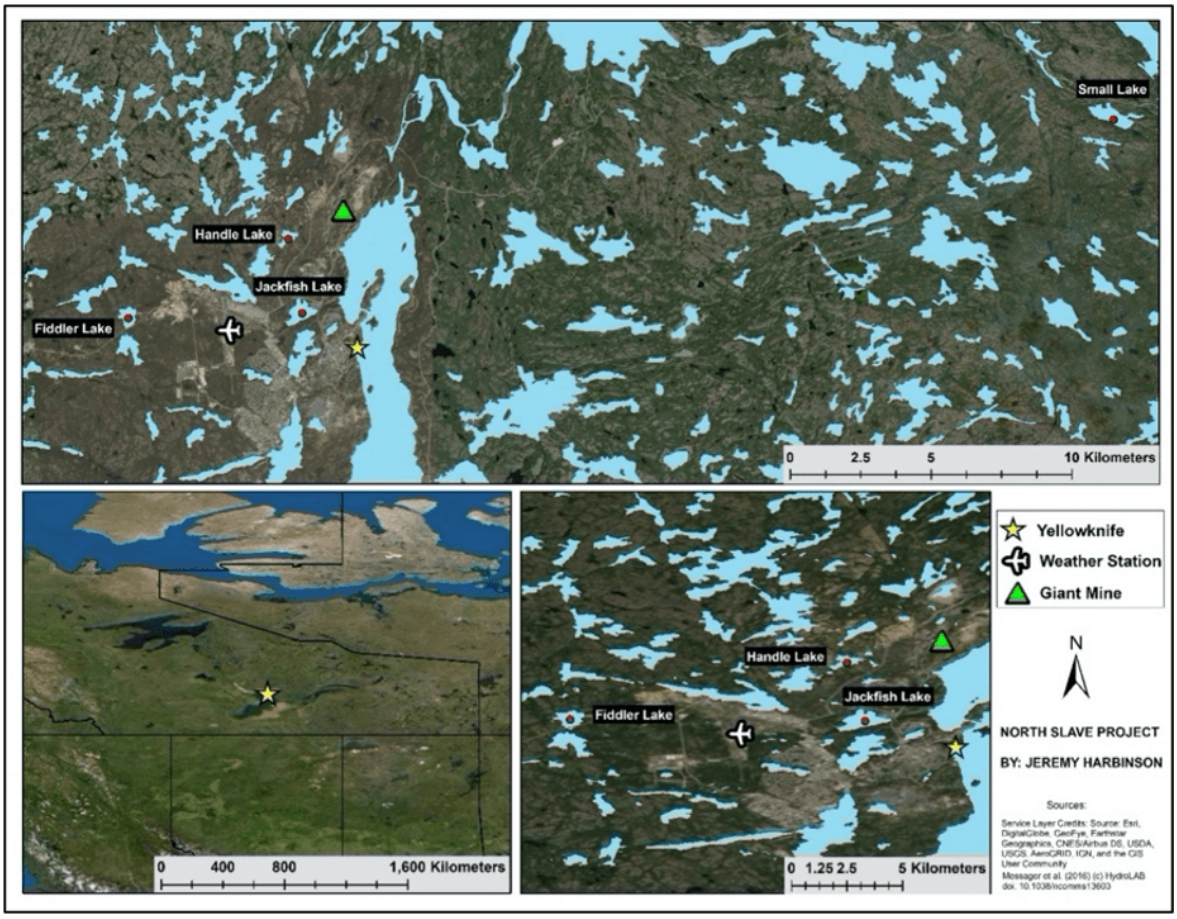

Figure 1.1 Map showing the North Slave Region, NT and locations of the study lakes, and the Giant Mine.

Table 1.2 Physical characteristics of selected lakes: Z_{Max} is the maximum depth, V is lake volume, A is lake area, SA:V is surface area lake volume ratio, and $D_{Giant\ Mine}$ is the distance from Giant Mine.

Lake	*Lat (°N)*	*Lon (°W)*	*Z_{max} (m)*	*V (m^3)*	*SA (m^2)*	*SA:V*	*$D_{Giant\ Mine}$ (km)*
Handle	62.49	114.39	3.5	390 525	210 000	0.54	2.2
Fiddler	62.47	114.51	6.5	1 103 741	290 000	0.26	8.6
Jackfish	62.47	114.39	7.5	3 205 937	490 000	0.15	4.2
Small	62.52	113.82	12.5	4 016 371	780 000	0.19	27.4

2. Chapter 2: Materials and Methods

In this chapter, the materials and methods used for this study are described following a brief description of data analysis.

2.1 Field Sampling

Eight field visits to Handle Lake, Fiddler Lake, Jackfish Lake, and Small Lake occurred from November 2020 to October 2021.

2.1.1 Water Chemistry

Lake water samples were collected approximately monthly from November 2020 to October 2021 at all four study lakes during both the ice-covered and open-water periods. Samples were collected in the deepest section of each lake indicated in the bathymetry map in Fig. 3.1. Both total (unfiltered) and dissolved (filtered, 0.45 μm)) water samples were collected for water chemistry analysis (Table 2.4). Water samples were collected by a peristaltic pump equipped with Teflon lines attached to a sonde. Filtering of the water samples occurred in the field using an inline high-pressure filter (0.45 μm Versapor membrane). The high-pressure filter was attached to a separate Teflon line with a switch valve separating it from another Teflon line used for total fraction sampling. A calibrated depth cable was used to lower the attached intake Teflon line to the desired depth and the sonde cable was anchored in place. For each sample depth, the Teflon lines were rinsed for approximately two minutes with the depth water before sample collection occurred to prevent potential cross depth contamination. Water sample bottles and caps without a preservative were triple rinsed with associated depth water. Widely adopted field sampling protocols were followed including wearing sterile non-powdered latex gloves (CCME, 2011).

The Teflon lines were drained of any remaining lake water before field departure to minimize the amount of time excess water was in the lines. All Teflon lines were pre-washed with 5% hydrochloric acid (HCL) for 10 minutes, then rinsed with Milli-Q water for 10 minutes and placed in clean plastic bags. Cleaning the Teflon lines was carried out before and after each field visit to prevent potential cross contamination. Stratified depth sampling was conducted to establish a detailed water column profile.

Additionally, a field spectrophotometer (*Hach DR-1900*) was used to measure dissolved sulfide (S(-II)) and ferrous iron (Fe(II)) levels in lake waters when reducing/anoxic conditions were present. The phenanthroline method for ferrous iron and methylene blue method protocol for dissolved sulfide was followed (Hach, 2018; Hach, 2019). After leaving the field water samples were transported in coolers and delivered immediately to Taiga Environmental Laboratory in Yellowknife, NT.

An in-situ calibrated multi-parameter water quality sonde (*YSI EX02*) instrument was used during each field visit to measure physical lake characteristics of dissolved oxygen (DO, *mg/L* and %), pH, water temperature (℃), specific conductivity (SpC, $\mu S/cm$), water depth (m), oxidation-reduction potential (ORP, mV), and chlorophyll-*a* ($\mu g/L$) (YSI, 2022). Measurements from the multi-parameter sonde were recorded at 1-m intervals through the water column. Regular calibration of the multi-parameter sonde with industry standard reference solutions was performed (YSI, 2022).

2.1.2 Data Loggers

Continuous data loggers were deployed in the deepest section of each study lake during November 2020 to May 2021 to measure DO (*mg/L* and %), water temperature (℃), and light

intensity (lum/ft²) (Fig. 3.1 and Table 2.1). The data loggers were stringed every 1 m in depth until approximately 1 m above the lake sediment (Fig. 2.1). Sensor strings were anchored in a pvc-pipe on the lake ice (Fig. 2.1). A schematic diagram example of a sensor string is shown in Fig. 2.1. Table 2.1 summarizes the data loggers' parameters, setup, and frequency of measurement. The accuracy and resolution of the sensors are also summarized in Table 2.2.

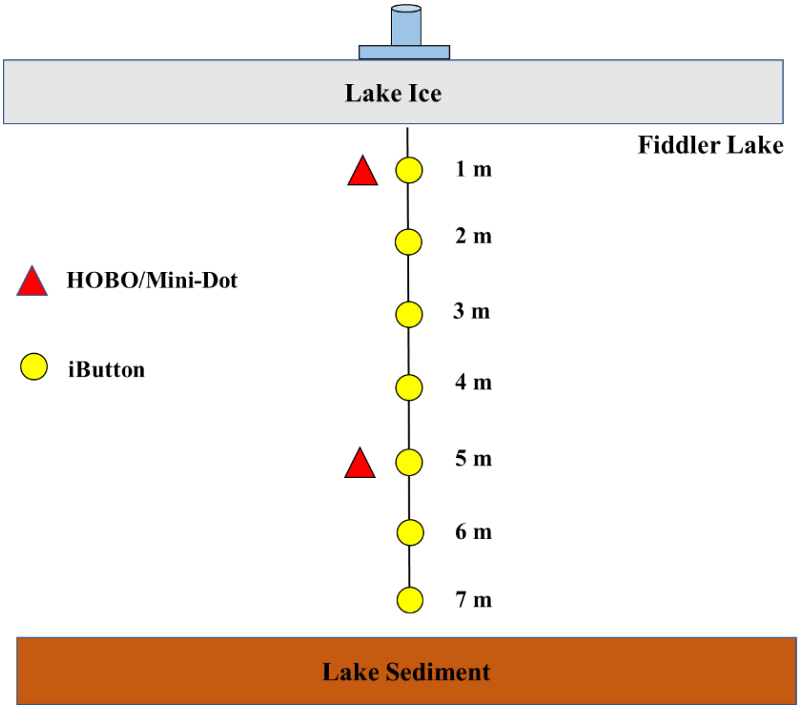

Figure 2.1 Schematic diagram of the data logger strings (*e.g.,* Fiddler Lake).

Table 2.1 Data logger information on logger type, depth location, parameters measured, frequency of measurement, coordinates, deployment, and retrieval dates for each study lake. Jackfish Lake did not have a data logger results due to field technical difficulties.

Fiddler Lake			
#1: Deployment: 2020-11-18; Retrieval: 2021-05-11 Lat/Long: 62°28'8.68"N 114°30'37.06"W			
Depth (m)	**Instrument**	**Parameter (Units)**	**Frequency of Measurement (min)**
1	iButton	Temp (°C)	120
2	iButton	Temp (°C)	120
3	iButton	Temp (°C)	120
4	iButton	Temp (°C)	120

5	iButton	Temp (°C)	120
6	iButton	Temp (°C)	120
7	iButton	Temp (°C)	120
#2: Deployment: 2021-01-27; Retrieval: 2021-05-11 Lat/Long: 62°28'8.68"N 114°30'37.06"W			
Depth (m)	**Instrument**	**Parameter (Units)**	**Frequency of Measurement (min)**
1	MiniDOT™	DO (%, mg/L), Temp (°C)	10
5	HOBO DO	DO (mg/L), Temp (°C)	30
Handle Lake			
#1: Deployment: 2020-11-16; Retrieval: 2021-05-12 Lat/Long: 62°29'31.25"N 114°23'43.90"W			
Depth (m)	**Instrument**	**Parameter (Units)**	**Frequency of Measurement (min)**
1	iButton	Temp (°C)	120
2	iButton	Temp (°C)	120
3	iButton	Temp (°C)	120
3.5	iButton	Temp (°C)	120
#2: Deployment: 2021-01-18; Retrieval: 2021-05-12 Lat/Long: 62°29'31.25"N 114°23'43.90"W			
Depth (m)	**Instrument**	**Parameter (Units)**	**Frequency of Measurement (min)**
1	MiniDOT™	DO (%, mg/L), Temp (°C)	10
2.5	MiniDOT™	DO (%, mg/L), Temp (°C)	10
Small Lake			
#1: Deployment: 2020-11-19; Retrieval: 2021-05-13 Lat/Long: 62°31'03.6"N 113°49'20.7"W			
Depth (m)	**Instrument**	**Parameter (Units)**	**Frequency of Measurement (min)**
1	iButton	Temp (°C)	120
	HOBO Light	Temp (°C), Light (lum/ft²)	60
2	iButton	Temp (°C)	120
3	HOBO Light	Temp (°C), Light (lum/ft²)	60
	iButton	Temp (°C)	120
4	iButton	Temp (°C)	120
5	iButton	Temp (°C)	120
6	HOBO Light	Temp (°C), Light (lum/ft²)	120
	iButton	Temp (°C)	120
7-12	iButton	Temp (°C)	120

Table 2.2 Continuous data logger accuracy and resolution specifications.

Sensor Type	***Parameter (Units)***	***Accuracy***	***Resolution***
HOBO	Temp (°C)	± 0.53°C from 0° to 50°C	0.14°C at 25°C
	Light (lum/ft²)		Range: 0 to 320,000 lux
MiniDOT™	DO (%, mg/L)	+/- 5%, 0.3 mg L−1	0.01 mg L−1
	Temp (°C)	+/- 0.1	
iButton	Temp (°C)	±1°C	0.5°C

2.1.3 Lake Sediment Cores

Lake sediment cores from each lake were collected in April 2021 using an 8.8 cm internal diameter gravity corer (*Uwitec*). Each sediment core was collected adjacent to the water sampling locations (Fig. 3.1). Approximately the top 30 cm of the lake sediment was optimal to examine general metal geochemistry. The gravity corer was carefully lowered and raised through a slush-free drilled ice hole, while maintaining the core tube in the upright position during the entire extraction process. Upon retrieval of the gravity core at the ice surface, a rubber plug was placed in the bottom of the tube before the core emerged from the water to safeguard from any significant loss of sediment. Each sediment core was visually inspected to ensure adequate lake water was collected above the sampled sediment (approximately half water to half sediment in the core tube), making sure the top of the sediment column was captured and intact. This aspect of sampling was important to ensure the top of the sediment column was sampled. Transportation of the sediment cores from the field to the lab was conducted using a tube rack keeping the cores in the upright position while allowing minimal movement. Extreme caution was taken to minimize disturbance to the sediment column in the core. This was important to minimize different layers in the sediment column from extensively mixing and settling. The collected sediment cores were temporarily stored in a 4°C refrigerator before slicing each core.

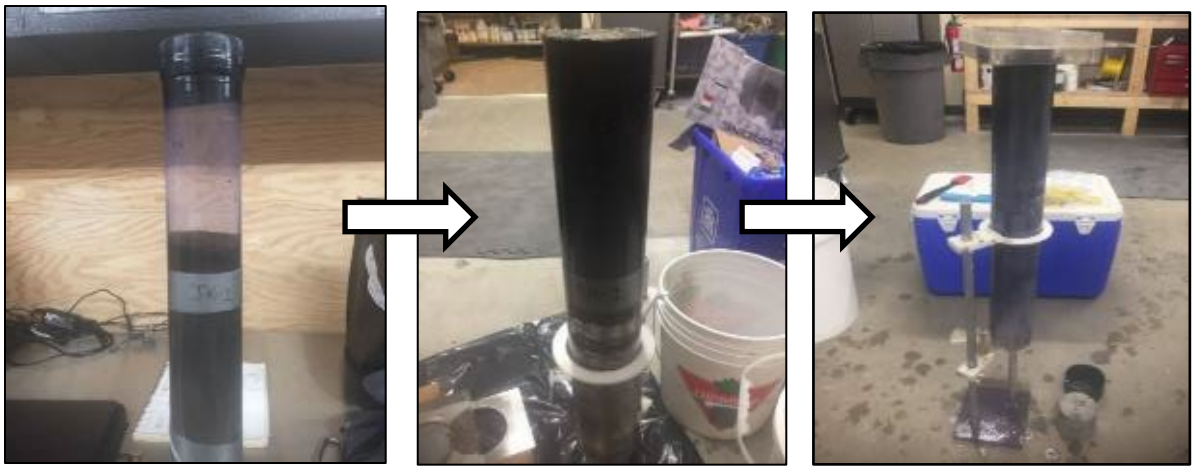

Figure 2.2 Sediment core slicing process into 1-cm sub-sections via a gravity corer (*Unwitec*).

Each sediment core was processed within 24-to-48-hours after collection (Fig. 2.2). Sub-sectioning of the cores involved, first removing any overhead water while confirming the surface organic matter layer was still intact (Fig. 2.2). Each sediment core was then sliced into 1 cm depth subsections (Fig. 2.2). Between each subsample, the slicing equipment was scrubbed with a phosphorus free soap and rinsed in warm water to prevent cross contamination. The 1 cm sectioned subsamples were individually packaged in sterile *Whirl-Pak* bags and immediately frozen in a freezer. A total of 117 subsamples from the 4 sediment cores was completed.

Next, the frozen lake sediment subsamples were freeze-dried in a vacuum sealed instrument to remove all moisture from the samples before laboratory analysis. Water content in each subsample was calculated using initial and post freeze-dried sediment mass weights.

The percentage of organic matter was calculated based on the Loss-on-Ignition (LOI) method by Heiri *et al.* (2001) by placing 2-grams of each subsample in a muffle furnace at 550°C for 4 hours, this was repeated for each sliced sub-section of the cores. Metal analysis of arsenic (As), iron (Fe), and manganese (Mn), among a suite of other parameters were completed for each

of the 0.5-gram freeze-dried subsamples. This analysis was conducted by the Analytical Services Unit (ASU) of Queens University Laboratory using ICP-OES and ICP-MS instruments. Duplicate subsamples were included in the sediment analysis for quality assurance control. Further laboratory quality assurance (QA) and quality control (QC) was ensured by ASU by operating two blank samples for each element analysis with a specified control targets for each ICP-OES and ICP-MS instruments.

2.1.4 Lake Bathymetry

Lake bathymetric maps for three of the study lakes (Fiddler Lake, Jackfish Lake, and Small Lake) were mapped in August and September 2021 utilizing a *Humminbird* depth sounder and chart plotter via a canoe. Multiple transects of each lakes' basin and boundary was performed with the depth sounder on the canoe to capture accurate representation of each lake. Handle Lake's bathymetry map data was previously surveyed by Michael Palmer and others from the Government of Northwest Territories in September 2017 using a *Garmin Fishfinder 250*.

The collected geo-referenced depth points were extracted to *Reef Master Software* where the file was converted to csv format. Depth point data was QA and QC by filtering and removing outlier measurement and clear error readings. Bathymetric maps were constructed in *ArcGIS* software. Data points from each study lake were interpolated separately in *ArcGIS* by spatial interpolation tools, specifically utilizing kriging, inverse distance weighted (IDW), or natural neighbor depending on the data set with each using a three-meter output resolution. Spatial analysis was conducted in *ArcGIS* involved surface-volume calculation on the lake raster files to determine lake volume and produce a two-dimensional surface area value. The final lake

bathymetry map layout symbology was collectively applied to each individual map to showcase a unified legend reference of lake depth.

2.1.5 Ice-on and ice-off dates

Approximate lake ice-on and ice-off dates for each study site was derived utilizing high-resolution satellite imagery (*Sentinel Playground)* and cross-referenced with in-situ photograph documentation of lake ice on the study lakes (Sentinel Hub, 2022). Results are presented in section 3.1.1 in Table 3.1.

2.1.6 Snow and Lake Ice

Measurements of snow depth, snow-water equivalent, and snow temperature were also recorded throughout the winter (Table 2.3). Snow depth was measured utilizing a *Snow-Hydro* magnaprobe equipped with a GPS (±10 m resolution) taking snow depth readings approximately every 10 paces across two transects approximately 300 m in length in both the North-South and East-West direction. Snow-water equivalent (SWE) and snow depth were recorded using a snow tube made of clear lexan. Snow-water equivalent was determined through weighing the snow tube with a snow core in the field and subtracting the weighing of the snow tube empty. A total of five SWE measurements were taken at each site. Snow temperatures were also taken at the surface and base of the snowpack using a thermometer.

Lake ice measurements of ice thickness, classification, and proportion of white ice to black ice was performed. Lake ice thickness was measured by a pre-calibrated pole and proportion of white and black ice was recorded via a measuring tape.

2.2 Data

Table 2.3 Summary of data collection parameters.

Component	***Parameter (Unit)***	***Field Instrument***	***Analysis***
Snow	Depth (cm), Snowpack Temp (°C), Snow-water-equivalent (SWE)	Magna-probe, Thermometer, Snow Tube	
Lake Ice	Depth (cm), Classification (white ice / black ice)	Measuring tool & tape	
Lake Bathymetry	Depth (m), Latitude/Longitude	Depth Sounder & Chart Plotter	ArcGIS: Interpolation, 3-D Analyst
Water (Chemistry)	Total & Dissolved Metal Suite (As, Fe, Mn), Dissolved organic carbon (DOC), Major Ions, Nutrients (Nitrogen, Phosphorus etc.)	Peristaltic pump / Teflon Lines	ICPMS3, DICPMS
	Fe2+, S2- (µg/L)	Field Spectrophotometer	
Water (Sonde/Loggers)	Dissolved oxygen (DO), pH, Temp (°C), Specific Conductivity (SpC), Oxidation reduction potential, Chlorophyll-a	YSI EXO2 Sonde MiniDot/HOBO/IButton	
Sediment Cores	Organic matter (%), Water content (%), Metals (µg/g).	Gravity Core ~ 30cm deep. Sectioned at 1 cm intervals.	Freeze-dried, Loss-on-Ignition (LOI), Metal Analysis

2.3 Data Analysis

2.3.1 Laboratory Analysis

Lab analysis of collected lake water samples were examined for major ions, nutrients, metalloids, and dissolved organic carbon at Taiga Environmental Laboratory in Yellowknife, NWT (Table. 2.4). Dissolved concentration results represent water samples that were filtered onsite through a high-pressured filter (0.45 µm) and total concentration results represent samples of unfiltered water. Dissolved and total metalloid concentrations were measured utilizing an inductively coupled plasma mass spectrometry (ICP-MS) following the EPA 200.8 protocol

(Creed *et al.,* 1994). Major ions concentrations were measured using an ion chromatography (SM4110) (APHA, 1992). Dissolved organic carbon was determined through a total carbon analyzer (SM5310) (APHA, 1992). Phosphorus was measured colorimetrically (SM4500P) (APHA, 1992). Percentage of particulate concentrations was calculated using dissolved and total concentration which is explained in the following section.

Table 2.4 List of water sample analysis measurements.

Parameter	***Unit***	***Instrument***
Total & Dissolved Metal Suite (As, Fe, Mn, …)	µg/L	ICP-MS3, DICPMS3
Fe2+, S2- (ferrous iron and sulfide)	µg/L	Field Hach spec. Hach DR1900 spectrometer
Dissolved organic carbon (DOC)	mg/L	Total carbon analyzer
Major Ions	mg/L	Ion chromatography
Nutrients (phosphorus, nitrogen, …)	µg/L, mg/L	IC Anion

2.3.2 Percent Particulate

Total and dissolved concentrations of As, Fe, and Mn were used to calculate the percentage of particulate (> 0.45 µm) of each element in the study lakes to understand the amount of particulate versus dissolved concentrations. Percentage of particulate was calculated through the following equation, (Equation 2.1):

$$\%\ Particulate = \frac{(\ Total\ [concentration]\ -\ Dissolved\ [concentration])}{Total\ [concentration]} \times 100$$

Instances of zero percent particulate represents that the dissolved concentrations exceeded total concentrations. The purpose of this calculation was to determine the percentage of dissolved concentration versus total concentration in each study lake's water column, as well as observe any seasonally changes through ice-on to open-water periods. Information on particulate As for

example is important to further understand As cycling relationship with other redox sensitive elements of Fe and Mn regarding processes like sorption and co-precipitation.

2.3.3 Volume Weighted Mean

Dissolved concentrations for As, Fe, and Mn from stratified lake samples from each study lake were used to calculate a volume weighted mean for each site visit (Table 2.5). A volume weighted mean is defined as a single concentration value which represents the entire lake for a site visit. The volume weighted mean calculation considered proportional volume of each depth layer based on the percentage of the total water volume in a lake (Table 2.5). An example of calculating the volume weighted mean of a lake is shown in equation 2.2 below, but first the volume of each depth layer in a lake was determined.

To determine the volume for each depth layer in a lake, the bathymetry data was analyzed through spatial analysis tools in *ArcGIS*. First, the bathymetry raster was projected to UTM 11, enabling the output value to be in meters using "Project Raster (Data Management)" tool. Next, the values were reclassified into 1 m intervals using the "Reclassify (Spatial Analyst)" tool. Finally, the "Zonal Statistics as Table" tool was used to calculate the statistics of the reclassified output. Once completed, the Zonal statistics results were exported to a "txt" file. Moving onto a spreadsheet, the first step was to find the area of different depths use the following formula: =SUMIF(A2:A10,">=(Depth)",B2:B10). Where the depth column (A2:A10) and area column (B2:B10) were added for all areas, whose depth is greater or equal to the depth in question. This process was repeated for each step to determine the area of all depth ranges. After the area was determined, it can be multiplied by the depth interval to determine the volume. Finally, the percentages of each volume were calculated, and their weights were determined. A complete list of the percentage volume per depth of each lake is listed in Table A.4 1 in the *Appendices*.

Table 2.5 Volume weighted As mean calculation example of Handle Lake for a field visit from 2020-11-16.

Sample Date	*Depth (m)*	*Percentage of Total Volume (%)*	*Dissolved As (µg/L)*	*Volume Weighted As (µg/L)*	*Volume Weighted As Mean (µg/L)*
2020-11-16	1	55	204	112.2	207.24
	2	27	208	56.16	
	3	18	216	38.88	

(Equation 2.2) **Example: Handle Lake, Sample Date: 2020-11-16**

Step 1: Assign each depth in the water column its calculated percentage of the total volume of Handle Lake = 390 525 m^3

(Table 3.1 and Table A.4.1, *Appendices*).

- $\%\ of\ Total\ Volume = Depth\ volume\ (m^3) \div Total\ lake\ Volume\ (m^3)$
- Example: 1 m depth, $\%\ of\ Total\ Volume = 214\ 357\ m^3 \div 390\ 525\ m^3$
- $\%\ of\ Total\ Volume$ = 0.55 or (55%)
- 1 m = 214 357 m^3 (55%), 2 m = 106 822 m^3 (27%), 3 m = 69 345 m^3 (18%)

Step 2: For each depth volume multiply the percentage of the total volume against the corresponding depth sample concentration.

- $Volume\ Weighted\ As\ = Dissolved\ concentration\ (\mu g/L) \times Percentage\ of\ total\ volume$
- $Volume\ Weighted\ As\ = 204\ (\mu g/L) * 0.55$
- $Volume\ Weighted\ As\ = 112.2\ (\mu g/L)$

Step 3: Total up all the weighted volume concentrations to produce a mean concentration.

- $Volume\ Weighted\ As\ Mean = (Volume\ weighted\ concentration\ (\mu g/L) + Volume\ weighted\ concentration\ (\mu g/L))$
- $Volume\ Weighted\ As\ Mean = (112.2\ (\mu g/L) + 56.16\ (\mu g/L) + 38.88\ (\mu g/L))$
- $\boldsymbol{Volume\ Weighted\ As\ Mean = 207.24\ (\mu g/L)}$

2.3.4 Seasonal Percent Change

Seasonal percent change of the volume weighted mean for As, Fe, and Mn was calculated to understand how much the concentration of each redox element changed through the seasons. Calculating the seasonal percent change was conducted for the ice-on period (November-April), spring ice-off (May-June), and the open-water period (June-October) (Equation 2.3). May was not included in the ice-on calculation despite ice conditions, to ensure the freshet period, particularly snowmelt, was not an external influence or factor on the winter season percent change calculation. Thus, the freshet event was captured separately, and May was included in the spring ice-off (May-June) period. Below is an example of the seasonal percent change calculation between elemental concentrations during spring ice-off (May-June):

Example: $$\% \text{ Change over spring ice-off} = \frac{[\text{June}] - [\text{May}]}{[\text{May}]} \times 100 \qquad \text{(Equation 2.3)}$$

This type of calculation is important to assist in understanding how lake ice, freshet, and atmosphere exchange of dissolved oxygen with the water during the open-water period could control surface water chemistry of As and other redox elements.

3. Chapter 3: Results

3.1 Physical Characteristics

3.1.1 Lake Morphology

The morphometric properties of the four subarctic lakes (Handle Lake, Fiddler Lake, Jackfish Lake, and Small Lake) are summarized in Table 3.1. Based on field and satellite observations, none of the lakes have defined inflow or outflow channels and are likely

hydrologically disconnected from surrounding watersheds in most years (Fig. 3.1). However, some hydrologic connectivity through surrounding wetlands may exist in wet years (Fig. 3.1). Handle Lake is the closest study lake to Giant Mine, approximately 2.2 km from a decommissioned roaster stack. Handle Lake is the shallowest lake with a maximum depth (Z_{max}) of 3.5 m, lake volume (V) of 390 525 m^3, and a surface area (SA) of 210 000 m^2 (Table. 3.1 and Fig. 3.1 A). The bathymetric map of Handle Lake (Fig. 3.1 A) shows the lake is comprised of a single basin. Additionally, Handle Lake has the highest calculated surface area to volume (SA: V) ratio of 0.54 among the four study lakes (Table 3.1). The SA:V ratio is calculated to determine the proportionality of surface area to volume in a lake for a basis to assist in understanding how any differences physical lake characteristics may influence solute concentrations like As.

Fiddler Lake is the second shallowest lake with a Z_{max} of 6.5 m, V of 1 103 741 m^3, and a SA of 290 000 m^2 (Table 3.1 B). Lake bathymetry displayed in Fig. 3.1 B shows that much of the lake is less than 3 m deep in the southern basin. The north basin is deeper reaching maximum depths of 6.5 m (Fig. 3.1 B). The SA:V ratio for Fiddler Lake is 0.26 and ranks second highest among the four lakes (Table 3.1). Fiddler Lake is bordered by Highway 3 to the south and has wetland connections on both east and west sides of the lake (Fig. 3.1 B).

Jackfish Lake has a Z_{max} of 7.5 m, V of 3 205 937 m^3 and a SA of 490 000 m^2 (Table. 3.1), with its shorelines being surrounded by a substantial amount of municipal infrastructure, including: a solid waste facility, highway to the north, a power generation station on the northeast shore, and cemetery to the southwest (Fig. 3.1 C). Consequently, much of the catchment for Jackfish Lake has been impacted by municipal development. The bathymetric map

of Jackfish Lake in Fig. 3.1 C displays that most of the main basin is between 6 and 7 m deep. Jackfish Lake has the lowest SA:V ratio of 0.15 (Table 3.1).

Small Lake is the deepest and largest lake of the study with Z_{max} of 12.5 m, V of 4 016 371 m^3, and SA of 780 000 m^2 (Table 3.1). The bathymetry map for Small Lake in Fig. 3.1 D shows the deepest part (12.5 m) of its basin is in the south-east section of the lake. Small Lake reported the second smallest SA:V ratio of 0.19 (Table 3.1). Small Lake is likely the least impacted lake from historical aerial emissions from mining sources in the region as it is not along the path of prevailing winds and is 27 km from Giant Mine (Fig. 3.1 D and Table 3.1). Based on field and satellite observations, Small Lake's basin has no channelized inflow or outflow and has a small pond in its northeast corner (Fig. 3.1 D)

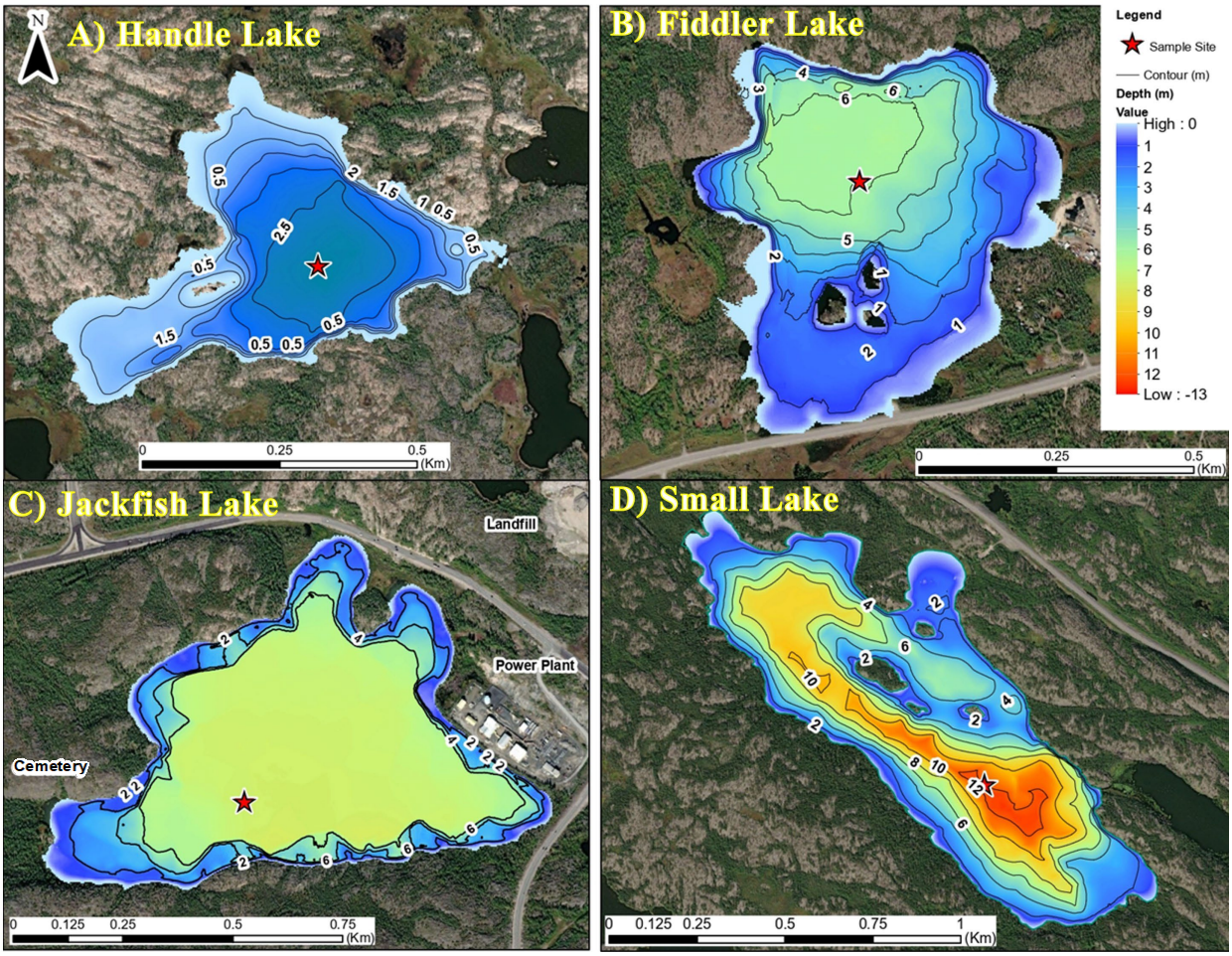

Figure 3.1 Bathymetric maps of A) Handle Lake, B) Fiddler Lake, C) Jackfish Lake, and D) Small Lake, NWT.

Table 3.1 Summary of physical properties of study lakes, including lake surface area, maximum depth, lake volume, estimated ice-on and ice-off dates, and distance of lake to Giant Mine.

Lake *Name*	***Lake Surface Area*** ***(m^2)***	***Max Depth (m)***	***Lake Volume (m^3)***	***Surface Area : Lake Volume Ratio***	***Ice-on Date (Estimated)***	***Ice-off Date (Estimated)***	***Distance to Giant Mine (km)***
Handle	210 000	3.5	390 525	0.54	2020-10-29	2021-05-27	2.2
Fiddler	290 000	6.5	1 103 741	0.26	2020-10-29	2021-05-27	8.6
Jackfish	490 000	7.5	3 205 937	0.15	2021-11-06	2021-05-25	4.2
Small	780 000	12.5	4 016 371	0.19	2020-10-24	2021-06-14	27.4

3.1.2 Water Temperature

Water temperature profiles were recorded during site visits to all four lakes from November 2020 to October 2021 (Fig. 3.2).

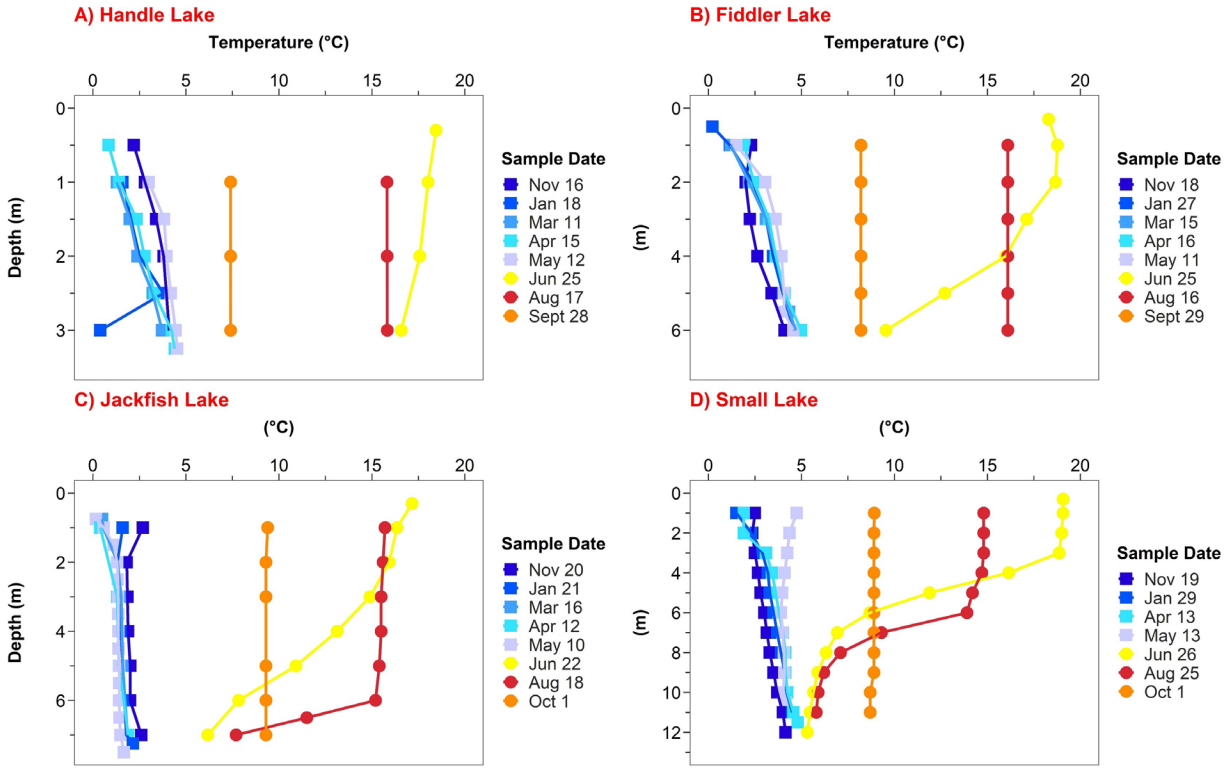

Figure 3.2 Water temperature profiles for Handle Lake, Fiddler Lake, Jackfish Lake, and Small Lake during November 2020 to October 2021. Squares = Ice-on, Circles= Ice-off.

During the ice-covered period (November to May) all lakes developed inverse thermal stratification, except for Jackfish Lake which remained isothermal throughout the ice-covered season between 1°C and 3°C (Fig. 3.2 C). In the open-water season, vertical temperature gradients were observed in all lakes, except Handle Lake (Fig. 3.2 A). Surface waters warmed rapidly in all lakes once the ice-cover disappeared, with temperatures increasing approximately

15°C between May 10th and June 26th (Fig. 3.2). Handle Lake was isothermal during the open-water season with water temperatures that ranged between 7.4°C and 19°C (Fig. 3.2 A). A detailed thermal profile of Handle Lake in Fig. 3.3 shows the relative stability of the water column under-ice. The densest water (approximately 4°C) in Handle Lake accumulated near the sediment boundary during the continuous data logger deployment (Fig. 3.3).

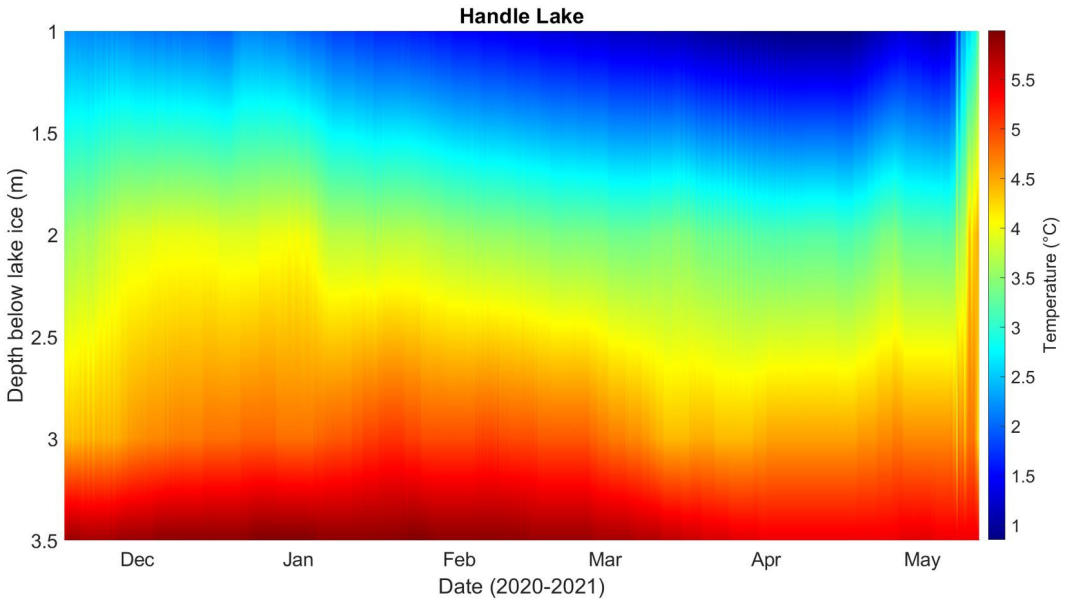

Figure 3.3 Water temperature (°C) time series for Handle Lake during November 2020 to May 2021 via a string of continuous data loggers.

In Fiddler Lake, there was a steep gradient observed in the water temperature early in the open-water period (June 25th), and temperatures decreased from 18°C at the surface to 9°C in the bottom waters (Fig. 3.2 B). On August 16th, Fiddler Lake was isothermal at 16°C and was observed isothermal again on September 29th at 8.2°C (Fig. 3.2 B). Like Handle Lake, the detailed under-ice thermal profile for Fiddler Lake showed a stable and inversely stratified water column under-ice (Fig. 3.4). Although Fiddler Lake and Jackfish Lake are similar in Z_{max} and

bathymetry, Jackfish Lake displayed periods of thermal stratification during the summer (Fig. 3.2 B and C).

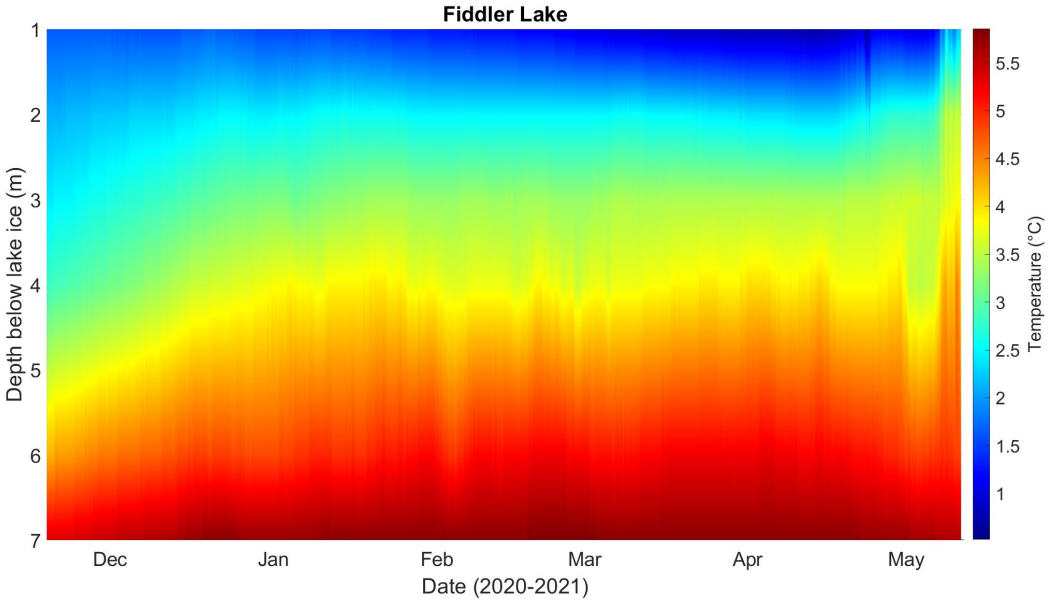

Figure 3.4 Water temperature time series for Fiddler Lake during November 2020 to May 2021 via a string of continuous data loggers.

The thermal regime of Small Lake was distinct from all other study lakes during the open-water period (Fig. 3.2 D). Thermal stratification developed early in Small Lake during the open-water period and persisted through to lake turnover in autumn (Fig. 3.2 D). Clear water temperature boundaries were distinguished between the epilimnion, metalimnion, and hypolimnion in Small Lake (Fig. 3.2 D and Fig. 3.5). The thickness of the epilimnion in Small Lake increased in size from 3 m on May 13th to approximately 7 m on August 25th, deepening the thermocline (Fig. 3.2 D).

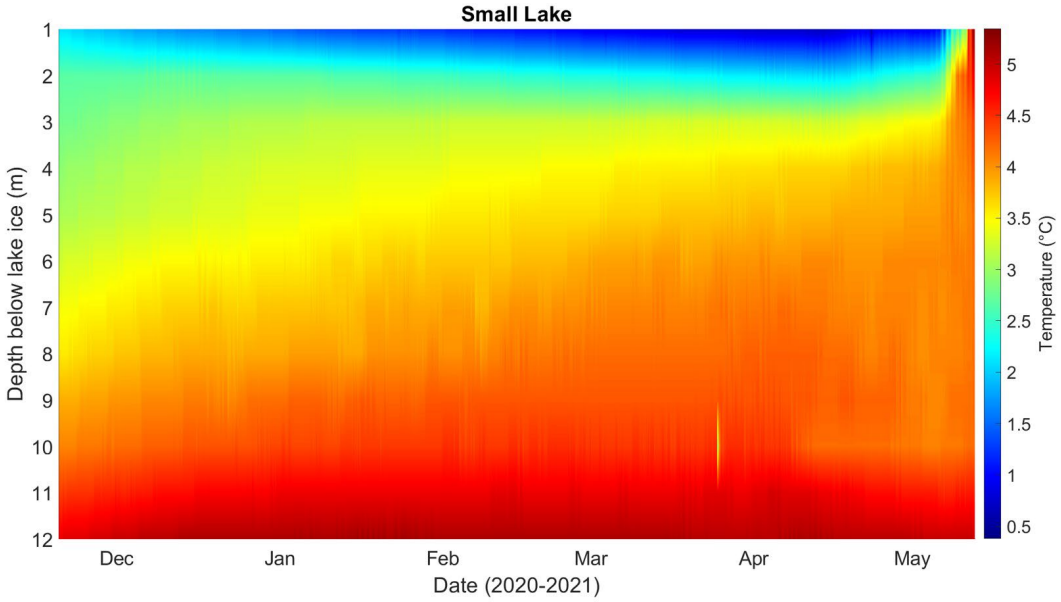

Figure 3.5 Water temperature (°C) time series for Small Lake during November 2020 to May 2021 via a string of continuous data loggers.

3.1.3 Dissolved Oxygen (DO)

Dissolved oxygen (DO) concentrations (mg/L) for each study lake were recorded at site visits from November 2020 to October 2021 and are shown in Fig. 3.6 below.

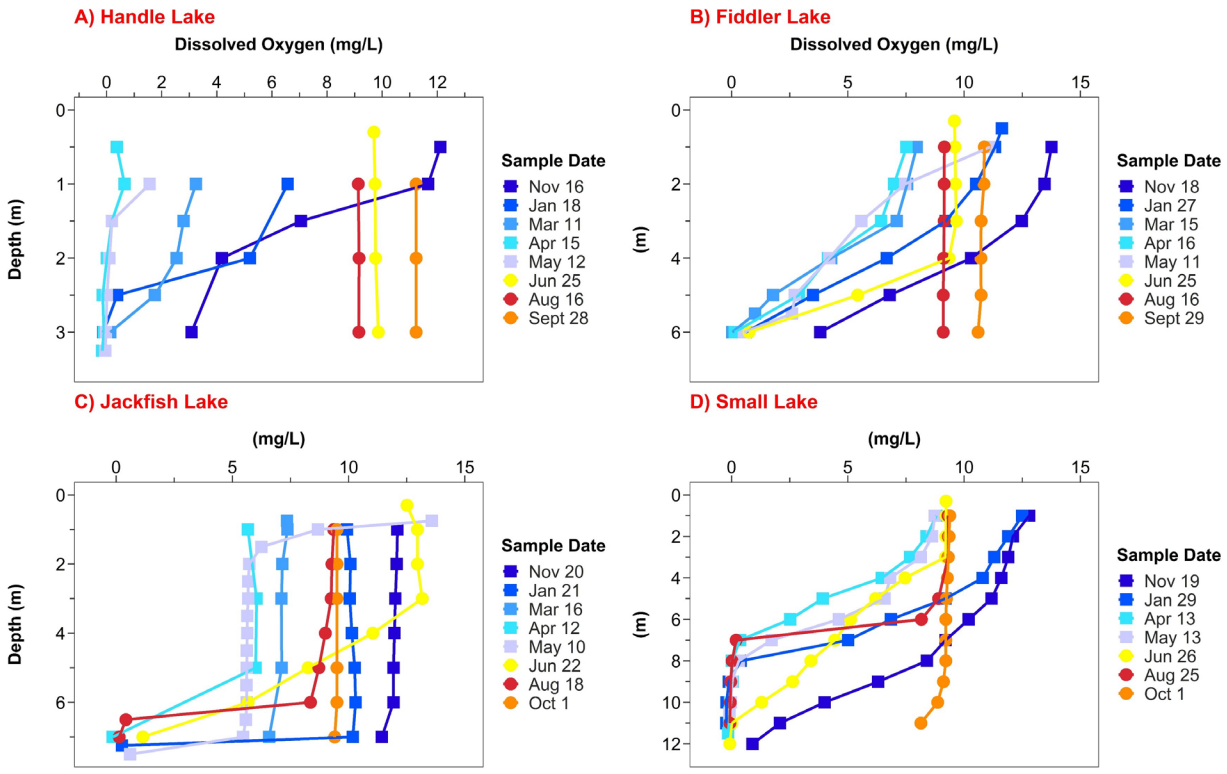

Figure 3.6 Dissolved oxygen concentrations (mg/L) for Handle Lake, Jackfish Lake, Fiddler Lake, and Small Lake during November 2020 to October 2021. Squares = Ice-on, Circles= Ice-off.

Dissolved oxygen levels progressively decreased in all the study lakes through the winter period from ice-on (November) until ice-off (May) (Fig. 3.6). Full water column anoxia (< 0.5 mg/L) was observed in Handle Lake from mid-April to the end of the ice-cover season (May 12th) (Fig. 3.6 A and Fig. 3.7). A steep gradient in DO conditions was reported in Fiddler Lake's water column throughout the ice-cover season (Fig. 3.6 B and Fig. 3.8). The bottom 1 m of Fiddler Lake's water column was anoxic during the March 15th and April 16th sampling periods (Fig. 3.6 B and Fig. 3.8).

In contrast to Handle Lake and Fiddler Lake, there was no DO gradient in the water column during the ice cover season in Jackfish Lake, which remained well oxygenated (>5

mg/L) (Fig. 3.6). However, a thin anoxic layer (approximately 0.5 m) was often measured near the sediment boundary during the ice-covered season in Jackfish Lake (Fig. 3.6 C).

Like Handle Lake and Fiddler Lake, DO concentrations in Small Lake decreased in the water column in conjunction with decreasing depth over the ice-covered season (Fig. 3.6 D). Hypolimnetic anoxia was observed in Small Lake's bottom 4 m of its water column from April 13th to ice-off (Fig. 3.6 D). Once the lake ice left the study lakes in late-May and early June, lake waters were quickly re-oxygenated (Fig. 3.6). During the open-water season hypolimnetic anoxia was observed in two of the study lakes of Jackfish Lake and Small Lake (Fig. 3.6 C and D). The anoxic zone in Jackfish Lake was relatively thin and appeared intermittently (Fig. 3.6 C). Small Lake's water column profile developed hypolimnetic anoxia during the open-water season in the bottom 4 to 5 m of the lake and was stable through the summer until fall turnover (Fig. 3.6 C and D).

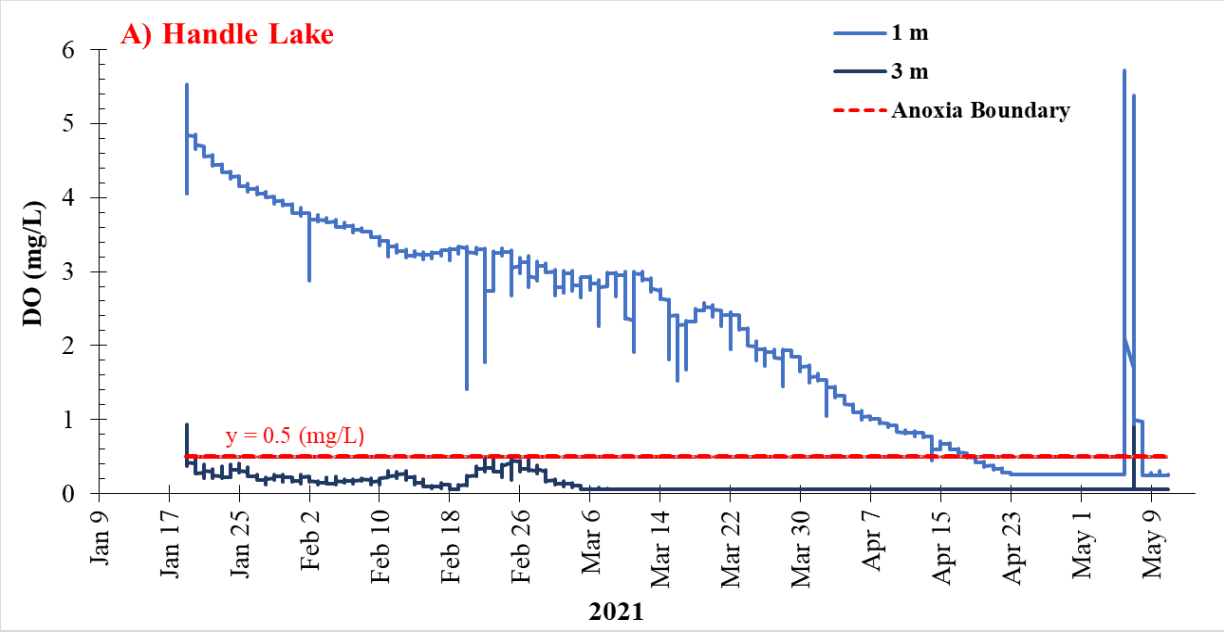

Figure 3.7 Dissolved oxygen concentration time series profile for Handle Lake at 1 m and 3 m depths from January 2021 to May 2021. Anoxia boundary represents 0.5 mg/L.

Figure 3.8 Dissolved oxygen concentration time series profile for Fiddler Lake at 1.5 m and 5 m depths during January 2021 to May 2021. Anoxia boundary represents 0.5 mg/L.

3.2 Nutrients

A summary table representing nutrient data for nitrogen (N), phosphorus (P), and chlorophyll-*a* (Chl-*a*) from each study lake is presented in Table 3.2 below. The goal of reporting this background nutrient data was to determine general productivity or trophic status of each lake, which is explored in section 3.2.4. Calculated mean, maximum, and minimum of total nitrogen **(**reported as total**)** and dissolved nitrogen concentrations (mg/L), total and dissolved phosphorus concentrations (µg/L), and chlorophyll-a concentrations (µg/L) for Handle Lake, Fiddler Lake, Jackfish Lake, and Small Lake during November 2020 to October 2021. In occurrences where a result reading was below method detection level**,** the result value (equalling the method detection limit) was divided in half when included in mean calculations to appropriately represent the sample mean. For example, the method detection value of phosphorus was 10 µg/L. Therefore, data reported less than the method detection value

of 10 µg/L was represented as half of the detection level as 5 µg/L. The justification for this was to proportionally represent concentration results that were below the method of detection.

Based on the nutrient data in Table 3.2, Jackfish Lake was the most productive lake during the study followed by Handle Lake, Small Lake, and Fiddler Lake. Jackfish Lake had the highest level of phosphorus (total P mean = 54.70 (µg/L), dissolved P mean = 16.72 (µg/L)) and chlorophyll-*a* (Chl-*a* mean= 7.83 (µg/L)), which are key indicators of a productive lake (Table 3.2). Comparatively, Handle Lake measured the highest level of nitrogen (total N mean = 2.49 (mg/L), dissolved N mean = 2.19 (mg/L) in all the study lakes (Table 3.2). Small Lake also produced moderate concentrations of both dissolved and total phosphorus, ranking second in phosphorus among the study lakes (Table 3.2). Fiddler Lake's nutrient levels over the study were generally low as Fiddler Lake ranked last in each nutrient parameter, except for dissolved phosphorus (Table 3.2).

Table 3.2 Calculated mean, maximum, and minimum of total nitrogen (reported as total) and dissolved nitrogen concentrations (mg/L), total and dissolved phosphorus concentrations (µg/L), and chlorophyll-a concentrations (µg/L) for Handle Lake, Fiddler Lake, Jackfish Lake, and Small Lake during November 2020 to October 2021. Dissolved and total nitrogen's method detection level was 0.06 mg/L through the ISO/TR 11905:1997(E) test method. Dissolved and total phophorus's method dection limit was 10 µg/L via the EPA200.8 test method. In occurrences where a result reading was below method detection level, the result value (equalling the method detection limit) was divided in half when included in mean calculations to appropriately represent the sample mean. For example, the method detection value of phosphorus was 10 µg/L. Therefore, data reported less than the method detection value of 10 µg/L was represented as half of the detection level as 5 µg/L. The justification for this was to proportionally represent concentration results that were below the method of detection.

Lake	***Mean***	***Maximum***	***Minimum***	***N***
Total N (mg/L)				
Handle	2.49	3.84	1.4	17
Fiddler	0.59	0.91	0.49	18
Jackfish	1.23	2.08	0.89	19
Small	0.72	1.68	0.57	34
Dissolved N (mg/L)				
Handle	2.19	3.64	1.15	23
Fiddler	0.52	0.89	0.39	32
Jackfish	0.97	5.82	0.67	35
Small	0.65	1.44	0.52	46
Total P (µg/L)				
Handle	16.76	33	5	21
Fiddler	11.83	108	5	24
Jackfish	54.70	491	5	20
Small	24.89	131	5	38
Dissolved P (µg/L)				
Handle	6.88	23	5	26
Fiddler	7.41	41	5	41
Jackfish	16.72	395	5	39
Small	11.36	102	5	64
Chlorophyll-a (µg/L)				
Handle	2.2	7.2	1	6
Fiddler	0.9	1.8	0.5	9
Jackfish	7.8	27.9	1.6	9
Small	1.4	2.5	1	7

3.2.1 Chlorophyll-a (Chla)

Analysis results for chlorophyll-*a* (Chl-*a*) samples for Handle Lake, Fiddler Lake, Jackfish Lake, and Small Lake are shown in Table 3.2 above. The highest mean concentrations

of chlorophyll-*a* were recorded in Jackfish Lake (mean = 7.8 µg/L) with the other study lakes reported values much lower with Handle Lake (mean= 2.2 µg/L), Small Lake (mean= 1.4 µg/L), and Fiddler Lake (mean= 0.9 µg/L) (Table 3.2). Overall, all the study lakes apart from Jackfish Lake measured very low Chl-*a*, with concentrations being less than or equal to 2.2 µg/L or below the method detection limit of 1 µg/L (Table 3.2). Jackfish Lake's maximum Chl-*a* concentration of 27.8 µg/L over the study period occurred on October 1st (Table. 3.2). Maximum Chl-*a* levels were observed in other study lakes during the late open-water fall period. Additional data for the water column profiles from an in-situ sonde of Chl-*a* concentrations for each study lake is presented in the *Appendices* A.2 (Fig**.** A2.1 and A2.2).

3.2.2 Phosphorus (P)

Phosphorus (P) concentrations of both the filtered (dissolved) and unfiltered (total) fractions is shown for each of the study lakes in Table 3.2 above. Total phosphorus (TP) and dissolved phosphorus (DP) was low for most study lakes over the sampling period (Table 3.2). Specifically, TP and DP in Handle Lake and Fiddler Lake were near or below the method detection limit of 10 µg/L for much of the study period. Considering several phosphorus results measured less than the method detection level of 10 µg/L. Phosphorus concentrations less than the method detection limit of 10 µg/L included in mean calculations were divided in half to be reported as 5 µg/L, to appropriately represent the overall mean phosphorus concentration in each of the study lakes (Table 3.2). The highest average concentrations of TP were reported in Jackfish Lake (mean = 54.70 µg/L) followed by Small Lake (mean = 24.89 µg/L), Fiddler Lake (mean = 11.83 µg/L), and Handle Lake (mean = 16.76 µg/L) (Table 3.2). In comparison, highest

mean concentrations of DP were observed in Jackfish Lake (mean = 16.72 µg/L) followed by Small Lake (mean = 11.36 µg/L), with Fiddler Lake (mean = 7.41 µg/L) and Handle Lake (mean = 6.88 µg/L) both reporting below the detection limit of 10 µg/L (Table 3.2).

3.2.3 Nitrogen (N)

Nitrogen (N) concentrations in both the filtered (dissolved) and unfiltered (total) fractions is presented in Table 3.2. The highest average concentrations of dissolved nitrogen (DN) were reported in Handle Lake (mean = 2.19 mg/L) followed by Jackfish Lake (mean = 0.97 mg/L), Small Lake (mean = 0.65 mg/L), and Fiddler Lake (mean = 0.52 mg/L) (Table 3.2). Highest to lowest mean total fraction concentrations of nitrogen is reported in the ranking of Handle Lake (mean = 2.49 mg/L) followed by Jackfish Lake (mean = 1.23 mg/L), Small Lake (mean = 0.72 mg/L), and Fiddler Lake (mean = 0.59 mg/L) (Table 3.2).

3.2.4 Trophic Status

The categorization of the trophic status for each study lake was determined according to the Carlson (1977) trophic state index (TSI) methodology (Table A.2.1). TSI equations used the mean total phosphorus and chlorophyll-*a* levels for each lake from Table 3.2. Secchi depth data is not available for this study, thus, trophic state index equations for total phosphorus (TSI_{TP}) and mean chlorophyll-a ($TSI_{CHL\text{-}a}$) were solely used in the index calculations. Mean chlorophyll-*a* and total phosphorus from each study lake was entered into a trophic state index (TSI) index. First, mean chlorophyll-*a* concentrations for a lake was entered as (CHL) in the following index TSI(CHL) = 9.81 ln(CHL) + 30.6, following mean total phosphorus concentrations for a lake was entered as (TP) in the following index TSI(TP) = 14.42 ln(TP) + 4.15 (Carlson, 1977). Next,

these two indexes are entered into the Carlson Trophic Status Index (CTSI) producing a value, which is then compared to Table A.2 1 in the *Appendices* to determine the trophic status (Carlson, 1977). Trophic status for each lake is presented in Table 3.3 below.

Table 3.3 Trophic state index (TSI) calculations based on Carlson (1977) Trophic Status Index (CTSI) and trophic status in Table A.2.1 in the *Appendices*. Mean chorophyll-a and total phoruphus values from each study lake in Table 3.2 were used in the TSI calculations.

Lake	***TSI_{CHL-a}*** *9.81 ln(CHL-a) + 30.6*	***TSI_{TP}*** *14.42 ln(TP) + 4.15*	***CTSI*** *$[TSI_{CHL-a} + TSI_{TP}]/2)$*	***Trophic Status***
Handle	38.33	44.80	41.57	Oligotrophic
Fiddler	29.7	39.78	34.74	Oligotrophic
Jackfish	50.99	61.86	56.43	Eutrophic
Small	33.61	50.50	42.06	Mesotrophic

The TSI_{CHL-a} ranged for all the study lakes was from 29.7 to 50.99 and TSI_{TP} ranged was from 39.78 to 61.86. Based on the TSI_{CHL-a} and TSI_{TP} for each study lake from (November 2020 - October 2021) the trophic status was determined and presented in Table 3.3. The ranking of trophic status from lowest to highest is as follows; Handle Lake and Fiddler Lake as oligotrophic, followed by Small Lake as mesotrophic, and Jackfish Lake as eutrophic. Thus, Jackfish Lake ranked the highest along the trophic gradient, which is reflective of the lake's high nutrient results in Table 3.3.

3.3 Water Chemistry

3.3.1 Arsenic (As)

Substantial seasonal variation in water column dissolved arsenic (As) concentrations was observed for most study lakes over both the ice-on (November-May) and the open-water (June-October) period (Fig. 3.9). All lakes except Fiddler Lake observed increases in dissolved As over

winter and decrease in As over spring ice-off (Fig. 3.9). An increase of As was observed in all the study lakes over the open-water period (Fig. 3.9).

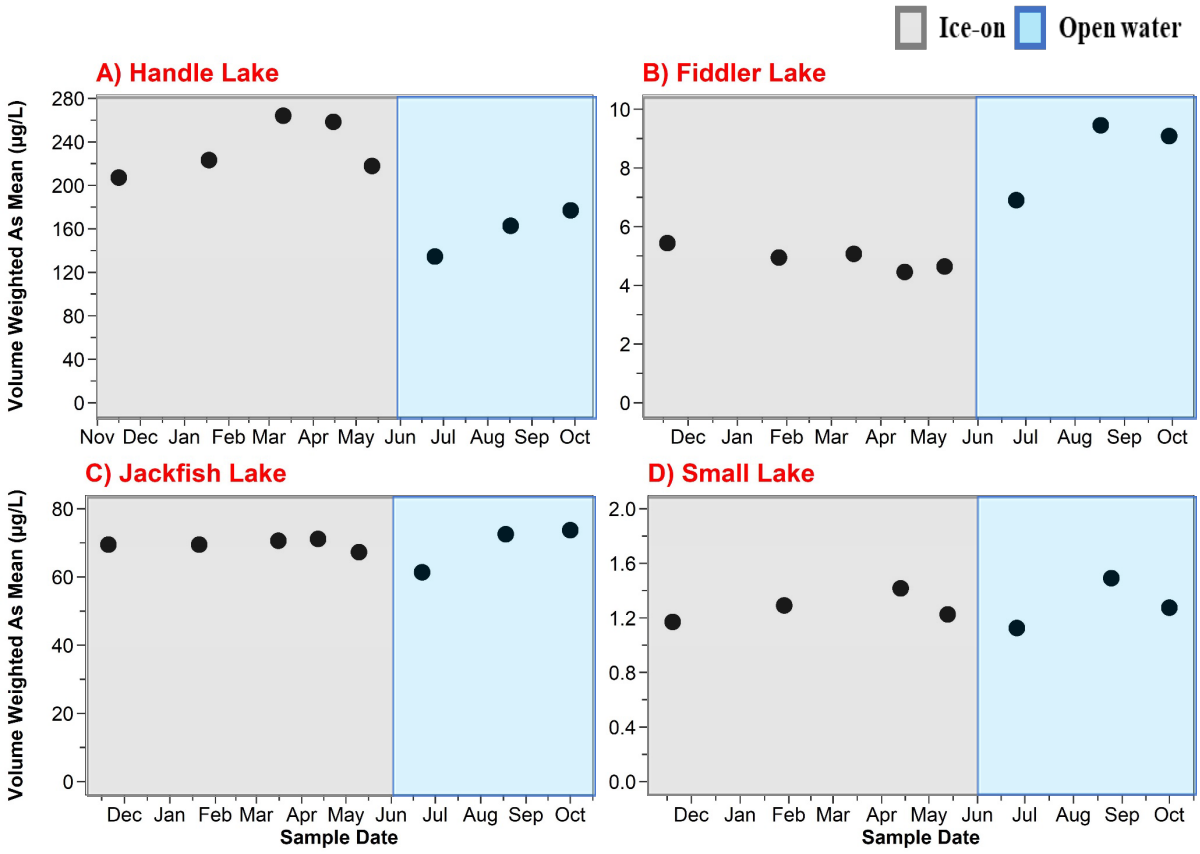

Figure 3.9 Volume weighted As mean for Handle Lake, Fiddler Lake, Jackfish Lake, and Small Lake during November 2020 to October 2021.

The highest concentrations of dissolved As were measured in Handle Lake (mean= 208.46 µg/L, max= 377 µg/L), followed by Jackfish Lake (mean= 69.28 µg/L, max= 74.8 µg/L), Fiddler Lake (mean= 6.35 µg/L, max= 11.8 µg/L), and Small Lake (mean= 1.43 µg/L, max= 5.8 µg/L) (Fig. 3.10). Each lake recorded its maximum As level in summer except for Handle Lake (Fig. 3.9 and 3.10).

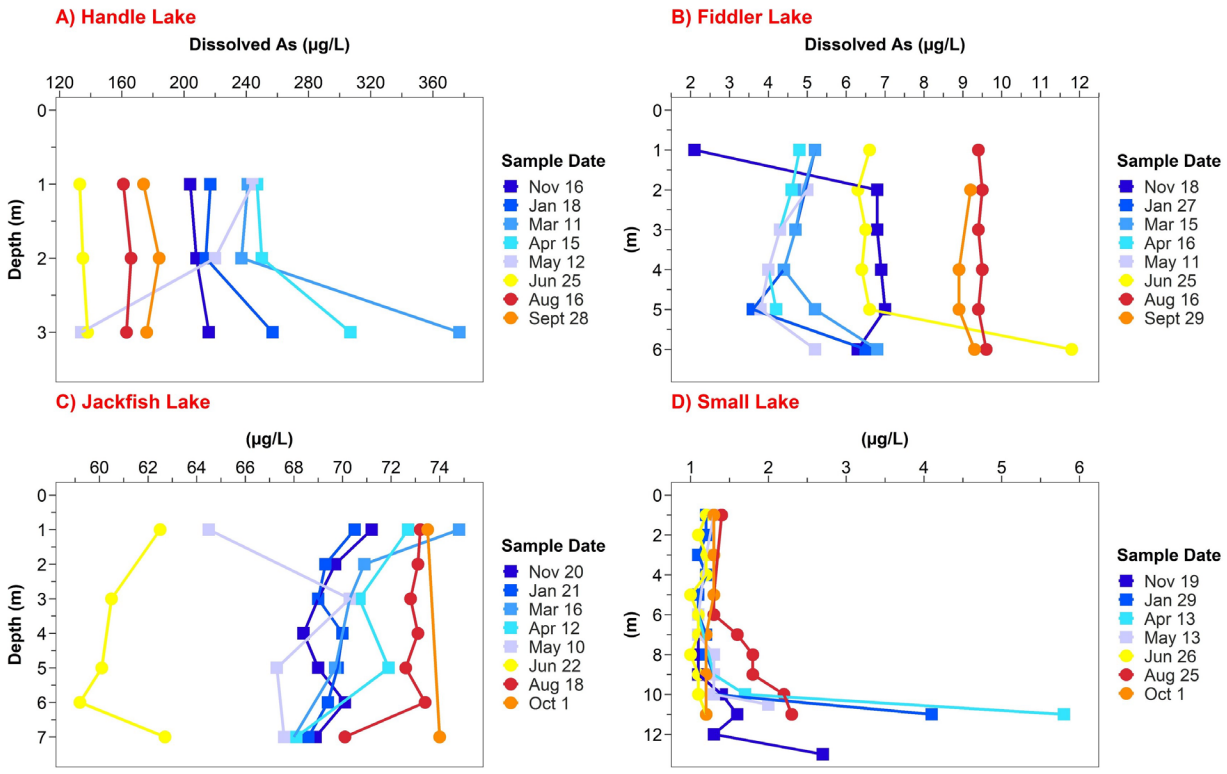

Figure 3.10 Dissolved (filtered < 0.45 µm) arsenic concentrations (µg/L) for Handle Lake, Fiddler Lake, Jackfish Lake, and Small Lake from November 2020 to October 2021. Squares = Ice-on, Circles= Ice-off. Detection level = 0.2 µg/L. Test method = EPA200.8

Most lakes shared a consistent pattern of enrichment of dissolved As concentration near the sediment water interface (SWI) primarily in the winter period, with exception of Jackfish Lake (Fig. 3.10). The volume weighted As mean for Handle Lake shows distinct seasonal patterns in lake water As (Fig. 3.9 A). Arsenic concentrations increased 25% over the ice-covered period (from 207 to 258 µg/L), decreased 62% (from 217 to 134 µg/L) during the spring ice-out period and subsequently increased again by 32% (from 134 to 177 µg/L) over the open-water season (Table 3.4).

Table 3.4 Percentage (%) change in volume weighted As mean for Handle Lake, Fiddler Lake, Jackfish Lake, and Small Lake over winter (Nov 2020-May 2021), spring ice off (May-June 2021), over summer (June-October 2021).

Volume Weighted % change of As			
Lake	***% change over winter***	***% change over spring ice-off***	***% change over summer***
Handle	25	-62	32
Fiddler	-18	49	32
Jackfish	2	-9	20
Small	21	-8	13

Water column profile sampling in Handle Lake showed vertical As gradients during the ice-on period, but not during the open-water season (Fig. 3.10 A). Dissolved As concentrations in Handle Lake were consistently enriched near the SWI during the ice-on period (November 2020 to April 2021) (Fig. 3.10 A). A maximum filtered As concentration of 377 µg/L in Handle Lake was measured near the SWI on March 11th (Fig. 3.10 A). An inverse vertical gradient in dissolved As was measured in Handle Lake during May, with As decreasing from approximately 240 µg/L near the water surface to 120 µg/L near the SWI (Fig. 3.10 A). Once the ice-cover disappeared in early June, there was a substantial decrease in dissolved As to 130 µg/L through the water column in Handle Lake (Fig. 3.9 A). Overall, dissolved As in Handle Lake's water column in the open-water period was lower than ice-covered period (Fig. 3.9 A). Water column As in Handle Lake was predominately in the dissolved phase (< 0.45 um) since particulate As (Fig. 3.11 A) only accounted for approximately 5% of total As in the water column over the sampling period. During the ice-off period (May-June) there was limited (mean= 3%) particulate fraction of As in Handle Lake (Fig. 3.11 A).

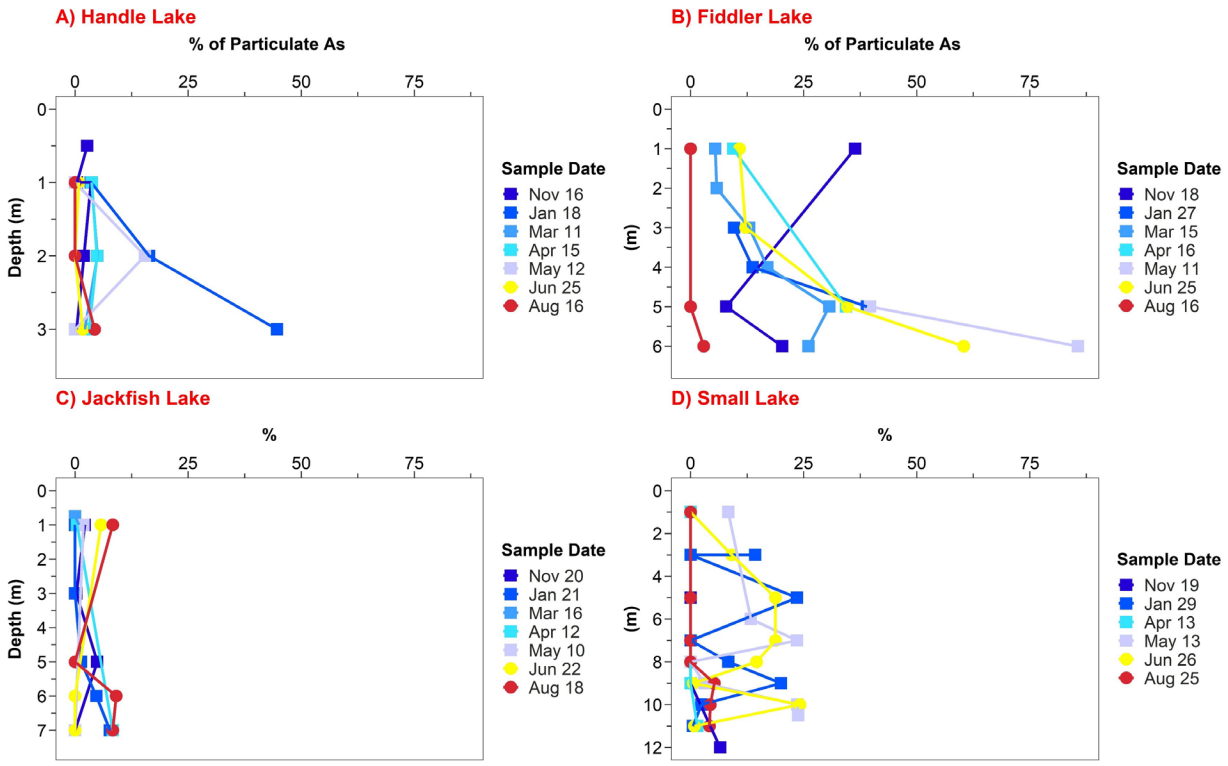

Figure 3.11 Percentage of particulate As for Handle Lake, Fiddler Lake, Jackfish Lake, and Small Lake during November 2020 to August 2021. Squares = Ice-on, Circles= Ice-off.

Concentrations of dissolved As in Fiddler Lake ($D_{Giant\ Mine}$= 8.6 km) were lower than the other lakes Handle ($D_{Giant\ Mine}$= 2.2 km) and Jackfish ($D_{Giant\ Mine}$= 4.2 km) within Yellowknife city limits (Fig. 3.10 B). During the ice-covered period, Fiddler Lake was the only study lake to measure a decrease (18%) in the volume weighted mean concentration of dissolved As from 5 µg/L to 4 µg/L (Fig. 3.9 B and Table 3.4). Fiddler Lake was also the only lake where an increase (49%) in dissolved As occurred after ice breakup in early June, from 4 µg/L to 7 µg/L and continued to rise by 32% over the duration of the open-water season (Fig. 3.9 B and Table 3.4). The water column profile of Fiddler Lake shown in Fig. 3.10 B showcases As enrichment observed near the SWI in both ice-on and ice-off periods, however, enrichment at the SWI was

less pronounced in the summer (Fig. 3.10 B). Water column As at Fiddler Lake was predominately in the dissolved phase (< 0.45 μm), but the percentage of particulate As measured in Fiddler Lake was higher than Jackfish and Handle Lake (Fig. 3.11) and was consistently around 22% of total As (Fig 3.12 B). Higher proportions of particulate As were consistently measured near the SWI in Fiddler Lake, especially during the sample visits on May 11th and June 25th (Fig. 3.11 B).

Jackfish Lake (7.5 m) is similar in maximum depth and bathymetry to Fiddler Lake (6.5 m), but As concentrations and patterns were considerably different between the lakes. Specifically, dissolved As varied little at Jackfish over winter compared to Fiddler and Handle lakes (Fig. 3.9 C). The volume weighted mean of As in Jackfish Lake displayed in Fig. 3.9 C exhibited relatively stable As concentrations (2% change) during the ice-on period (69 μg/L to 71 μg/L) (Table 3.4). A slight decrease of 9% in volume weighted mean of As was observe during the spring ice-off period at Jackfish Lake (67 μg/L to 61 μg/L) and was followed by a gradual increase (20%) over the rest of the open-water season (Table 3.4 and Fig. 3.9 C). Chemical profiles in the water column of Jackfish Lake shown in Fig. 3.10 C indicate there was little vertical variation in dissolved As throughout the water column. In comparison to the other study lakes, Jackfish Lake did not have a pronounced enrichment of dissolved As near the SWI (Fig. 3.10). The proportion of total As particulate was low in Jackfish Lake compared to the other study lakes (Fig. 3.11 C). During the sampling period an average of 3% of total As in the water column was associated with the particulate fraction (Fig. 3.11 C).

Concentrations of dissolved As in the water column of Small Lake were much lower (max= 5.8 μg/L) than the other study lakes (Fig. 3.10 D). In Small Lake there was much less

seasonal variation in volume weighted mean of As (Fig. 3.9 D and Table 3.4). Detailed profile sampling of dissolved As shown in Fig. 3.10 D of Small Lake highlights bottom water enrichment of As during summer and winter in association with hypolimnetic anoxia. Water column As at Small Lake was mainly in the dissolved phase (< 0.45 μm), as particulate As accounted for only approximately 8% of total As in the water column over the study (Fig. 3.11 D).

3.3.2 Iron (Fe) and Manganese (Mn)

3.3.2.1 Fe

The highest concentrations of dissolved Fe recorded by lake occurred as follows: Handle Lake (mean= 122.31 μg/L, max= 1600 μg/L), Small Lake (mean= 64.02 μg/L, max= 947 μg/L), Fiddler Lake (mean= 58.05 μg/L, max= 372 μg/L), and Jackfish Lake (mean= 31.33 μg/L, max= 124 μg/L). Collectively, all the study lakes had enrichment of dissolved Fe near the sediment boundary during at least one of the sampling visits, with Fiddler Lake and Small Lake being more common to have enrichment predominantly under ice-on-conditions (Fig. 3.12). Water column enrichment of dissolved Fe was observed through the ice-covered season in Handle Lake and Fiddler Lake (Fig. 3.12 and Fig. 3.13). Fe enrichment was more pronounced in the bottom waters of Fiddler Lake and in the anoxic hypolimnion of Small Lake during the ice-covered period (Fig. 3.12 and Fig. 3.6). Dissolved Fe concentrations were typically low in the open-water season through the upper water column of the study lakes, apart from Fiddler Lake (Fig. 3.12).

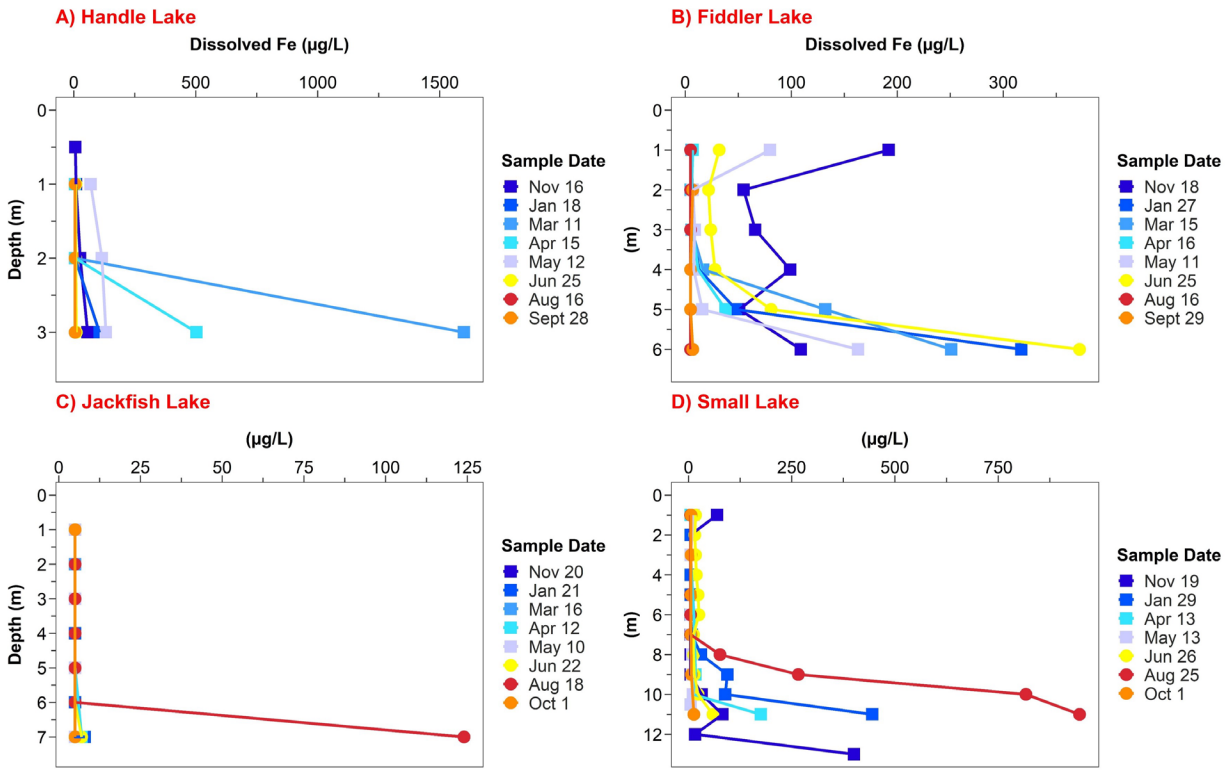

Figure 3.12 Dissolved iron concentrations (µg/L) for Handle Lake, Fiddler Lake, Jackfish Lake, and Small Lake during November 2020 to October 2021. Squares = Ice-on, Circles= Ice-off. Detection level = 5 µg/L. Test method = EPA200.8.

The volume weighted mean of Fe in Handle Lake displayed in (Fig. 3.13 A) shows a clear peak of Fe concentration of 288 µg/L in March and a significant increase in percentage change of 325% from (22 µg/L to 93 µg/L) over the ice-on period (Table 3.5). Dissolved Fe measured a slight increase in Handle Lake during the ice-on period can be associated with depletion of dissolved oxygen in the water column mid to late winter (Fig. 3.12 A, Table 3.5, and Fig. 3.6).

The volume weighted mean of Fe in Fiddler Lake displayed in (Fig. 3.13 B) shows peaks in Fe concentrations of 67 µg/L in May and 60 µg/L in June and a decrease in percentage change of 80% from (66 µg/L to 13 µg/L) over the ice-on period (Table 3.5)

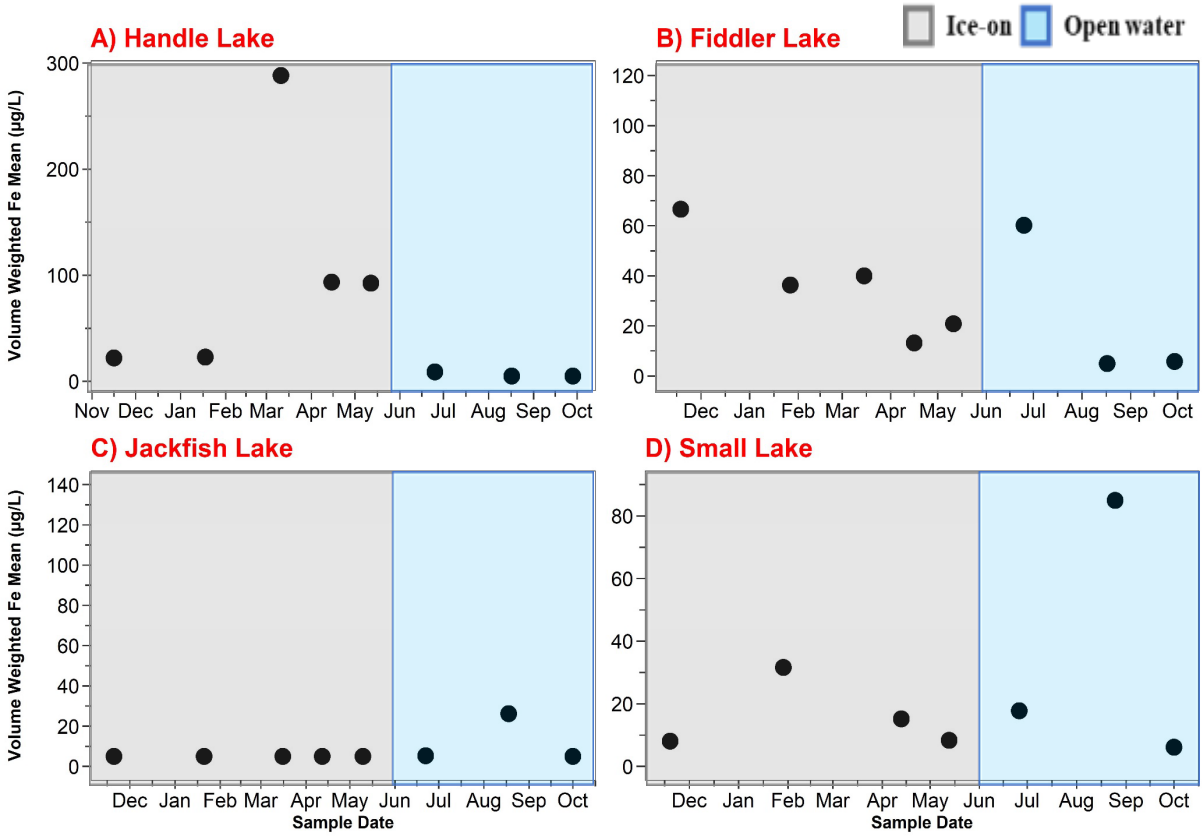

Figure 3.13 Volume weighted mean of Fe for Handle Lake, Fiddler Lake, Jackfish Lake, and Small Lake during November 2020 to October 2021.

Table 3.5 Volume weighted percentage (%) change of Fe for Handle Lake, Fiddler Lake, Jackfish Lake, and Small Lake over winter (Nov 2020-May 2021), spring ice off (May-June 2021), over summer (June-October 2021).

Volume Weighted % change of Fe			
Lake	***% change over winter***	***% change over spring ice-off***	***% change over summer***
Handle	325	-340	-44
Fiddler	-80	188	-90
Jackfish	0	7	-7
Small	88	114	-66

Over the spring ice-off period integrative mean Fe in Fiddler Lake saw a significant increase of 188% with concentrations decreasing 90% in the summer from (60 µg/L to 5 µg/L) (Table 3.5). Enrichment of Fe near the SWI was measured consistently during the under-ice sampling period, from 109 µg/L on November 18th to approximately 150 µg/L on May 11th (Fig. 3.12 B). The highest recorded dissolved Fe concentrations occurred on June 25th recently after ice breakup and ranged between 22 µg/L at the surface to 372 µg/L near the sediment boundary (Fig. 3.12 B). During the rest of the open-water season dissolved Fe concentrations were low and close to the analytical detection limit of 5 µg/L (Fig. 3.12 B). Particulate fraction of Fe in Fiddler Lake over the period of the study had a mean percentage of 69% (Table 3.6). The highest percentage of particulate Fe of 95% in Fiddler Lake occurred late in the open-water period (Table 3.6).

Dissolved Fe concentrations were higher through the water column in Fiddler Lake than most other study lakes (Fig. 3.12 B). Dissolved Fe concentrations were well above the method detection limit of 5 µg/L throughout Fiddler Lake's water column in November, but decreased for most of the winter (Fig. 3.12 B). Although, near the sediment boundary Fe enrichment was noted throughout the winter in Fiddler Lake (Fig. 3.12 B). Fiddler Lake's upper water column enrichment in dissolved Fe was noted again in June, with a subsequent decrease in dissolved Fe throughout the rest of the summer (Fig. 3.12 B). No bottom water enrichment in dissolved Fe was noted in Fiddler Lake during August or September in association with the well-mixed water column (Fig. 3.12 B and Fig. 3.2 B).

Table 3.6 Calculated mean, maximum, and minimum percentage (%) of particulate Fe for Handle Lake, Fiddler Lake, Jackfish Lake, and Small Lake during November 2020 to August 2021. *(0% particulate Fe = dissolved fraction exceeded total).

Lake	***Mean % of Particulate Fe***	***Max % of Particulate Fe***	***Min % of Particulate Fe***	***N***
Handle	58	83	0	22
Fiddler	69	95	2	24
Jackfish	38	81	0	23
Small	61	95	0	36

Dissolved Fe concentrations in Jackfish Lake were low throughout the study, except in a bottom water sample collected in August, which was likely associated with anoxia (<0.5 mg/L) near the sediment-water interface at 6.5 m deep (Fig. 3.6 and Fig. 3.12 C). Particulate fraction of Fe in Jackfish Lake over the period of the study had a mean percentage of 38% (Table 3.6). The highest percentage of particulate Fe of 81% in Jackfish Lake occurred late in the open-water period (Table 3.6).

Dissolved Fe concentrations were typically low in the epilimnion of Small Lake during the study (Fig. 3.12 D). Significant enrichment in dissolved Fe was observed in the hypolimnion during periods of summer and winter stratification (Fig. 3.12 D). Particulate fraction of Fe in Small Lake over the period of the study had a mean percentage of 61% (Table 3.6). The highest percentage of particulate Fe of 95% in Small Lake occurred late in the open-water period (Table 3.6).

3.3.2.2 Manganese

Dissolved Mn concentrations were low in the upper water column of all study lakes over the open-water season (Fig. 3.14). Mn enrichment (Fig. 3.15 A) was observed in Handle Lake over winter in association with the depletion of oxygen in the water column (Fig. 3.6 A). Further,

Mn enrichment corresponded with the enrichment of other redox sensitive elements of As and Fe (Fig. 3.10 A and Fig. 3.14 A). Mn enrichment was also measured in the bottom waters of most study lakes when stratified (Fig. 3.14 and Fig. 3.2). The Mn enrichment near the sediment water interface can be associated with As and Fe enrichment. Particulate Mn results from each of the study lakes is presented in Table 3.7. Results of the mean percentage of particulate Mn was the highest in Jackfish Lake at 75% followed by Small Lake (57%), Fiddler Lake (55%), and Handle Lake (46%) over the study period (Table 3.7).

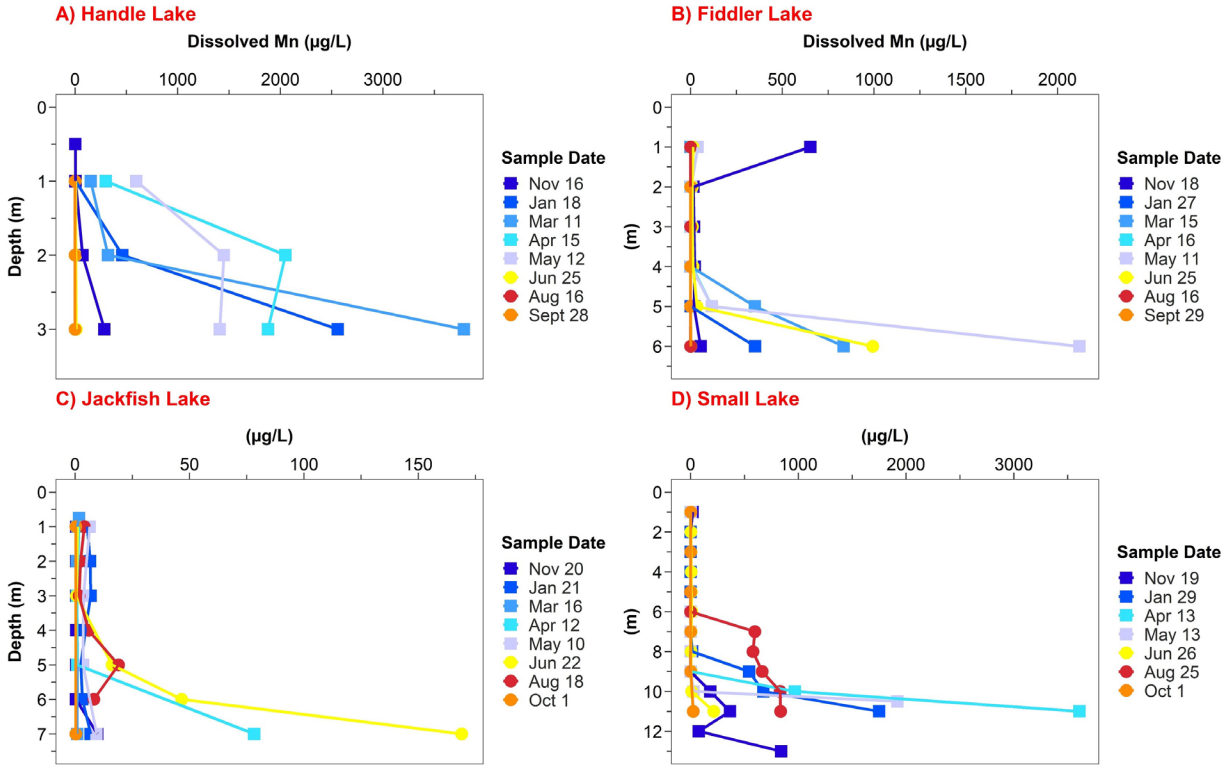

Figure 3.14 Dissolved manganese concentrations (µg/L) for Handle Lake, Fiddler Lake, Jackfish Lake, and Small Lake during November 2020 to October 2021. Squares = Ice-on, Circles= Ice-off. Detection level = 0.1 µg/L. Test method = EPA200.8

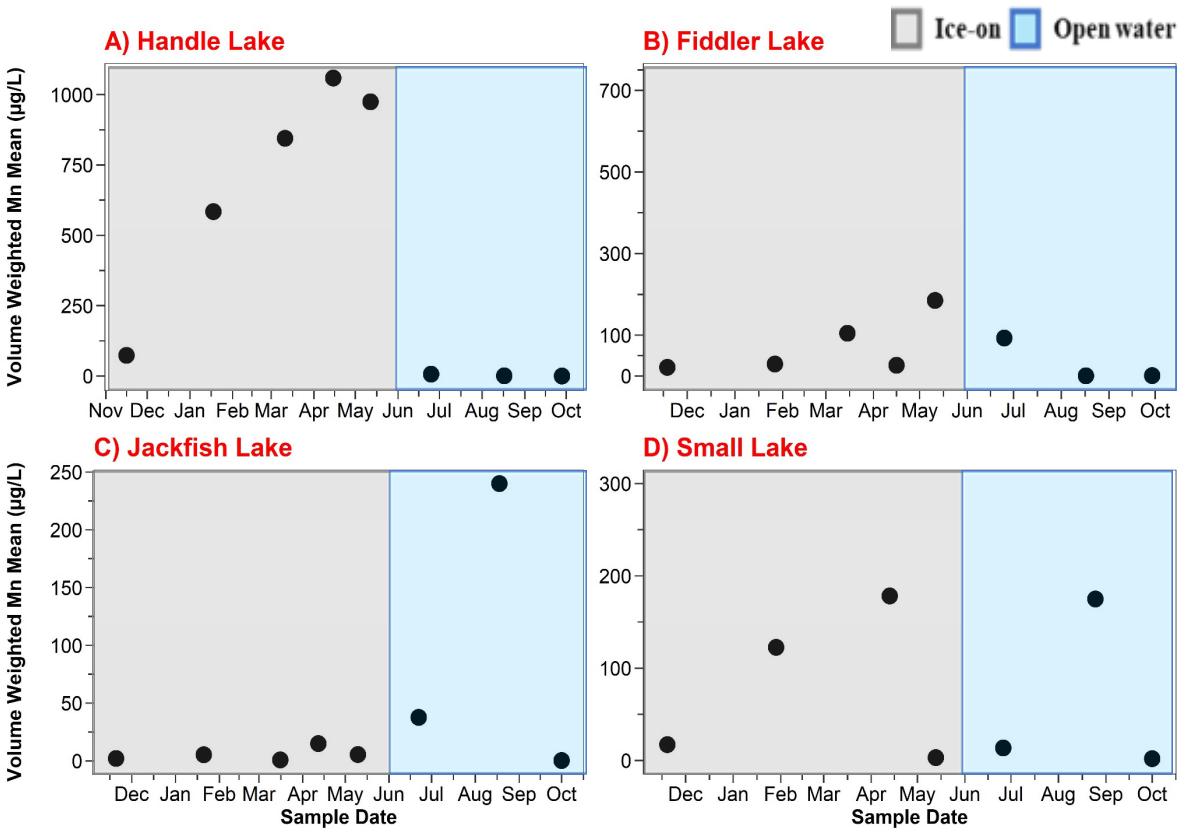

Figure 3.15 Volume weighted mean of Mn for Handle Lake, Fiddler Lake, Jackfish Lake, and Small Lake during November 2020 to October 2021.

Table 3.7 Calculated mean, maximum, and minimum of percentage (%) of particulate Mn for Handle Lake, Fiddler Lake, Jackfish Lake, and Small Lake during November 2020 to August 2021. *(0% particulate As = dissolved fraction exceeded total).

Lake	*Mean % of Particulate Mn*	*Max % of Particulate Mn*	*Min % of Particulate Mn*	*N*
Handle	46	99	0	24
Fiddler	55	99	0	22
Jackfish	75	98	0	21
Small	57	100	0	37

Collectively, increases in dissolved As, Fe, and Mn concentrations (Fig. 3.10, Fig. 3.12, and Fig. 3.14) in Handle Lake and the hypolimnion of the other lakes can be associated with

period of low dissolved oxygen levels (Fig. 3.6). Small Lake and Handle Lake showcased that the three metals of As, Fe, and Mn shared similar concentration trends in response to the timeframe periods (Fig. 3.10, Fig. 3.12, and Fig. 3.14). Specific takeaways from Handle Lake and Small Lake include metal concentration increases during ice-on and decrease in open-water period (Fig. 3.9, Fig. 3.12, and Fig. 3.15). In comparison, Fiddler Lake observed the opposite result of decrease in As concentration over the ice-on and increase in the open-water period, while Jackfish remained an outlier (Fig. 3.9, Fig. 3.12, and Fig. 3.15).

3.3.2.3 Fe & As Ratio

The ratio of Fe to As in filtered water samples was calculated for all sites to represent and explore seasonal ratio change between As and Fe as dissolved oxygen levels in the study lake changes. The ratio of volume weighted means of dissolved As to Fe was calculated and presented in Table. 3.8 and Fig. 3.16 below.

Table 3.8 Ratio of volume weighted mean of Fe:As (dissolved).

Sample Date	***Fe:As***
Handle	
2020-11-16	0.1
2021-01-18	0.1
2021-03-11	1.1
2021-04-15	0.4
2021-05-12	0.4
2021-06-25	0.1
2021-08-17	0.0
2021-09-28	0.0
Fiddler	
2020-11-18	12.3
2021-01-27	7.4
2021-03-15	7.9
2021-04-16	3.0

Sample Date	***Fe:As***
2021-05-11	4.5
2021-06-25	8.7
2021-08-17	0.5
2021-09-29	0.6
Jackfish	
2020-11-20	0.1
2021-01-21	0.1
2021-03-16	0.1
2021-04-12	0.1
2021-05-10	0.1
2021-06-22	0.1
2021-08-18	0.4
2021-10-01	0.1
Small	
2020-11-19	6.9
2021-01-29	24.5
2021-04-13	10.7
2021-05-13	6.8
2021-06-26	15.8
2021-08-25	57.0
2021-10-01	4.8

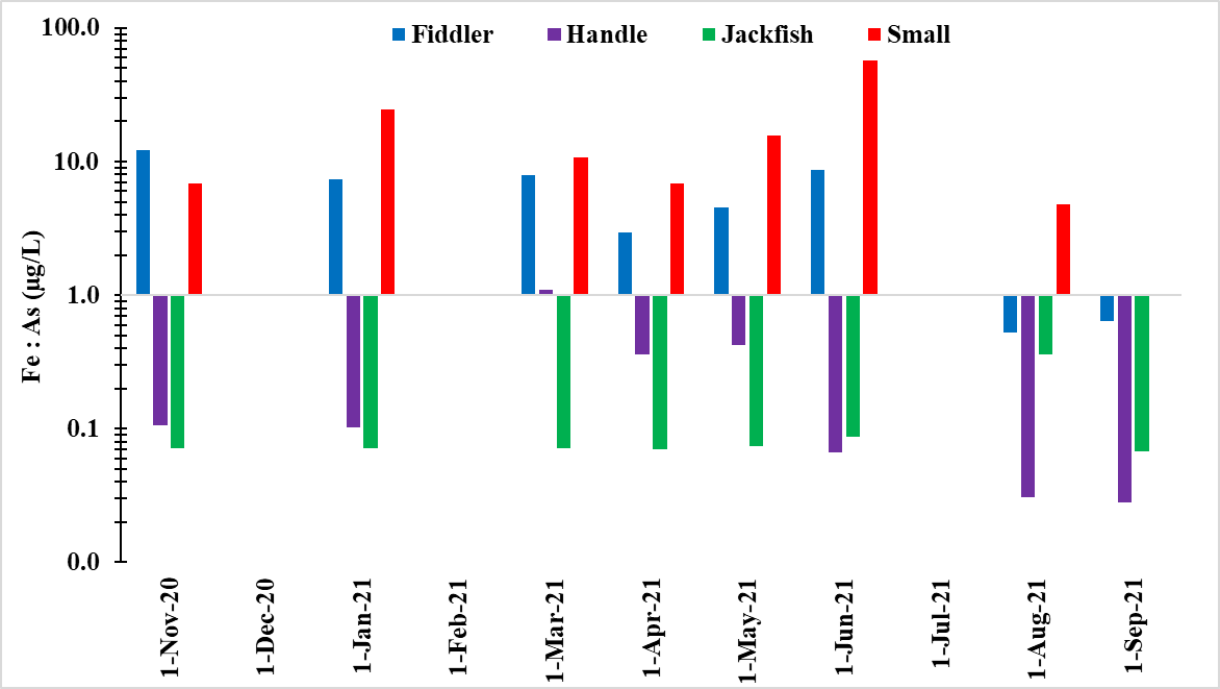

Figure 3.16 Ratio of volume weighted mean of Fe:As (dissolved) displayed on a based ten logarithmic scale through November 2020 to September 2021.

A distinct outcome emerged that both Fiddler Lake and Small Lake held the two highest Fe to As ratios among the study lakes (Fig. 3.16 and Table 3.8). This indicates that both Fiddler Lake and Small Lake have excess Fe relative to As concentrations in their lake waters. In comparison, Handle Lake and Jackfish Lake had very low Fe to As ratios, signaling a low proportion of Fe concentrations relative to excess As concentrations in the lakes (Fig. 3.16 and Table 3.8). The top ranked ratios of volume weighted mean of Fe to As shown in Table 3.9 highlights the highest ratios are mostly from Small Lake and the largest ratio from Small Lake occurred late in the open-water period.

Table 3.9 Ratio rank of the top 15 volume weighted mean of Fe:As from ranked from highest to lowest.

Rank	***Sample Date***	***Lake***	***Fe:As***
1	2021-08-25	Small	56.97
2	2021-01-29	Small	24.47
3	2021-06-26	Small	15.82
4	2020-11-18	Fiddler	12.25
5	2021-04-13	Small	10.71
6	2021-06-25	Fiddler	8.72
7	2021-03-15	Fiddler	7.89
8	2021-01-27	Fiddler	7.35
9	2020-11-19	Small	6.91
10	2021-05-13	Small	6.80
11	2021-10-01	Small	4.81
12	2021-05-11	Fiddler	4.50
13	2021-04-16	Fiddler	2.96
14	2021-03-11	Handle	1.09
15	2021-09-29	Fiddler	0.64

3.4 Sediment

3.4.1 Physical properties of sediments

3.4.1.1 Water content

Sediment water content of the lake sediment cores from the study sites is presented in Fig. 3.17 below.

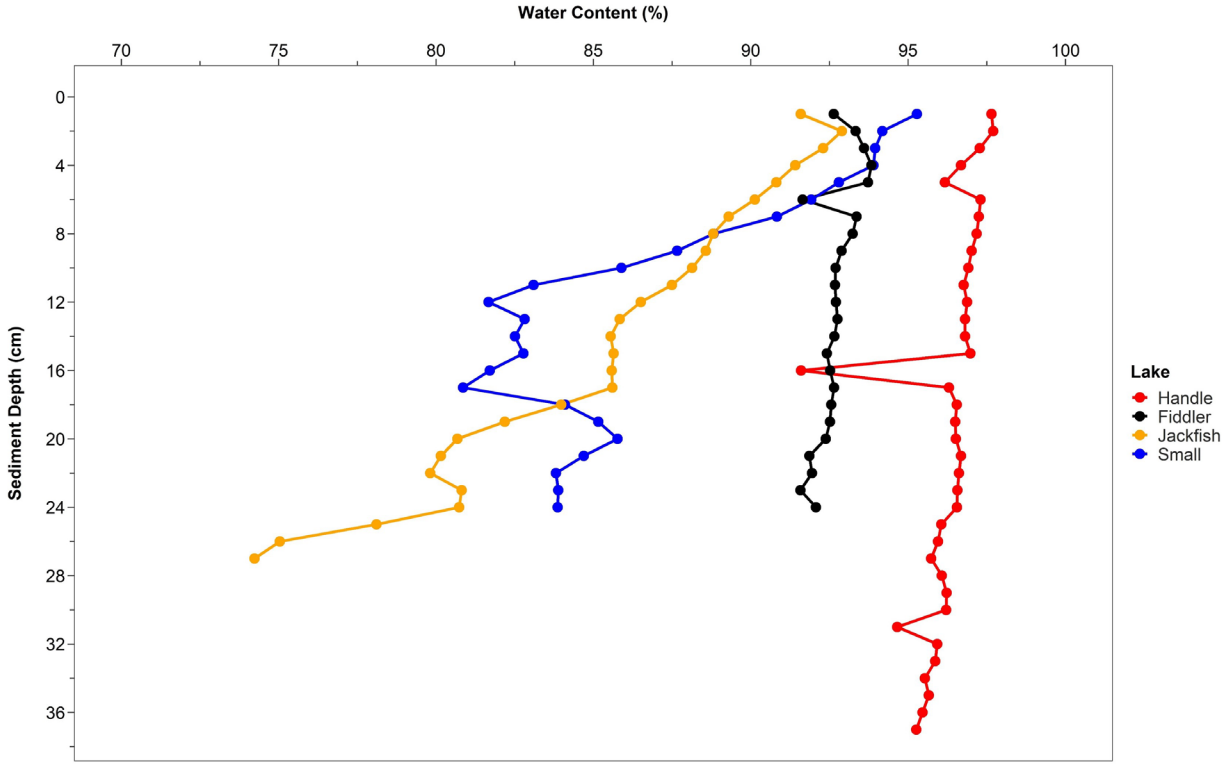

Figure 3.17 Percentage of water content in each sediment core from Handle Lake, Fiddler Lake, Jackfish Lake, and Small Lake.

Overall, Handle Lake (mean= 96%) had the highest water content among the collected sediment cores, followed by Fiddler Lake (mean= 92%), Small Lake (mean= 86%), and Jackfish Lake (mean= 85%). Furthermore, both Handle Lake and Fiddler Lake (Fig. 3.17 A and B) maintained relative consistent and high-water content through the sediment profile. Whereas, in Jackfish Lake and Small Lake both measured lower percentage of water content deeper in the sediment column with Jackfish Lake (min= 74%) and Small Lake (min= 81%) (Fig. 3.17 C and D).

3.4.1.2 Organic Matter from Loss on Ignition (LOI)

Percentage of organic matter (OM) from the loss on ignition results are presented in Fig. 3.18 and Table 3.10 for all the study lakes.

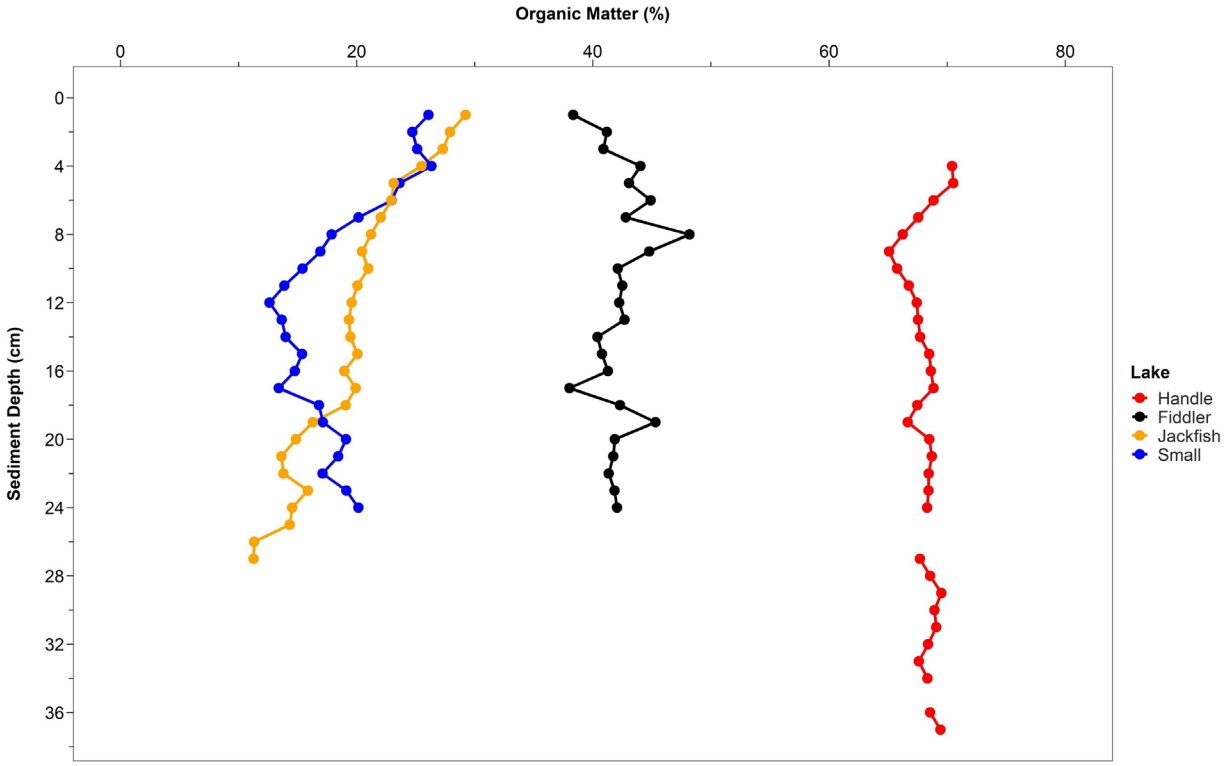

Figure 3.18 Percentage of organic matter in each sediment core at a 1 cm depth interval from Handle Lake, Fiddler Lake, Jackfish Lake, and Small Lake.

Table 3.10 Calculated mean, maximum, and minimum of percentage of organic matter in each sediment core at a 1 cm depth intervals and specifically the top 5 cm from Handle Lake, Fiddler Lake, Jackfish Lake, and Small Lake.

Sediment Organic Matter (%)				
Lake	***Mean (Top 5 cm)***	***Mean***	***Max***	***Min***
Handle	70	68	71	65
Fiddler	42	42	48	38
Jackfish	27	19	29	11
Small	25	19	26	13

Overall, Handle Lake (mean= 68%) had the most organic rich sediments, followed by Fiddler Lake (mean= 42%), Jackfish Lake (mean= 19%), and Small Lake (mean= 19%) (Table 3.10). Surficial enrichment of organic matter occurred in both Jackfish Lake (27%) and Small Lake (25%) (Table 3.10) with mean percentages in the top 5 cm of the sediment greater than the rest of their profile (Fig 3.18). In contrast, Fiddler Lake's sediment core (Fig. 3.18) maintained a relatively consistent percentage of organic matter (42%) with sediment depth (Table 3.10). The top 5 cm mean calculations presented in Table 3.10 above shows rich organic matter content in Handle Lake (70%).

3.4.2 Metal(loid)s

3.4.2.1 Arsenic

Sediment arsenic (As) concentrations from sectioned sediment cores for each study lake are presented in Fig. 3.19 below.

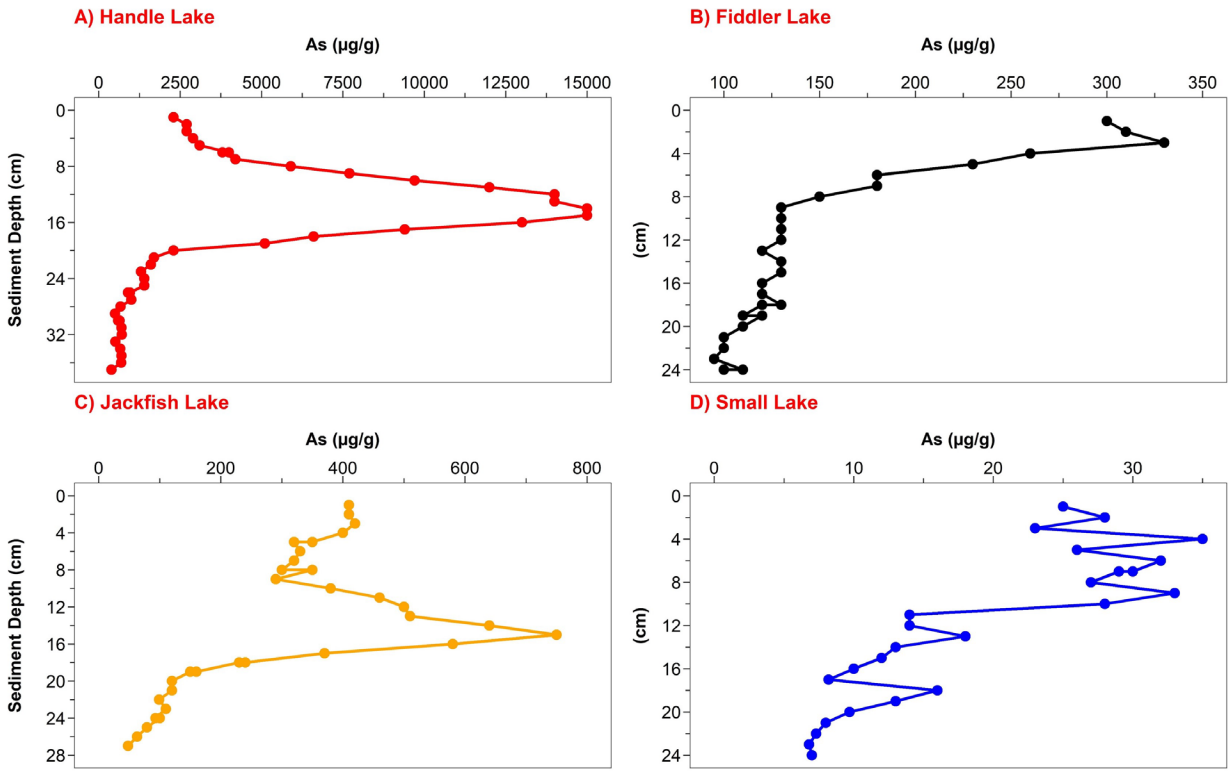

Figure 3.19 Sediment As profiles at 1 cm intervals from Handle Lake, Fiddler Lake, Jackfish Lake, and Small Lake (µg/g).

Mean sediment As concentrations for the top 10 cm of each core shown in Table 3.11 indicates the highest As concentration were in Handle Lake (mean = 4 455 µg/g; max = 15 000 µg/g), followed by Jackfish Lake (mean = 357 µg/g; max = 750 µg/g), Fiddler Lake (mean = 213 µg/g; max = 330 µg/g) and Small Lake (mean = 29 µg/g; max = 35 µg/g) (Fig. 3.19).

Table 3.11 Calculated mean arsenic (As), iron (Fe), manganese (Mn), and sulfur (S) concentration (µg/g) in each lake sediment core from the top 0 to 10 cm sectioned depth from Handle Lake, Fiddler Lake, Jackfish Lake, and Small Lake.

Mean Sediment (µg/g) (0 to 10 cm)				
Lake	***As***	***Fe***	***Mn***	***S***
Handle	4 455	13 818	656	20 909
Fiddler	213	49 333	513	9 692
Jackfish	357	19 583	423	6 358
Small	29	27 545	563	5 473

Significant enrichment of As (15 000 µg/g) occurred through the 12-15 cm intervals in Handle Lake and decreased to approximately 390 µg/g at the deepest sediment interval of the core of 37 cm deep (Fig. 3.19 A). A sediment As maxima was also recorded at depth in Jackfish Lake at 15 cm (750 µg/g) (Fig. 3.19 B). In Jackfish Lake's sediment profile, there was a slight decrease from 410 µg/g at the surface to 290 µg/g at 9 cm, before increasing towards the As maxima at 15 cm (Fig. 3.19 C).

Sediment As concentrations in Fiddler Lake (Fig. 3.19 B) were the highest near the sediment-water interface 330 µg/g and decreased with depth to approximately 100 µg/g at the base of the sediment core (Fig. 3.19 B).

Finally, sediment As concentrations in the top 10 cm of sediment in Small Lake (Fig. 3.19 D) were relatively low (mean= 29 µg/g) in comparison to the other study lakes (Table 3.11). In addition, Small Lake's sediment profile measured higher concentrations 35 µg/g at 4 cm in the upper sediments before a steady decline from 28 µg/g at 10 cm to 7 µg/g at 24 cm (Fig. 3.19 D).

3.4.2.2 Iron

Iron (Fe) concentrations from sectioned sediment cores for each study lake are outlined in Fig. 3.20 with accompanying summary statistics shown in Table 3.11.

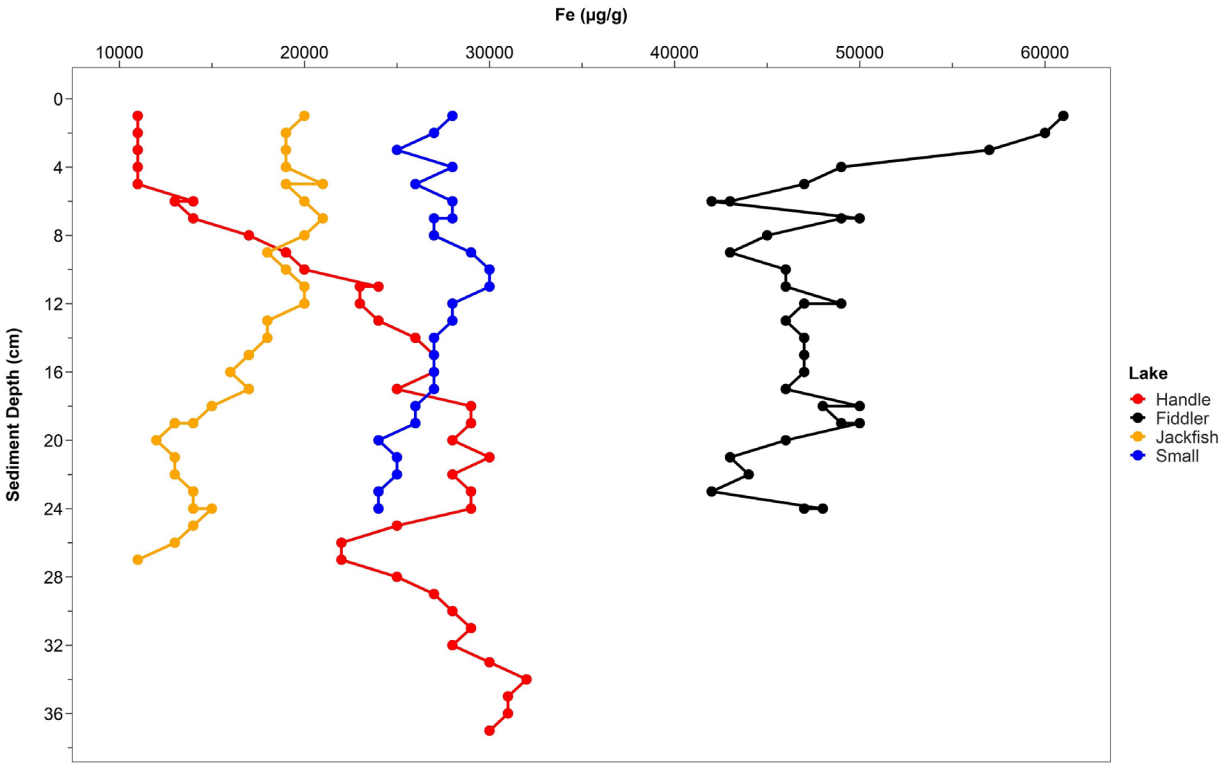

Figure 3.20 Sediment profile plots of the cross-comparison of Handle Lake, Fiddler Lake, Jackfish Lake, and Small Lake examining sediment iron (Fe) concentration (µg/g) at 1 cm depth intervals.

Sediment Fe concentrations were highest in Fiddler Lake with a mean of 49 333 µg/g and a maximum level of 61 000 µg/g, followed by Small Lake (mean= 27 545 µg/g), Jackfish Lake (mean= 19 583 µg/g), and Handle Lake (mean= 13 818 µg/g) (Table 3.11).

Sedimentary Fe levels increased with depth in Handle Lake, as the maximum Fe concentration was measured at 34 cm deep (Fig. 3.20). In contrast, sediment Fe concentrations decreased with depth in the other three lakes (Fig. 3.20). Surficial Fe enrichment was most

pronounced in the Fiddler Lake sediment core with a maximum concentration of 61 000 µg/g recorded (Fig. 3.20). Sediment Fe concentrations in Fiddler Lake subsequently declined until 6 cm sediment depth before varying slightly in depth to the base of the sediment core at 24 cm (Fig. 3.20). Fe concentrations in Jackfish Lake (Fig. 3.20) showed a consistent concentration around 20 000 µg/g for much of the sediment profile. Sedimentary Fe concentration in Small Lake's sediment profile (Fig. 3.20) was consistent around 26 000 µg/g, with slight increase to 30 000 µg/g at 10 to 11 cm. Both sedimentary Fe profiles for Small Lake and Jackfish Lake had little variation with depth.

3.4.2.3 Manganese

Sediment manganese (Mn) concentrations from sectioned sediment cores for each study lake are presented in Fig. 3.21 with mean concentration shown in Table 3.11.

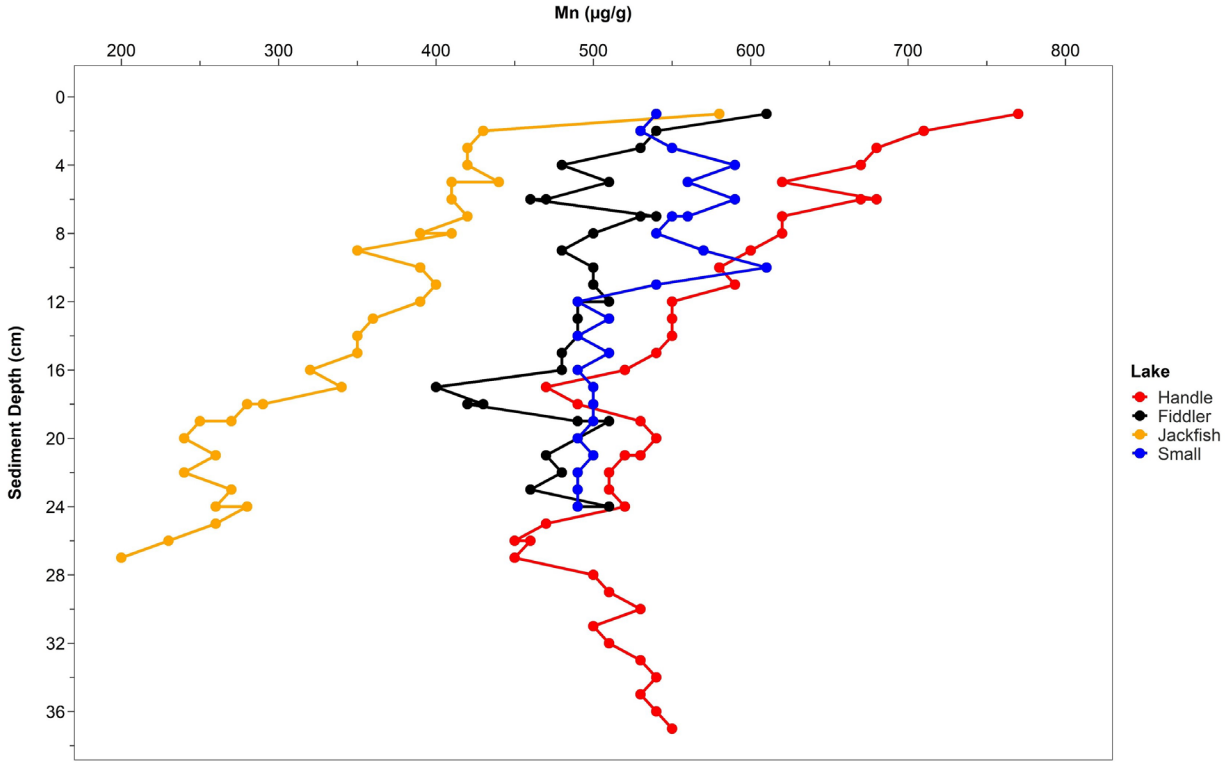

Figure 3.21 Sediment profile plots of the cross comparison of Handle Lake, Fiddler Lake, Jackfish Lake, and Small Lake examining manganese (Mn) concentration (µg/g) at 1 cm depth intervals.

In summary, sedimentary Mn was highest in Handle Lake (mean = 656 µg/g; max = 770 µg/g), followed by Small Lake (mean= 563 µg/g), Fiddler Lake (mean= 513 µg/g) and Jackfish Lake (mean= 423 µg/g) (Table 3.11). Sedimentary Mn concentrations in Handle Lake, Fiddler Lake, and Jackfish Lake were highest in the upper part of the core and declined with depth (Fig. 3.21). There was less vertical variation in sediment Mn concentrations in Small Lake's core compared to the other three study lakes (Fig. 3.21).

3.4.2.4 Sulfur

Sediment sulfur (S) concentrations from each study lake are presented in Fig 3.22 and Table 3.11.

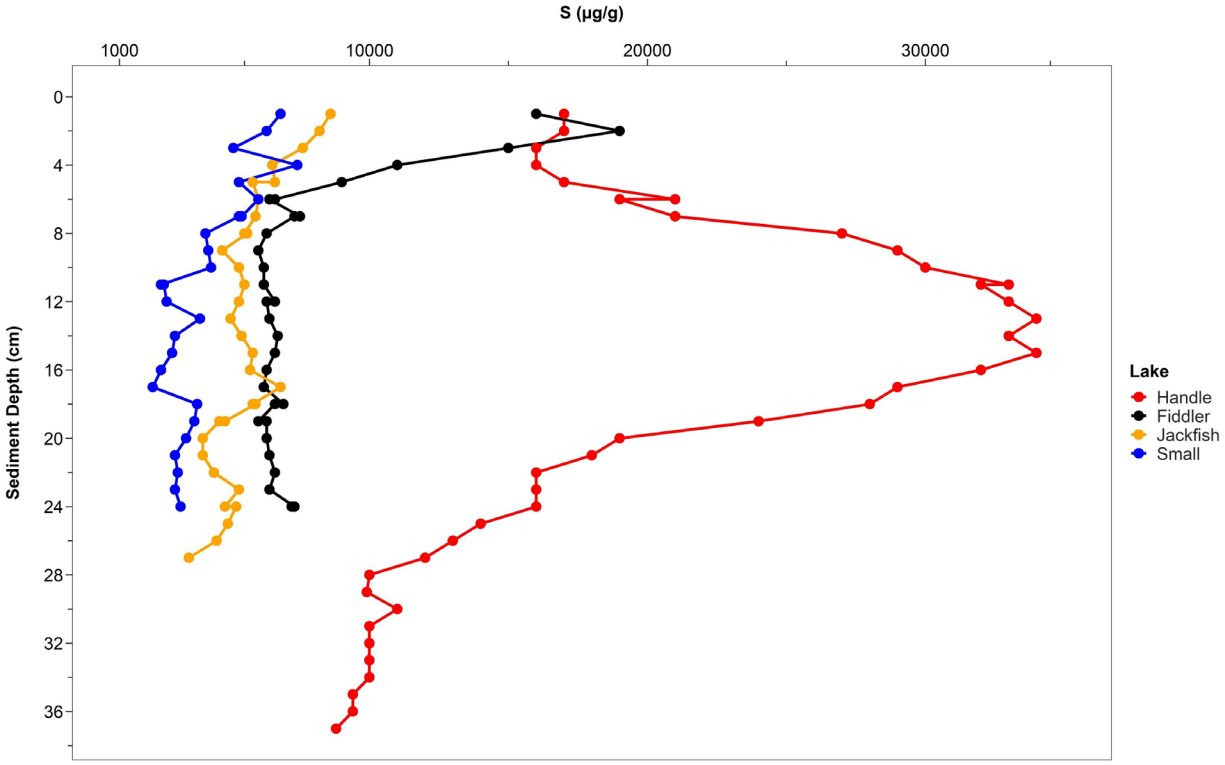

Figure 3.22 Sediment profile plots of the cross comparison of Handle Lake, Fiddler Lake, Jackfish Lake, and Small Lake examining sulfur (S) concentration (µg/g).

Mean sediment S concentrations in the top 10 cm of each core were the highest in Handle Lake (mean = 20 909 µg/g; max = 34 000 µg/g), followed by, Fiddler Lake (mean = 9 692 µg/g; max = 19 000 µg/g), Jackfish Lake (mean = 6 358 µg/g; max = 8 600 µg/g), and Small Lake (mean = 5 473 µg/g; max = 7 400 µg/g) (Table 3.11). Sedimentary S concentrations generally decreased with depth in the study lake sediment core except for Handle Lake (Fig. 3.22).

Maximum S sediment concentration in Handle Lake appear to be coincided with maximum As sediment concentrations at approximately 15 cm (Fig. 3.23 and Fig. 3.24).

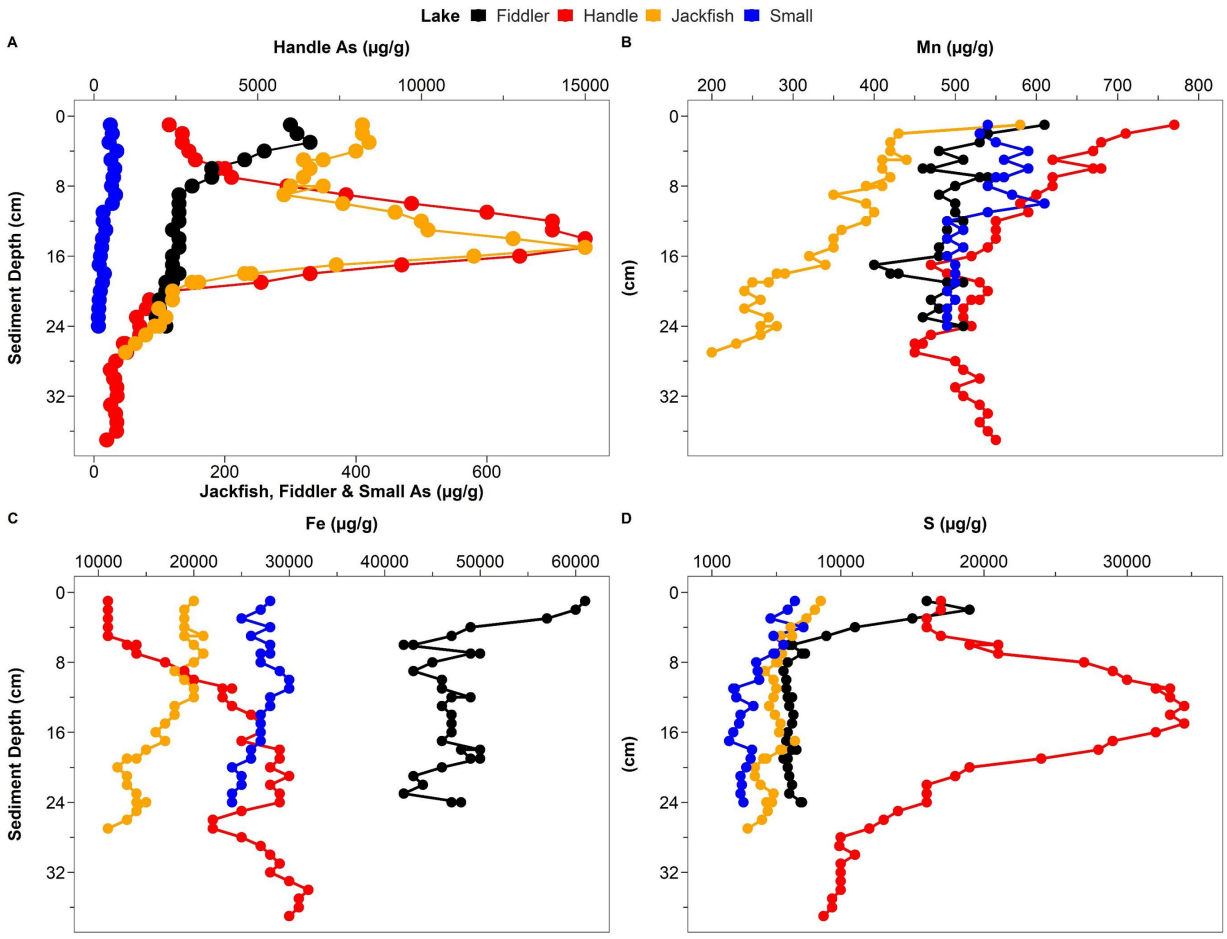

Figure 3.23 Elemental analysis (As, Mn, Fe, S) from sediment core profile of Handle Lake, Fiddler Lake, Jackfish Lake, and Small Lake.

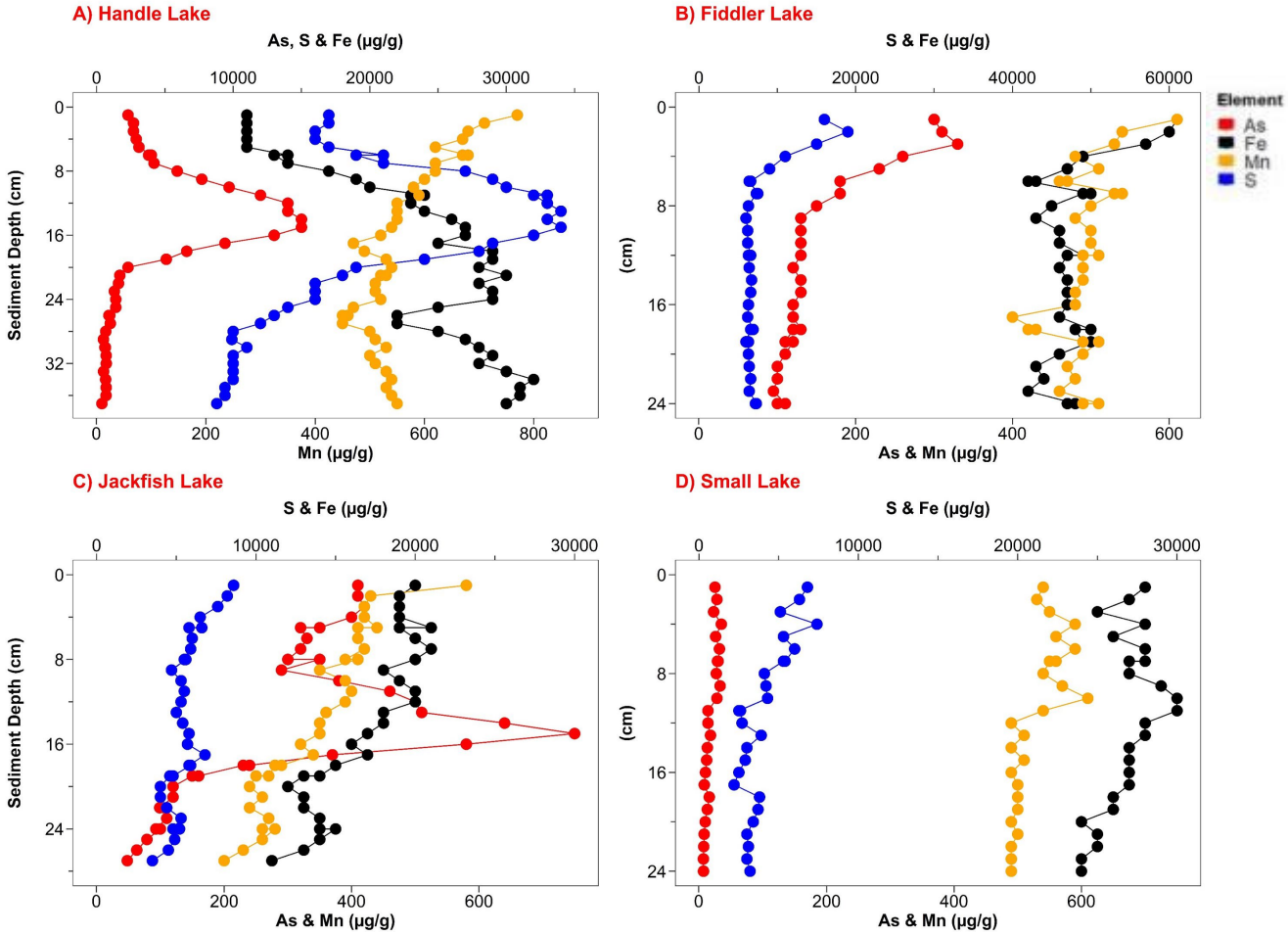

Figure 3.24 Elemental analysis (As, Mn, Fe, S) from sediment core profile of Handle Lake, Fiddler Lake, Jackfish Lake, and Small Lake.

4. Chapter 4: Discussion

This study investigated how winter can influence As cycling in small subarctic lakes near Yellowknife, NT, Canada, by examining seasonal changes of As concentration profiles under the ice in subarctic shield lakes. Arsenic concentrations in a series of lakes with different basin morphologies were compared to examine seasonal changes in As cycling. Substantial variation in surface water As highlighted the importance of seasonality in all study lakes (Fig. 3.9 and

Table 3.4). Each study lake manifested distinct results based on its physical characteristics and processes (Fig. 3.1 and Fig. 3.10). Further, we observed that differences in lake mixing regimes among lakes was more important than differences in morphometric properties in driving differences in As concentrations among small subarctic lakes (Fig. 3.2 and Fig. 3.10). Evidence of SWI As enrichment was frequently measured in the study lakes, particularly during winter, when lake circulation was limited due to the presence of an ice-cover (Fig. 3.10). During ice-on conditions oxygen depletion generating reducing condition within a lake is the key driver in enrichment of As especially near the SWI. Thus, the position of an oxic/anoxic boundary shaped redox conditions in each lake influencing As enrichment at the SWI and in the lower lake water column (Fig. 3.10, Fig. 3.1, and Fig. 3,7). These findings and observations from this study can collectively contribute to furthering the knowledge of seasonal differences in As mobility in small lakes.

4.1 Significant seasonal variation of As concentration in small subarctic lakes between ice-covered and open-water conditions.

The field data indicated that seasonality, accentuated by development of annual ice-cover, drives the As variability in these small subarctic lakes (Fig. 3.9 and Table 3.4). During the ice-cover period, lake sediments in both Handle Lake and Small Lake were a source of As to overlying waters, as demonstrated by the frequent measurement of As enrichment near the SWI (Fig. 3.10 and Fig. 3.19). In comparison, there was little indication that the lake sediments supplied As to overlying waters under-ice in Fiddler Lake and Jackfish Lake (Fig. 3.10 and Fig. 3.19).

4.1.1 Ice-on

The development of lake ice on the study lakes profoundly influenced lake water As and associated redox elements Fe and Mn concentrations, which is presented in section 3.3. Results showed increased As concentrations under ice-covered conditions, especially for Handle Lake. The greatest increase occurred in Handle Lake by 25%, followed by Small Lake (21%) and Jackfish Lake (2%), respectively (Table 3.4). In contrast, As concentrations in the water column of Fiddler Lake decreased by 18% over the winter (Table 3.4). The progressive depletion of DO concentration in the water column from the onset of ice development throughout winter was observed in most study lakes, except in Jackfish Lake (Fig. 3.6). The limited supply of DO in the study lakes can be explained mainly due to the presence of ice, which effectively prevents the free exchange of oxygen between the atmosphere and lake waters (Duthie, 1979). Moreover, these lakes are largely hydrologically disconnected and likely do not receive continuous inflow and outflow of water bringing an exchange of DO (Fig. 3.6, Fig. 3.7, and Fig. 3.8), therefore consumption of dissolved oxygen via sediment processes depleted DO levels within the water column of the study lakes.

Depleted DO supply eventually led to the development of anoxia through the water column in the shallowest lake (Handle Lake) and the bottom waters of the deepest lake (Small Lake) (Fig. 3.6 A and D). Handle Lake, specifically, observed no oxic boundary due to fully anoxic conditions through the water column (Fig. 3.6 A). Hypolimnetic anoxia can enable more upward diffusion of As in the water column from the bottom waters, in addition to anoxic conditions in the lake sediment (Fig. 3.10 and Fig. 3.6) (Hollibaugh *et al.*, 2005; Spliethoff *et al.,* 1995). This upward diffusion of As into the water column corresponded with the onset of

reducing conditions (Fig. 3.6 and Fig. 3.10) (Deshpande *et al.,* 2015; Mathias & Barica, 1980). These findings are consistent with a study by Palmer *et al.* (2019), where they also found increases in As concentrations in the lake waters to be connected to the onset of anoxia in the water column of shallow lakes.

Lake ice formation leads to cryoconcentration of lake water solutes through the exclusion of solutes in the ice (Bergmann & Welch, 1985; Belzile *et al.*, 2002; Deshpande *et al.*, 2015). In shallow lakes, this can affect the concentration of solutes, such as As, in the underlying water, which could be linked to why As enrichment was more pronounced in Handle Lake (Fig. 3.10 A, Fig. 3.2, and Table 1.1) (Bergmann & Welch, 1985; Belzile et al., 2002; Deshpande et al., 2015). Evidence from Palmer *et al.* (2019) study also found solute exclusion during the development of lake ice to be linked to increases in surface water As concentrations during the early winter period. This could partially explain the differences in As concentration between shallower and deeper lakes in the study, aside from the obvious geographic factor of lake proximity to historical mining operations (Fig. 3.2 and Table 1.1).

4.1.2 Open-water

The freshet transition from ice-cover to open-water during May to June showed a rapid decrease in volume weighted mean of As in most study lakes, except in Fiddler Lake (Fig. 3.9 and Table 3.4). Results from Fiddler Lake showed an increase of As concentration by 49% (Table 3.4). The greatest decrease occurred in Handle Lake by 62% (Table 3.4), followed by Jackfish Lake (9%) and Small (8%) Lake, respectively. This sudden decrease in As concentrations in Handle Lake during the freshet period can largely be attributed to the re-

oxygenation and dilution of the water column from the influx of DO and during meltwater incursion (Fig. 3.9 and Fig. 3.6) (Joung *et al.,* 2017; Palmer *et al.,* 2019; Schroth *et al.,* 2017). Increased oxygen production from benthic microbial mats may also drive spring increases in lake water DO prior to the onset of snowmelt (Bertilsson *et al.,* 2013; Joung *et al.,* 2017; Nelligan *et al.,* 2019; Palmer *et al.,* 2020). Photosynthesis from microbial activity and algae production in the lake would be triggered by improved light conditions in the water column with the melt of overlying snow and ice cover, as well the longer daylight hours during spring (Leppäranta, 2014; Joung *et al.,* 2017).

The timing and influx of meltwater into the lakes can be reflected in the data of specific conductivity and DO, as shown in Fig. A.1.1 and Fig. 3.6. Specific conductivity levels in each lake clearly showed a significant reduction from dilution in the spring melt period between May and June (Fig. A.1.1). DO concentrations rapidly reoxygenated throughout the water column after the ice-off field visit in June (Fig. 3.6). Particulate As was observed to be the more prevalent fraction in the open-water and transitional freshet period versus under the ice (Fig. 3.11). This is also shown in the study by Palmer *et al.* (2020), which was related to Fe (oxy)hydroxide minerals and As particle adsorption (Belzile & Tessier 1990; Root *et al.,* 2007).

After As concentration dropped during the freshet period in the spring, As concentrations typically began to increase in the water column of all the lakes over the open-water period (Fig. 3.9 and Fig. 3.10). The concentration of As continued to increase during the open-water period to a point where the maximum As concentrations were observed in most lakes, except in Handle Lake (Fig. 3.9 and Fig. 3.10). Factors likely driving As concentration increases in the water column during the open-water period could be associated with the processes of thinning of the

oxic boundary within the lake sediment, increased microbial activity, and evapoconcentration (Barrett *et al.,* 2019; Gibson *et al.,* 1998; Nelligan *et al.,* 2019; Schuh *et al.,* 2019; Spence, 2006; Van Den Berghe *et al.,* 2018).

During the open-water period, warming of the lake sediment can increase As released into the bottom waters (Barrett *et al.,* 2019; Nelligan *et al.,* 2019). The increased sediment temperatures in open-water conditions can facilitate heightened microbial respiration activity, which could be linked to the dissimilatory reduction of Fe oxides and organic carbon oxidation, causing As to be released into the overlying waters (Barrett *et al.,* 2019).

Handle Lake's shallow depth (Z_{max} = 3.5 m) causes it to be a well-mixed and susceptible to heating up quickly, indicative of the observed isothermal conditions in the summer (Fig. 3.2 A), which can enhance evapoconcentration. Loss of water via evapoconcentration has been reported in the literature on low-volume lakes like Handle Lake (Table 3.1) (Gibson *et al.,* 1998; Spence, 2006). Evaporation of water leading to less water volume in a lake can increase solute concentration, thus, facilitating increasing As concentrations among other elements (Fig. 3.2 and Table 3.1) (Gibson *et al.,* 1998; Spence, 2006). The hydrological balance between precipitation input into the study lakes and the rate of evaporation and loss of water volume could be a suggestive component toward a better understanding of As concentration variations (Palmer *et al.,* 2019; Gibson *et al.,* 1998; Spence, 2006).

During the open-water period, As concentrations were typically lower overall in the water column of deeper study lakes (Fig. 3.9 and Fig. 3.10). The lower As concentrations could be related to the co-precipitation and sorption reactions of As onto Fe (III) ferric oxides particles and settling out of the water column into the sediment (Aggett & O'Brien, 1985; Martin &

Pedersen, 2002; Kneebone *et al.,* 2002; Root *et al.,* 2007; Couture *et al.,* 2010). This was shown in an equivalent case in a study by Barrett *et al.* (2019), where As concentrations were lower in oxic waters and was found to be related to the sorption of As onto particles settling into sediments (Dixit & Hering 2003; Tufano & Fendorf, 2008; Vitre *et al.,* 1991). The particle reactivity of As, specifically arsenate As(V), is well known in the literature and a widely accepted process behind As being scavenged from the water column by Fe (oxy)hydroxides under oxic conditions (Smedley & Kinniburgh, 2002; Kneebone *et al.,* 2002; Root *et al.,* 2007).

4.2 Lake mixing regime regulates the position of redox boundaries within the water column and controls As cycling.

This section shows that lake mixing regime classification was found to be a more pivotal factor than morphometric properties in driving changes in As concentrations. Key differences in As concentrations amongst different lake mixing regimes was observed throughout the study (Fig. 3.10). In this study, we found that hypolimnetic enrichment of As was observed in dimictic versus polymictic lakes (Fig. 3.10). Lake stratification in the lakes dictated the redox boundary position within the water column and regulated As mobility (Fig. 3.2 and Fig. 3.10). Thermal stratification of the lakes largely isolated the enrichment of As in the bottom waters (Fig. 3.2 and Fig. 3.10). There was varied implications for each lake mixing regime driven by redox gradients and hypolimnetic enrichment in the lakes (Fig. 3.2 and Fig. 3.10).

4.2.1 Lake Mixing Regime

Small Lake can be classified as a dimictic lake mixing regime, where stratification is established once in winter and again in the summer, with mixing occurring in spring and fall

(Fig. 3.2 D). Small Lake was thermally stratified for most of the open-water period and resulted in bottom water enrichment of both As and Fe (Fig. 3.2 D, Fig. 3.10 D, and Fig. 3.12 D). Barrett *et al.* (2019) also found As enrichment to be linked to anaerobic hypolimnetic water during stratification in the open-water period (Aggett & O'Brien 1985; Azcue & Nriagu 1995; Senn *et al.,* 2007; Barringer *et al.,* 2011). This finding is consistent with Sprague and Vermaire (2018) study in Cobalt, ON, where thermal stratification of their lakes had an influence on the mobility of As in the water column. Two periods of hypolimnetic anoxia occurred in Small Lake and the area expanded in depth from the June to August sample period (Fig. 3.2 D and Fig. 3.6 D). The redox gradient thus moved higher up in the water column of Small Lake over the course of the open-water period (Fig. 3.2 D and Fig. 3.6 D). This observation aligns with Aggett and Kriegman (1988) study, where it was noted that the duration of the stratification period is central for the extent of As concentration in lake waters.

In contrast, Handle Lake and Fiddler Lake would be classified as cold-polymictic lakes that do not stratify and are well mixed throughout the open-water season. This was evident in the frequent or consistent occurrence of isothermal and isochemical conditions (Fig. 3.2 A and B). However, these cold polymictic lakes showed much different patterns of As concentrations due to differences in lake depth and oxygen depletion in the water column (Fig. 3.1, Fig 3.7, and Fig. 3.10). Handle Lake had a large amount of variation in As concentrations due to being a shallow and low volume lake, which lead to rapid DO depletion in the winter and quicker sediment warming in the summer enabling diffusion of As from the lake sediments (Fig. 3.1 A, Fig 3.7 A, and Fig. 3.10 A). In comparison to Fiddler Lake, As conditions did not change as much due to being a higher volume lake (Fig. 3.1 B, Table 3.1, and Fig. 3.10 B). Barrett *et al.* (2019) also

studied As in shallow polymictic lakes in a temperate region. The polymictic lake reported in Barrett *et al.* (2019) never stratified and was slower to recover from elevated As concentrations. However, our study presents new information based on what Barrett *et al.* (2019) findings proposed. Our study showcases supportive evidence that water depth and volume are also important secondary factors in addition to polymictic mixing regime in regulating As concentrations (Fig. 3.1, Fig 3.7, Table 3.1, and Fig. 3.10).

Jackfish Lake stratifies intermittently during the open-water season, depending on air temperature and wind speeds in the region (Fig. 3.2 C). Intermittent stratification and subsequent development of an anoxic hypolimnion in Jackfish Lake resulted in bottom water enrichment of redox sensitive species including As (Fig. 3.2 C and Fig. 3.6 C). This result is consistent with Barrett *et al.* (2019) study that found in stratified lakes, elevated As concentrations typically reside within the hypolimnion of a lake. In contrast, the water column of Jackfish Lake is well mixed with isothermal conditions during ice-covered conditions due to the power plant's water intake connection in the lake (Fig. 3.1 C and Fig. 3.6 C).

4.2.2 Evaluation of As concentrations in shallow versus deep lakes

Differences in As concentrations between shallow and deep lakes were observed, with more variation in shallower lakes, like Handle (Fig. 3.10). Shallow lakes have less water volume, thus, lead to more limited DO supply causing greater susceptibility to water column anoxia and greater variation of As in the winter (Fig. 3.1, Fig. 3.6, Table 3.1, and Fig. 3.10). In open-water conditions, the shallow morphology of Handle Lake (Z_{max} = 3.5 m) allowed for a well-mixed and oxygen-rich water column due to frequent physical mixing from winds (Fig. 3.1, Table 3.1, and

Fig. 3.6) (Vincent *et al.*, 2008). In addition, the lower water volume of Handle Lake enables greater increases in concentration of As that are diffused from the lake sediments (Table 3.1 and Fig. 3.10 A). These characteristics of Handle Lake led it to be more susceptible to high As in its surface waters in open-water conditions because of continuous entrainment and re-deposition of As from lake sediments through greater mixing (Nelligan *et al.*, 2019).

The range of reducing conditions from depleted DO within the lakes' water column was largely dependent on the depth and volume of the lakes (Fig. 3.1, Fig. 3.6, and Table 3.1). This also influenced the position of the redox boundary or chemocline, where As species among other redox elements could be mobilized upwards from the sediment source (Fig 3.3, Fig. 3.6, and Fig. 3.10). Andrade *et al*. (2010) discussed the redoxcline as a key barrier to preventing the upward migration of As concentrations from the lake sediment. Redox boundaries influence on As concentrations was evident between Small Lake and Handle Lake (Fig. 3.6 A and B, Fig. 3.10).

As cycling in deep lakes like Small Lake, were likely regulated by the water column temperature and density gradients through the establishment of an epilimnion, metalimnion, and hypolimnion (Fig. 3.2 D and Fig. 3.6 D). Deep and large volume lakes like Small would have higher capacity to dilute solute concentrations like As (Table 3.1 and Fig. 3.10 D). The deep lake of Small experienced stratification for most of the open-water period which facilitated reducing conditions in the hypolimnion (Fig. 3.2 D). The development of a stable hypolimnion in Small Lake allowed for the upward migration of the oxic boundary in the water column (Fig. 3.6 D and Fig. 3.10 D). A study conducted by Barrett *et al.* (2019) found As concentrations in the water column below the thermocline were elevated and was attributed to the lake sediment as the source. Water temperature and density gradients can limit the upward migration of As

concentrations throughout the water column from the bottom waters (Hall *et al*., 1999). Vincent *et al.* (2008) echoes that with more water volume in deep lakes comes greater heat capacity to distribute thermal energy, which can shape the thermal structure of a water column and redox conditions for As. Small Lake's reducing conditions were limited to the bottom waters or hypolimnion, versus Handle Lake where reducing conditions were present through the water column by mid to late winter (Fig. 3.6 A and B).

Little variation in As concentrations was observed in the medium depth lakes of Fiddler (Z_{max} = 6.5 m) and Jackfish (Z_{max} = 7.5 m). These lakes are associated with intermittent stratification and limited subsequent development of an anoxic hypolimnion (Fig 3.3, Fig. 3.6, and Fig. 3.10). These medium sized lakes also observed less influence from the SWI on the overlying water, because of the transitory nature of the development of a hypolimnion (Fig. 3.10 B and C). The smaller variation in As concentrations can be connected to the high occurrence of isochemical and isothermal conditions, indicating the water column was well-mixed (Fig. 3.2 and Fig. 3.6). This was especially the case for Jackfish Lake with its external influence from the power plant likely generating year-round physical mixing of the water column from the water intakes (Fig. 1.1 C). In contrast, Fiddler Lake measured lower As concentrations than anticipated, despite the lake being relatively close in distance to the historical mining operations (Fig. 3.10 B, Fig. 3.1, and Table. 1.1).

4.3 High Fe in sediments and water from a shallow non-stratified lake demonstrates Fe attenuation of As from the water column.

This section investigates the relationship between As and Fe in lake waters and how this may influence As cycling within the water column. High Fe levels were measured in the sediments and lake waters of Fiddler Lake compared to the other study lakes. Here, the use of Fe as an amendment for As removal is discussed, using Fiddler Lake as a field observation of a high Fe to As system.

4.3.1 High Fe to As ratio observed in lake waters

A high Fe to As ratio was observed in the water column of Fiddler Lake throughout the study period, and suggested the potential attenuation of As from the water column by Fe precipitates in Fiddler Lake (Table. 3.10, Table 3.6 and Fig. 3.16). Under oxic conditions, Fe-oxyhydroxides can readily adsorb and co-precipitate with As (Dixit & Hering, 2003; Kneebone *et al.,* 2002; Root *et al.,* 2007). The high percentage (mean= 69%) of particulate Fe in Fiddler Lake's water column suggests the presence of Fe precipitates and could allow for the sequestration of As from the water column via sorption and co-precipitation processes (Table 3.6 and Fig. 3.10 B) (Dixit & Hering, 2003; Kneebone *et al.,* 2002; Root *et al.,* 2007; Palmer *et al.,* 2020). Enriched sedimentary Fe concentrations were also measured in Fiddler Lake in addition to high Fe in the lake waters (Fig. 3.20 B and Table 3.11). The high Fe concentrations in Fiddler Lake's sediment further suggests the settling of Fe particles from the water column (Fig. 3.20 B and Table 3.11). Arsenic concentrations in near surface sediments is related to Fe mobility, as Fe oxyhydroxide minerals in oxidized environments highly adsorb or co-precipitate with dissolved

As (Fig. 3.19 B and Table 3.11) (Bennett *et al.,* 2012; Ferguson & Gavis, 1972). The origin of the anomalously high levels of Fe in surface waters and sediments of Fiddle Lake merits consideration about what external factors or internal drivers of Fe historically and/or presently contribute to Fe in Fiddler Lake (Fig. 3.1, Fig. 3.12 B, and Fig. 3.13 B). Potential current external sources of Fe input could be partially attributed to the adjacent horse stable farm on the NE shoreline of Fiddler Lake or the highway bordering south of lake (Fig. 3.1 B).

4.3.2 Spatial context of Fe and As concentrations in small lakes around the Yellowknife region

Fiddler Lake measured extremely high Fe concentration (mean= 49 333 µg/g) in the top 10 cm of the sediment compared to the other study lakes (Fig. 3.20 and Table 3.11) and nearly twice as high as Small Lake, which had the second highest levels of Fe in near surface sediments (mean= 27 545 µg/g). Iron concentrations in the near-surface sediment of Jackfish Lake (mean= 19 583 µg/g) and Handle Lake (mean= 13 818 µg/g) were much lower (Fig. 3.20 and Table 3.11).

When comparing Fe levels in the lake sediments in conjunction with the water column, a key difference was showcased in Fiddler Lake (Fig. 3.12 B, Fig. 3.13 B, Fig. 3.20, and Table 3.11). This large reservoir of Fe in Fiddler Lake's sediment could represent the settling of high Fe particulate from the water column of Fiddler Lake (Fig. 3.20, Table 3.6, and Table 3.11). The high Fe levels in Fiddler Lake sediment can also potentially allow for a sustained supply of Fe available to be fluxed into the overlying waters through internal loading from the lake sediments if conditions were to allow (Fig. 3.20 and Fig. 3.12) (Martin & Pederson, 2002). Dissolved Fe levels were also highest in Fiddler Lake during the open-water season compared to the other

study lakes (Fig. 3.12, Fig. 3.13, and Table 3.5). This was evident in Fiddler Lake's water column, as SWI enrichment was frequently observed and reached a maximum level of Fe after the spring freshet period (Fig. 3.12 B). Under oxidizing conditions during the open-water period, dissolved Fe concentrations in the surface waters of the study lakes were the highest in Fiddler Lake (mean= 18.42 µg/L), followed by Small Lake (mean= 11.79 µg/L), and Handle Lake (mean= 4.45 µg/L), with the lowest levels in Jackfish Lake (mean= 2.50 µg/L) (Fig. 3.12 and Fig. 3.13). Small Lake was the other comparable lake that measured SWI enrichment of Fe in the hypolimnion, which was associated with periods of summer and winter stratification (Fig. 3.12 D and Fig. 3.2). Jackfish Lake consistently measured low or below detection limit of Fe levels (Fig. 3.12 C and Fig. 3.13 C). During the ice-water period, the volume weighted percentage change of Fe in Fiddler was the only lake to observe a decrease (80%) in Fe (Table 3.5 and Fig. 3.13 B). Fiddler Lake evidently stood out among the study lakes in its regard to Fe concentration dynamic between its water column and enriched lake sediment (Fig. 3.12 B and Fig. 3.20).

Sampling records from a previous survey done by Palmer *et al.* (2015) of other surrounding lakes in the Yellowknife region showcased a wide variation in Fe and As concentrations across 96 lakes sampled in September 2012 and 2014. The reported Fe concentrations in Fiddler Lake (mean= 18.4 µg/L, max= 372 µg/L) (Fig. 3.10 B) during this study period (November 2020 to October 2021) was elevated in comparison to historical studies of other regional lakes' Fe concentrations. Specifically, Palmer *et al.* (2015) found the surveyed lakes that were similar in depth to Fiddler Lake (N = 30) to have a mean Fe concentration of 4.2 µg/L and max Fe concentration of 23 µg/L. Most immediate lakes surrounding Fiddler Lake were classified in a lower Fe concentration range (Palmer *et al.,* 2015). This previous regional

study from Palmer *et al.* (2015) further supports Fiddler Lake as an anomaly in its elevated Fe concentration.

Arsenic concentrations reported in Handle Lake, Jackfish Lake, Fiddler and Small Lake (Fig. 3.10) were comparable to Palmer *et al.* (2015) examination of other regional lakes As levels. Palmer *et al.* (2015) found that surface water As decreased sharply until 17.5 km from historical mining operations, after which As concentrations were typically below 10 ug/L (Palmer *et al.,* 2015). Most of the lakes in the present study were within this 17.5 km marker distance, with exception to Small Lake being 27.4 km in distance away from historical mining operations (Fig. 1.1 and Table 1.1). This was reflected in Small Lake's considerably lower As concentrations (mean= 1.43 µg/L) relative to other lakes in this study (Fig. 3.10). Clark and Raven (2004) investigated surface water pollution in tailing ponds on the historic mining grounds to contain As concentrations of 8 000 µg/L and water underground of the mine over 4 000 000 µg/L. A stark comparison to this study's highest recorded As concentration of 377 µg/L in Handle Lake. Despite Fiddler Lake being in close proximity (8.6 km) and downwind of historical mining operations, it was surprising to find As concentrations (mean= 6.35 µg/L) to be relatively low.

4.3.3 Fe use as an amendment for As removal from lake water and related implications

Iron is well known to be used as an additive to lakes for As remediation (Gallegos-Garcia *et al.,* 2012; Hao *et al.,* 2018; Lenoble *et al.,* 2005). Removal of As via Fe can occur through different processes of chemical coagulation-precipitation, adsorption, and membrane separation (Gallegos-Garcia *et al.,* 2012; Hao *et al.,* 2018; Jiang, 2001; Lenoble *et al.,* 2005). In relation to

the study lake of Fiddler Lake, the high Fe found in both its lake waters and sediment warrants speculation if there was an external source of Fe in its watershed (Fig. 3.10, Table. 3.13, and Fig. 3.20 C). A study by Kumpiene *et al.* (2021) highlights the longevity and effectiveness of Fe amendments (specifically zerovalent) in soils over a 15-year elapsed period where As immobilization remained high. Enriched surficial Fe concentrations in Fiddler Lake's sediment core marks a large source susceptible for remobilization to occur into the lake waters (Table. 3.13 and Fig. 3.20 C). This cyclical process encompassing the settlement of Fe out of the water column into the lake sediment and then remobilization from a large Fe reservoir in lake sediments, could be indicative to how Fiddler Lake sustains high levels of Fe (Martin & Pedersen, 2002)

5. Chapter 5: Conclusion

This research examined seasonal differences in As cycling within four small subarctic shield lakes near Yellowknife, NWT, Canada. Overall, distinct differences in the cycling of As was observed among lakes. Seasonality drove As concentrations in all lakes, where each study lake established different results based on lake mixing regime and lake depth. In the shallowest lake (max depth = 3.5 m), anoxia developed throughout the water column under-ice and was associated with increase in under-ice concentrations of As. Hypolimnetic anoxia developed in the deepest lake during open-water season and under-ice resulting in bottom-water enrichment of As. Minimal arsenic variation was found in medium depth lakes, likely due to frequent isothermal conditions and intermittent stratification. During the freshet transition, an influx of

DO during meltwater input into the lakes induced a sudden decrease of As concentrations in three of the four lakes.

Furthering this knowledge of the biogeochemical cycling of As in lakes year-round is especially critical in subarctic lakes, where ice-covered conditions can persist up to half the calendar year. Other significant findings from this research indicated that the lake mixing regime of the study lakes was an important factor in controlling the redox conditions, and ultimately influencing the mobility of As. The morphometric property of lake depth was observed to be more influential in As cycling within shallow lakes than in deep lakes. A key observation from a shallow lake was a high Fe to As ratio in its lake waters and sediment, which showcased an applied example of Fe as an amendment of As from the water column. These results are important in the advancement towards understanding the chemical reclamation of subarctic lakes from As contamination.

Limitations of this research includes the interpretation of the results cannot be universally applied to a whole lake, as sampling only occurred at the deepest point in each lake and variation spatially across each lake is likely. Further, water chemistry results are a snapshot in time as water sampling only captures point data and conditions can evolve. In addition, these lakes are largely hydrologically disconnected which does not allow for comparison to other lakes that are hydrologically connected systems with defined inflow and outflow connections. Future work outside the scope of this study could examine the study lakes with other comparable lakes in different regions, as well as having more sampling variability of depth in each lake. These limitations are reflective of logistical challenges and realistic scope of the study to successful conduct the research within a defined period and not easily addressed. Other future

advancements of this research could involve gaining more information on temporal lake sediment temperatures to better quantify when As fluxes from the sediments increase. This, combined with detailed pore water concentration analysis could address a remaining question of: exactly how much diffusion of As occurs from the sediment-water interface? In addition, fabricating a simple mass balance of As in each study lake through temporal water level information would allow for a quantification of the effect of evapoconcentration on As concentrations. Thus, future work is justified to further advance the understanding of the biogeochemistry of As during the subarctic's long period of lake ice conditions and the dynamic transition during freshet. Ultimately, advancing the research into the vastly understudied discipline of winter limnology continues to be much needed, especially in dynamically changing northern regions like the subarctic.

Finally, information gained from this study will contribute to the understanding of the biogeochemical cycling of As seasonally between ice-covered and open-water periods in small sub-arctic shield lakes. Results from this study are an important step towards strengthening the knowledge surrounding the complex chemical recovery of small subarctic lakes from legacy anthropogenic As pollution.

Appendices

A.1 Specific Conductivity (SpC)

Specific conductivity (SpC) measurements (µs/cm) for each study lake from November 2020 to October 2021 are shown in Fig. A.1. The rank of highest to lowest SpC levels recorded by lake occurred as follows: Jackfish Lake (mean = 466.08 µs/cm), Handle Lake (mean = 298.76 µs/cm), Fiddler Lake (mean = 241.57 µs/cm), and Small Lake (mean = 163.66 µs/cm). SpC for all four lakes followed a similar pattern during the ice cover period (November-May), where SpC progressively increased in the water column through winter. During the ice-cover season, higher SpC was recorded near the lake bottom for most lakes. SpC levels dropped abruptly during the spring freshet and remained lower than under-ice conditions for the duration of the open-water season (Fig. A.1.). Although Fiddler Lake's SpC levels were comparable to Handle Lake one difference stood out in Fiddler Lake that its top 1 m of water (272.7 µs/cm) also experienced elevated SpC levels together with the bottom 1 m (272 µs/cm) during ice-on period, except on May 11th (Fig. A.1. B). Jackfish Lake was unique in that it held its high SpC levels 480 µs/cm to 520 µs/cm during the entire ice cover period and showed no significant change across the whole water column (Fig. A.1. C). Once the open-water period began in June, Jackfish Lake's SpC levels did not change drastically with SpC readings only dropping to 145 µs/cm on June 22nd from 166.2 µs/cm on May 10th (Fig. A.1.C). June 26th (range from 144.9 µs/cm to 163.50 µs/cm).

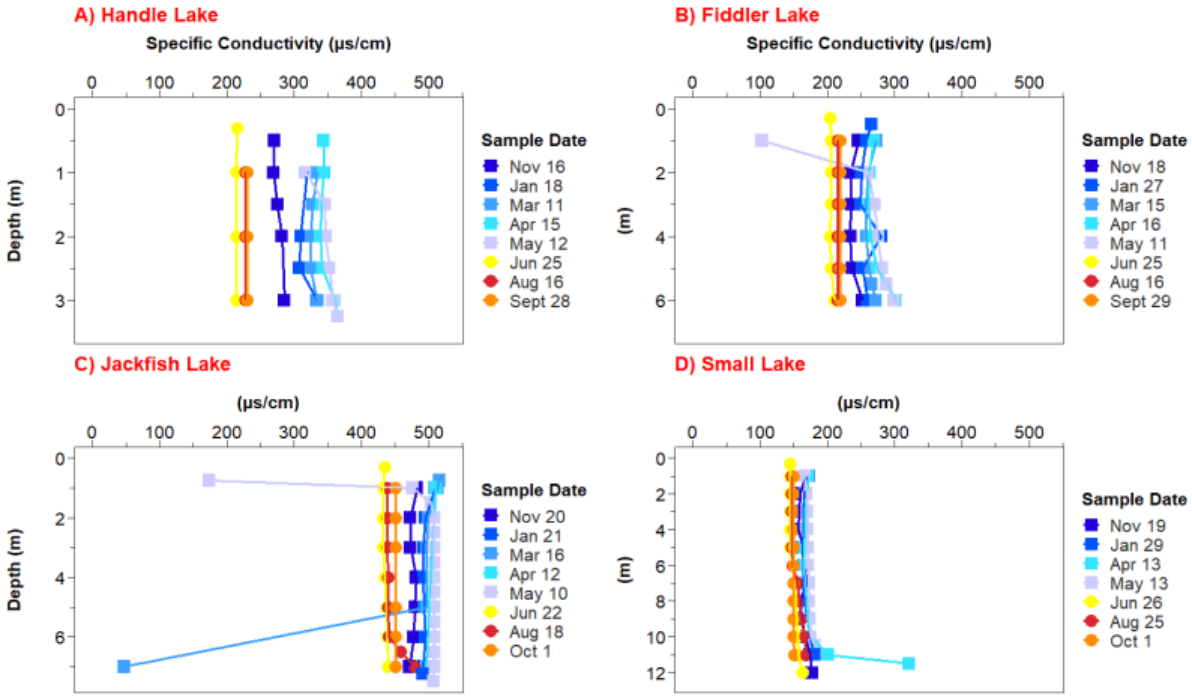

Figure A.1 1 Specific conductivity (SpC) (µs/cm) for Handle Lake, Jackfish Lake, Fiddler Lake, and Small Lake during November 2020 to October 2021. Squares = Ice-on, Circles= Ice-off.

A.2 Nutrients

Chlorophyll-*a* (Chl-*a*) sample results for much of the study period held Chl-a levels below < 5 µg/L (Fig. A.2.1). Sonde readings of Chl-*a* via a multi-parameter water quality sonde (YSI EXO2) were measured at each study lake Handle Lake, Fiddler Lake, Jackfish Lake, and Small Lake during field visits through November 2020 to October 2021 are shown in Fig A.2.2 below.

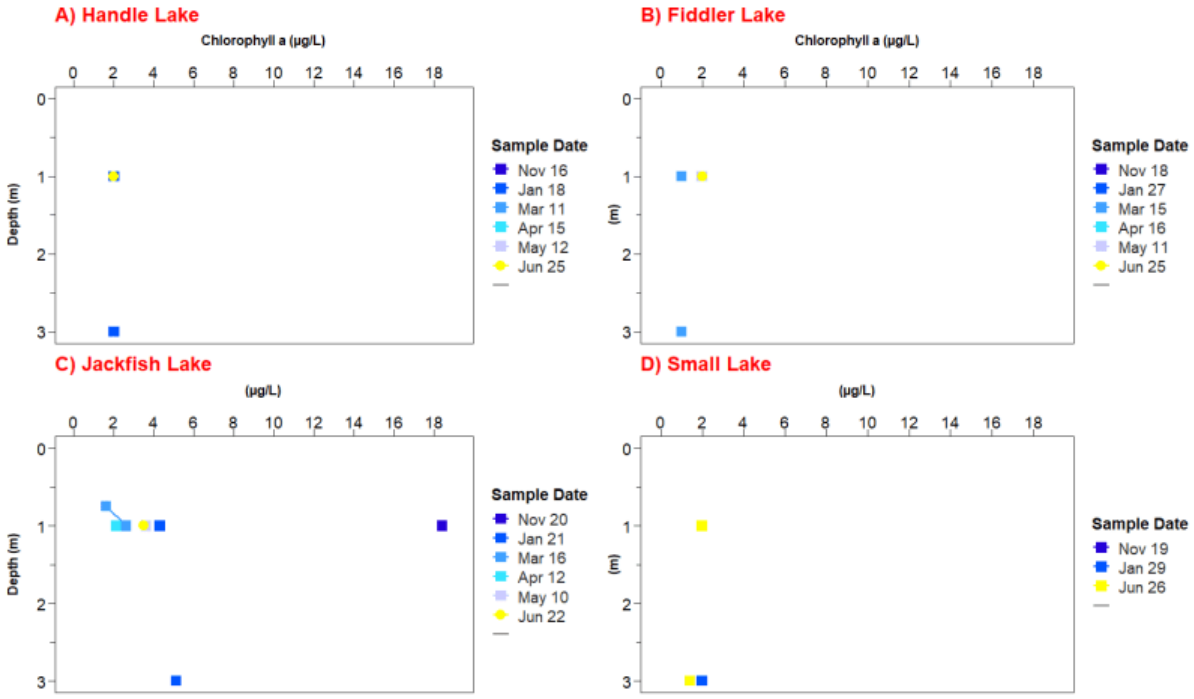

Figure A.2 1 Total chlorophyll-a (µg/L) levels result from total fraction water samples from Handle Lake, Fiddler Lake, Jackfish Lake, and Small Lake. Squares = Ice-on, Circles= Ice-off. Detection level = 1 µg/L from ICP-MS

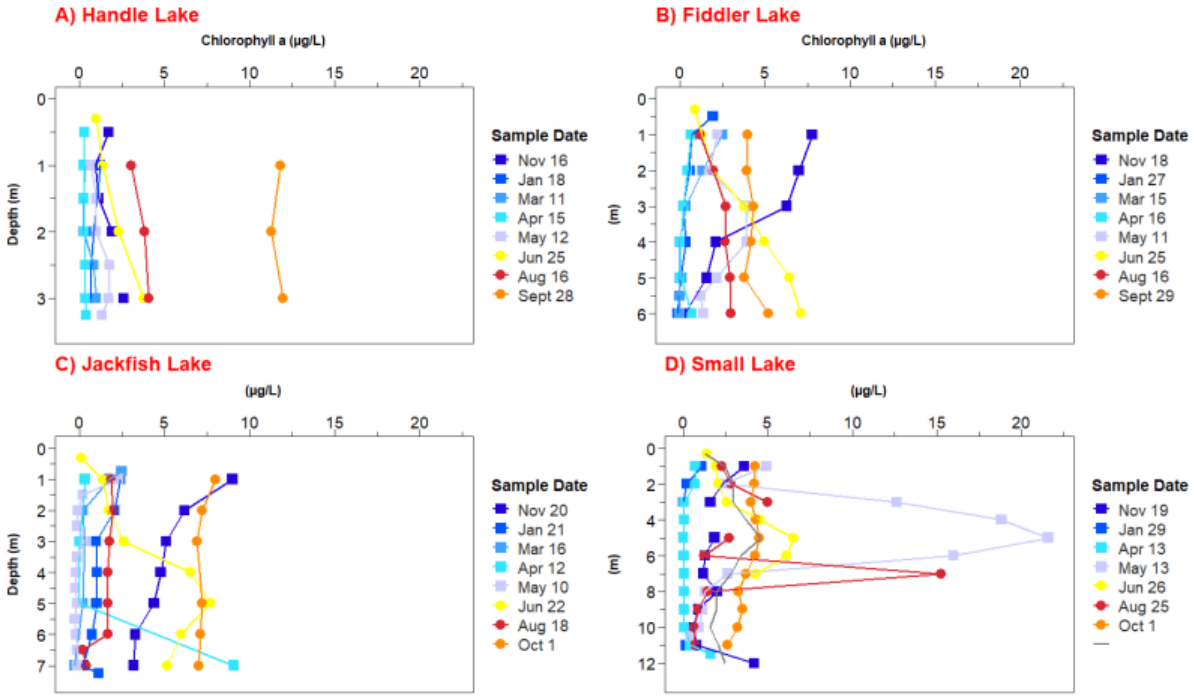

Figure A.2 2 Chlorophyll-a (µg/L) sonde reading via EXO2 from Handle Lake, Fiddler Lake, Jackfish Lake, and Small Lake through November 2020 to October 2021. Squares = Ice-on, Circles= Ice-off.

Table A.2 1 Carlson's trophic state index values and classification of lakes table from (Carlson, 1977), (A. G. Devi Prasad *et al,* 2012).

TSI values	***Trophic Status***	***Attributes***
< 30	Oligotrophic	Clear water, oxygen throughout the year in the hypolimnion
30-40	Oligotrophic	A lake will still exhibit oligotrophy, but some shallower lakes will become anoxic during the summer
40- 50	Mesotrophic	Water moderately clear, but increasing probability of anoxia during the summer
50-60	Eutrophic	Lower boundary of classical eutrophy: Decreased transparency, warm-water fisheries only
60-70	Eutrophic	Dominance of blue-green algae, algal scum probable, extensive macrophyte problems
70-80	Eutrophic	Heavy algal blooms possible throughout the summer, often hypereutrophic
>80	Eutrophic	Algal scum, summer fish kills, few macrophytes

A.3 Metals

Table A.3 1 Volume weighted percentage change of Mn for Handle Lake, Fiddler Lake, Jackfish Lake, and Small Lake over winter (Nov 2020-May 2021), spring ice off (May-June 2021), over summer (June-October 2021).

Volume weighted % change of Mn			
Lake	***% change over winter***	***% change over spring ice-off***	***% change over summer***
Handle	1349	-13928	-97
Fiddler	25	-50	-99
Jackfish	601	580	-99
Small	934	348	-85

Table A.3 2 Percentage (%) of particulate Fe for Handle Lake, Fiddler Lake, Jackfish Lake, and Small Lake during November 2020 to August 2021. *(0% particulate Fe = dissolved fraction exceeded total).

Handle Lake		
Date	***Depth (m)***	***% of Particulate Fe***
2020-11-16	0.5	80
2020-11-16	1	70
2020-11-16	2	58
2020-11-16	3	50
2021-01-18	1	72
2021-01-18	2	69
2021-01-18	3	76
2021-03-11	1	58
2021-03-11	2	55
2021-03-11	3	0
2021-04-15	1	38
2021-04-15	2	29
2021-04-15	3	28
2021-05-12	1	0
2021-05-12	2	57
2021-05-12	3	79
2021-06-25	1	67
2021-06-25	2	71
2021-06-25	3	64
2021-08-17	1	83

2021-08-17	2	83
2021-08-17	3	83
Fiddler Lake		
Date	***Depth (m)***	***% of Particulate Fe***
2020-11-18	1	78
2020-11-18	5	32
2020-11-18	6	37
2021-01-27	3	79
2021-01-27	4	77
2021-01-27	5	72
2021-03-15	1	74
2021-03-15	2	81
2021-03-15	3	81
2021-03-15	4	78
2021-03-15	5	56
2021-03-15	6	37
2021-04-16	1	65
2021-04-16	5	78
2021-05-11	1	2
2021-05-11	5	90
2021-05-11	6	91
2021-06-25	1	62
2021-06-25	3	70
2021-06-25	5	68
2021-06-25	6	71
2021-08-17	1	95
2021-08-17	5	95
2021-08-17	6	95
Jackfish Lake		
Date	***Depth (m)***	***% of Particulate Fe***
2020-11-20	1	0
2020-11-20	3	0
2020-11-20	5	0
2020-11-20	7	44
2021-01-21	1	0
2021-01-21	3	29
2021-01-21	5	17
2021-01-21	5	50
2021-01-21	6	38
2021-01-21	7	50
2021-01-21	7	67

2021-03-16	1	0
2021-04-12	1	0
2021-04-12	7	67
2021-05-10	1	17
2021-05-10	7	64
2021-06-22	1	38
2021-06-22	6	78
2021-06-22	7	81
2021-08-18	1	62
2021-08-18	5	71
2021-08-18	6	67
2021-08-18	7	34
Small Lake		
Date	***Depth (m)***	***% of Particulate Fe***
2020-11-19	1	23
2020-11-19	5	76
2020-11-19	9	67
2020-11-19	12	69
2021-01-29	3	0
2021-01-29	5	50
2021-01-29	7	67
2021-01-29	8	57
2021-01-29	9	56
2021-01-29	10	62
2021-01-29	11	61
2021-04-13	1	58
2021-04-13	9	80
2021-04-13	11	44
2021-05-13	1	0
2021-05-13	6	81
2021-05-13	7	85
2021-05-13	8	83
2021-05-13	9	90
2021-05-13	10	91
2021-05-13	10.5	95
2021-06-26	1	55
2021-06-26	3	48
2021-06-26	5	58
2021-06-26	7	68
2021-06-26	8	70
2021-06-26	9	72

2021-06-26	10	73
2021-06-26	11	70
2021-08-25	1	77
2021-08-25	5	85
2021-08-25	7	94
2021-08-25	8	69
2021-08-25	9	38
2021-08-25	10	16
2021-08-25	11	11

Table A.3 3 Percentage (%) of particulate Mn for Handle Lake, Fiddler Lake, Jackfish Lake, and Small Lake during November 2020 to August 2021. *(0% particulate As = dissolved fraction exceeded total).

Handle Lake		
Date	***Depth (m)***	***% of Particulate Mn***
2020-11-16	0.5	88
2020-11-16	1	80
2020-11-16	2	51
2020-11-16	3	46
2021-01-18	1	95
2021-01-18	2	0
2021-01-18	3	0
2021-03-11	1	50
2021-03-11	2	32
2021-03-11	3	0
2021-04-15	1	21
2021-04-15	2	3
2021-04-15	3	0
2021-05-12	1	2
2021-05-12	2	0
2021-05-12	3	4
2021-06-25	1	88
2021-06-25	2	86
2021-06-25	3	78
2021-08-17	1	99
2021-08-17	2	99
2021-08-17	3	99
Fiddler Lake		
Date	***Depth (m)***	***% of Particulate Mn***
2020-11-18	1	13
2020-11-18	5	14
2020-11-18	6	26
2021-01-27	3	94

2021-01-27	4	97
2021-01-27	5	99
2021-03-15	1	68
2021-03-15	2	84
2021-03-15	3	90
2021-03-15	4	96
2021-03-15	5	39
2021-03-15	6	4
2021-04-16	1	0
2021-04-16	5	43
2021-05-11	1	0
2021-05-11	5	49
2021-05-11	6	0
2021-06-25	1	65
2021-06-25	3	73
2021-06-25	5	66
2021-06-25	6	5
2021-08-17	1	99
2021-08-17	5	99
2021-08-17	6	99
Jackfish Lake		
Date	***Depth (m)***	***% of Particulate Mn***
2020-11-20	1	98
2020-11-20	3	0
2020-11-20	5	98
2020-11-20	7	74
2021-01-21	1	82
2021-01-21	3	88
2021-01-21	5	94
2021-01-21	6	93
2021-01-21	7	84
2021-03-16	0.75	92
2021-03-16	1	95
2021-04-12	1	90
2021-05-10	1	35
2021-05-10	7	85
2021-06-22	1	97
2021-06-22	6	68
2021-06-22	7	46
2021-08-18	1	95
2021-08-18	5	80
2021-08-18	6	90
2021-08-18	7	0
Small Lake		
Date	***Depth (m)***	***% of Particulate Mn***
2020-11-19	1	4

2020-11-19	5	97
2020-11-19	9	98
2020-11-19	12	39
2021-01-29	3	95
2021-01-29	3	0
2021-01-29	5	96
2021-01-29	7	99
2021-01-29	8	94
2021-01-29	9	11
2021-01-29	10	8
2021-01-29	11	0
2021-04-13	1	54
2021-04-13	9	100
2021-04-13	11	7
2021-05-13	1	27
2021-05-13	6	98
2021-05-13	7	99
2021-05-13	8	99
2021-05-13	9	99
2021-05-13	10	84
2021-05-13	10.5	0
2021-06-26	1	74
2021-06-26	3	63
2021-06-26	5	65
2021-06-26	7	83
2021-06-26	8	86
2021-06-26	9	89
2021-06-26	10	88
2021-06-26	11	41
2021-08-25	1	96
2021-08-25	5	99
2021-08-25	7	12
2021-08-25	8	0
2021-08-25	9	0
2021-08-25	10	0
2021-08-25	11	0

A.4 Lake Volume

Table A.4 1 List of the percentage of total water volume for each study lake.

Lake	*Depth (m)*	*Depth Volume (m^3)*	*Percentage of Total Volume (%)*
Jackfish	1	532 722	17
Jackfish	2	495 762	15
Jackfish	3	458 901	14
Jackfish	4	416 518	13
Jackfish	5	379 361	12
Jackfish	6	352 400	11
Jackfish	7	323 309	10
Jackfish	8	246 964	8
Total Lake Volume = 3 205 937 m^3			
Handle	1	214 357	55
Handle	2	106 822	27
Handle	3	69 346	18
Total Lake Volume = 390 525 m^3			
Fiddler	1	318 828	29
Fiddler	2	249 456	23
Fiddler	3	184 397	17
Fiddler	4	147 299	13
Fiddler	5	115 493	10
Fiddler	6	88 269	8
Total Lake Volume = 1 103 741 m^3			
Small	1	670 507	17
Small	2	612 672	15
Small	3	536 614	13
Small	4	448 464	11
Small	5	380 580	9
Small	6	332 251	8
Small	7	279 878	7
Small	8	243 226	6
Small	9	203 446	5
Small	10	151 865	4
Small	11	98 950	2
Small	12	57 919	1
Total Lake Volume = 4 016 371 m^3			

References

Aggett, J., & O'Brien, G. A. (1985). Detailed model for the mobility of arsenic in lacustrine sediments based on measurements in Lake Ohakuri. *Environmental science & technology*, *19*(3), 231-238.

Aggett, J., & Kriegman, M. R. (1988). The extent of formation of arsenic (III) in sediment interstitial waters and its release to hypolimnetic waters in Lake Ohakuri. *Water Research*, *22*(4), 407-411.

APHA (1992) Compendium of methods for the microbiological examination (3rd ed.), American Public Health Association, Washington (1992) pp. 105–119, 325–367, 371–415, 451–469 & 637–658

Andrade, C. F., Jamieson, H. E., Kyser, T. K., Praharaj, T., & Fortin, D. (2010). Biogeochemical redox cycling of arsenic in mine-impacted lake sediments and co-existing pore waters near Giant Mine, Yellowknife Bay, Canada. *Applied Geochemistry*, *25*(2), 199-211.

Azcue, J. M., & Nriagu, J. O. (1995). Impact of abandoned mine tailings on the arsenic concentrations in Moira Lake, Ontario. *Journal of Geochemical Exploration*, *52*(1-2), 81-89.

Barrett, P. M., Hull, E. A., King, C. E., Burkart, K., Ott, K. A., Ryan, J. N., ... & Neumann, R. B. (2018). Increased exposure of plankton to arsenic in contaminated weakly-stratified lakes. *Science of the Total Environment*, *625*, 1606-1614.

Barrett, P. M., Hull, E. A., Burkart, K., Hargrave, O., McLean, J., Taylor, V. F., ... & Neumann, R. B. (2019). Contrasting arsenic cycling in strongly and weakly stratified contaminated lakes: Evidence for temperature control on sediment–water arsenic fluxes. *Limnology and oceanography*, *64*(3), 1333-1346.

Barringer, J. L., Szabo, Z., Wilson, T. P., Bonin, J. L., Kratzer, T., Cenno, K., ... & Hirst, B. (2011). Distribution and seasonal dynamics of arsenic in a shallow lake in northwestern New Jersey, USA. *Environmental geochemistry and health*, *33*(1), 1-22.

Bauer, M., and C. Blodau. (2006). Mobilization of arsenic by dissolved organic matter from iron oxides, soils and sediments. Sci. Total Environ. 354: 179–190. doi:10.1016/j.scitotenv.2005.01.027

Belzile, N., & Tessier, A. (1990). Interactions between arsenic and iron oxyhydroxides in lacustrine sediments. *Geochimica et Cosmochimica Acta*, *54*(1), 103-109.

Belzile, C., Gibson, J. A., & Vincent, W. F. (2002). Colored dissolved organic matter and dissolved organic carbon exclusion from lake ice: Implications for irradiance transmission and carbon cycling. *Limnology and Oceanography*, *47*(5), 1283-1293.

Bennett, W. W., Teasdale, P. R., Panther, J. G., Welsh, D. T., Zhao, H., & Jolley, D. F. (2012). Investigating arsenic speciation and mobilization in sediments with DGT and DET: a mesocosm evaluation of oxic-anoxic transitions. *Environmental science & technology*, *46*(7), 3981-3989.

Bergmann, M. A., & Welch, H. E. (1985). Spring meltwater mixing in small arctic lakes. *Canadian Journal of Fisheries and Aquatic Sciences*, *42*(11), 1789-1798.

Bertilsson, S., Burgin, A., Carey, C. C., Fey, S. B., Grossart, H. P., Grubisic, L. M., ... & Smyth, R. L. (2013). The under-ice microbiome of seasonally frozen lakes. *Limnology and Oceanography*, *58*(6), 1998-2012.

Bissen, M., & Frimmel, F. H. (2003). Arsenic—a review. Part I: occurrence, toxicity, speciation, mobility. *Acta hydrochimica et hydrobiologica*, *31*(1), 9-18.

Block, B. D., Denfeld, B. A., Stockwell, J. D., Flaim, G., Grossart, H. P. F., Knoll, L. B., ... & Hampton, S. E. (2019). The unique methodological challenges of winter limnology. *Limnology and Oceanography: Methods*, *17*(1), 42-57.

Bostick, B. C., & Fendorf, S. (2003). Arsenite sorption on troilite (FeS) and pyrite (FeS2). *Geochimica et cosmochimica Acta*, *67*(5), 909-921.

Bromstad, M. J., Wrye, L. A., & Jamieson, H. E. (2017). The characterization, mobility, and persistence of roaster-derived arsenic in soils at Giant Mine, NWT. *Applied geochemistry*, *82*, 102-118.

Canadian Council of Ministers of the Environment. (1999). Canadian sediment quality guidelines for the protection of aquatic life: Arsenic. In: Canadian environmental

quality guidelines, 1999, Canadian Council of Ministers of the Environment, Winnipeg

Canadian Council of Ministers of the Environment (CCME). 2002. Canadian Sediment Quality Guidelines for the Protection of Aquatic Life, in, Canadian Environment Quality Guidelines.

Canadian Council of Ministers of the Environment (CCME). 2011. Protocols manual for water quality sampling in Canada.

Canadian Public Health Association, *Task Force on Arsenic – Final Report, Yellowknife Northwest Territories* (Ottawa: CPHA, 1977).

Carlson, R. E. (1977). A trophic state index for lakes 1. *Limnology and oceanography*, *22*(2), 361-369.

Clark, I. D., & Raven, K. G. (2004). Sources and circulation of water and arsenic in the Giant Mine, Yellowknife, NWT, Canada. Isotopes in environmental and health studies, 40(2), 115-128.

Chen, G., Shi, H., Tao, J., Chen, L., Liu, Y., Lei, G., ... & Smol, J. P. (2015). Industrial arsenic contamination causes catastrophic changes in freshwater ecosystems. *Scientific reports*, *5*, 17419.

Couture, R. M., Gobeil, C., & Tessier, A. (2010). Arsenic, iron and sulfur co-diagenesis in lake sediments. *Geochimica et Cosmochimica Acta*, *74*(4), 1238-1255.

Creed, J. T., Brockhoff, C. A., & Martin, T. D. (1994). Method 200.8: Determination of trace elements in waters and wastes by inductively coupled plasma–mass spectrometry. Revision 5.4, EMMC Version. *Ohio, US Environmental Protection Agency*.

Deshpande, B. N., MacIntyre, S., Matveev, A., & Vincent, W. F. (2015). Oxygen dynamics in permafrost thaw lakes: Anaerobic bioreactors in the Canadian subarctic. *Limnology and Oceanography*, *60*(5), 1656-1670.

Dixit, S., & Hering, J. G. (2003). Comparison of arsenic (V) and arsenic (III) sorption onto iron oxide minerals: implications for arsenic mobility. *Environmental science & technology*, *37*(18), 4182-4189.

Duthie, H. C. (1979). Limnology of subarctic Canadian lakes and some effects of impoundment. *Arctic and Alpine Research*, *11*(2), 145-158.

Ecosystem Classification Group. (2007). Ecological Regions of the Northwest Territories–Taiga Plains. *Department of Environment and Natural Resources, Government of Northwest Territories, Yellowknife, Northwest Territories, Canada*.

Environment and Climate Change Canada. (2022). Historical Canadian daily climate data [WWW Document]. Environ. Canada URL. http://climate.weather.gc.ca/historical_data/search_historic_ data_e.html, Accessed date: 22 June 2022.

Ferguson, J. F., & Gavis, J. (1972). A review of the arsenic cycle in natural waters. *Water research*, *6*(11), 1259-1274.

Gallegos-Garcia, M., Ramírez-Muñiz, K., & Song, S. (2012). Arsenic removal from water by adsorption using iron oxide minerals as adsorbents: a review. *Mineral Processing and Extractive Metallurgy Review*, *33*(5), 301-315.

Galloway, J. M., Palmer, M., Jamieson, H. E., Patterson, R. T., Nasser, N., Falck, H., ... & Lemay, D. (2015). Geochemistry of lakes across ecozones in the Northwest Territories and implications for the distribution of arsenic in the Yellowknife region. *Part*, *1*, 10-4095.

Gibson, J. J., Reid, R., & Spence, C. (1998). A six-year isotopic record of lake evaporation at a mine site in the Canadian subarctic: results and validation. *Hydrological processes*, *12*(10-11), 1779-1792.

Golosov, S., Maher, O. A., Schipunova, E., Terzhevik, A., Zdorovennova, G., & Kirillin, G. (2007). Physical background of the development of oxygen depletion in ice-covered lakes. *Oecologia*, *151*(2), 331-340.

Gorham, E., & Boyce, F. M. (1989). Influence of lake surface area and depth upon thermal stratification and the depth of the summer thermocline. *Journal of Great Lakes Research*, *15*(2), 233-245.

Government of the Northwest Territories, H. and S. S. (2019, July 5). *Arsenic in Lake water around Yellowknife*. Arsenic in Lake Water Around Yellowknife. Retrieved

December 3, 2022, from https://www.hss.gov.nt.ca/en/newsroom/arsenic-lake-water-around-yellowknife

Hall, G. E., Pelchat, J. C., & Gauthier, G. (1999). Stability of inorganic arsenic (III) and arsenic (V) in water samples. *Journal of Analytical Atomic Spectrometry*, *14*(2), 205-213.

Hao, L., Liu, M., Wang, N., & Li, G. (2018). A critical review on arsenic removal from water using iron-based adsorbents. *RSC advances*, *8*(69), 39545-39560.

Hach. (2018). *Iron, ferrous 1,10-Phenanthroline Method Method 8146*. Retrieved December 19, 2021, from https://images.hach.com/asset-get.download-en.jsa?id=7639983720

Hach. (2019). *Sulfide USEPA1 Methylene Blue Method Method 8131*. Retrieved December 19, 2021, from https://images.hach.com/asset-get.download.jsa?id=7639983902

Health Canada (2006). Guidelines for Canadian Drinking Water Quality: Guideline Technical Document — Arsenic. Water Quality and Health Bureau, Healthy Environments and Consumer Safety Branch, Health Canada, Ottawa, Ontario.

Health Canada (2022). Guidelines for Canadian Drinking Water Quality—Summary Tables. Water and Air Quality Bureau, Healthy Environments and Consumer Safety Branch, Health Canada, Ottawa, Ontario.

Heiri, O., Lotter, A. F., & Lemcke, G. (2001). Loss on ignition as a method for estimating organic and carbonate content in sediments: reproducibility and comparability of results. *Journal of paleolimnology*, *25*(1), 101-110.

Hocking, D., Kuchar, P., Plambeck, J. A., & Smith, R. A. (1978). The impact of gold smelter emissions on vegetation and soils of a sub-arctic forest-tundra transition ecosystem. *Journal of the Air Pollution Control Association*, *28*(2), 133-137.

Hollibaugh, J. T., Carini, S., Gürleyük, H., Jellison, R., Joye, S. B., LeCleir, G., ... & Wallschläger, D. (2005). Arsenic speciation in Mono Lake, California: Response to seasonal stratification and anoxia. *Geochimica et Cosmochimica Acta*, *69*(8), 1925-1937.

Houben AJ, D'Onofrio R, Kokelj SV, Blais JM (2016) Factors Affecting Elevated Arsenic and Methyl Mercury Concentrations in Small Shield Lakes Surrounding Gold Mines

near the Yellowknife, NT, (Canada) Region. PLoS ONE 11(4): e0150960. doi:10.1371/journal.pone.0150960

Hutchinson, G. E. (1967). *A treatise on limnology, introduction to lake biology and the limnoplankton* (Vol. 2). Wiley.

Hutchinson, T., Aufreiter, S., & Hancock, R. (1982). Arsenic pollution in the Yellowknife area from gold smelter activities. *Journal of Radioanalytical and Nuclear Chemistry*, *71*(1-2), 59-73.

Joung, D., Leduc, M., Ramcharitar, B., Xu, Y., Isles, P. D., Stockwell, J. D., ... & Schroth, A. W. (2017). Winter weather and lake-watershed physical configuration drive phosphorus, iron, and manganese dynamics in water and sediment of ice-covered lakes. *Limnology and Oceanography*, *62*(4), 1620-1635.

Kerr, D. E., & Wilson, P. (2000). *Preliminary surficial geology studies and mineral exploration considerations in the Yellowknife area, Northwest Territories* (pp. 1-8). Natural Resources Canada, Geological Survey of Canada.

Keeling, A., & Sandlos, J. (2012). Giant Mine: Historical Summary.

Kneebone, P. E., O'day, P. A., Jones, N., & Hering, J. G. (2002). Deposition and fate of arsenic in iron-and arsenic-enriched reservoir sediments. Environmental science & technology, 36(3), 381-386.

Kokelj. S (2003). Hydrologic Overview of the North and South Slave Regions. Water Resources Division Indian and Northern Affairs Canada.

Kumpiene, J., Carabante, I., Kasiuliene, A., Austruy, A., & Mench, M. (2021). LONG-TERM stability of arsenic in iron amended contaminated soil. *Environmental Pollution*, *269*, 116017.

Lenoble, V., Laclautre, C., Deluchat, V., Serpaud, B., & Bollinger, J. C. (2005). Arsenic removal by adsorption on iron (III) phosphate. *Journal of hazardous materials*, *123*(1-3), 262-268.

Leppäranta, M. (2014). *Freezing of lakes and the evolution of their ice cover*. Springer Science & Business Media.

MacDonald, D. D., Smorong, D. E., Levy, D. A., Swain, L., Caux, P. Y., & Kemper, J. B. (2002). Guidance on the site-specific application of water quality guidelines in Canada: Procedures for deriving numerical water quality objectives. Report prepared for the Canadian Council of Ministers of the Environment and Environment Canada.

Martin, A. J., & Pedersen, T. F. (2002). Seasonal and interannual mobility of arsenic in a lake impacted by metal mining. *Environmental science & technology*, *36*(7), 1516-1523.

Mass, M. J., Tennant, A., Roop, B. C., Cullen, W. R., Styblo, M., Thomas, D. J., & Kligerman, A. D. (2001). Methylated trivalent arsenic species are genotoxic. *Chemical research in toxicology*, *14*(4), 355-361.

Mathias, J. A., & Barica, J. (1980). Factors controlling oxygen depletion in ice-covered lakes. *Canadian Journal of Fisheries and Aquatic Sciences*, *37*(2), 185-194.

Nelligan, C., Jeziorski, A., Rühland, K. M., Paterson, A. M., & Smol, J. P. (2019). Long-term trends in hypolimnetic volumes and dissolved oxygen concentrations in Boreal Shield lakes of south-central Ontario, Canada. *Canadian Journal of Fisheries and Aquatic Sciences*, *76*(12), 2315-2325.

Ng, J. C. (2005). Environmental contamination of arsenic and its toxicological impact on humans. *Environmental Chemistry*, *2*(3), 146-160.

Nikolaidis, N. P., Dobbs, G. M., Chen, J., & Lackovic, J. A. (2004). Arsenic mobility in contaminated lake sediments. *Environmental pollution*, *129*(3), 479-487.

O'Day P. A., Vlassopoulos D., Root R., and Rivera N. (2004) The influence of sulfur and iron on dissolved arsenic concentrations in the shallow subsurface under changing redox conditions. Proc. Natl. Acad. Sci. USA 101, 13703–13708.

Oremland, R. S., & Stolz, J. F. (2003). The ecology of arsenic. *Science*, *300*(5621), 939-944.

Palmer, M.J., Galloway, J.M., Jamieson, H.E., Patterson, R.T., Falck, H. and S.V. Kokelj. (2015). The concentration of arsenic in the lake waters of the Yellowknife area; Northwest Territories Geological Survey, NWT Open File 2015-06 25p.

Palmer, M. J., Chételat, J., Richardson, M., Jamieson, H. E., & Galloway, J. M. (2019). Seasonal variation of arsenic and antimony in surface waters of small subarctic lakes

impacted by legacy mining pollution near Yellowknife, NT, Canada. Science of the Total Environment, 684, 326-339.

Palmer, M. J., Chételat, J., Jamieson, H. E., Richardson, M., & Amyot, M. (2020). Hydrologic control on winter dissolved oxygen mediates arsenic cycling in a small subarctic lake. Limnology and Oceanography.

Petersen, W., Wallman, K., Pinglin, L., Schroeder, F., & Knauth, H. D. (1995). Exchange of trace elements at the sediment-water interface during early diagenesis processes. *Marine and Freshwater Research*, *46*(1), 19-26.

Pieters, R., & Lawrence, G. A. (2009). Effect of salt exclusion from lake ice on seasonal circulation. *Limnology and Oceanography*, *54*(2), 401-412.

Plumlee, G. S., & Morman, S. A. (2011). Mine wastes and human health. Elements, 7(6), 399-404.

Rahman, M. A., Hasegawa, H., & Lim, R. P. (2012). Bioaccumulation, biotransformation, and trophic transfer of arsenic in the aquatic food chain. Environmental research, 116, 118-135

Root, R. A., Dixit, S., Campbell, K. M., Jew, A. D., Hering, J. G., & O'Day, P. A. (2007). Arsenic sequestration by sorption processes in high-iron sediments. Geochimica et Cosmochimica Acta, 71(23), 5782-5803.

Santschi, P., Höhener, P., Benoit, G., & Buchholtz-ten Brink, M. (1990). Chemical processes at the sediment-water interface. *Marine chemistry*, *30*, 269-315.

Schroth, A. W., Giles, C. D., Isles, P. D., Xu, Y., Perzan, Z., & Druschel, G. K. (2015). Dynamic coupling of iron, manganese, and phosphorus behavior in water and sediment of shallow ice-covered eutrophic lakes. *Environmental science & technology*, *49*(16), 9758-9767.

Schuh, C. E., Jamieson, H. E., Palmer, M. J., Martin, A. J., & Blais, J. M. (2019). Controls governing the spatial distribution of sediment arsenic concentrations and solid-phase speciation in a lake impacted by legacy mining pollution. *Science of the Total Environment*, *654*, 563-575.

Senn, D. B., Gawel, J. E., Jay, J. A., Hemond, H. F., & Durant, J. L. (2007). Long-term fate of a pulse arsenic input to a eutrophic lake. *Environmental science & technology*, *41*(9), 3062-3068.

Sentinel Hub. (2022). Sentinel-Hub Playground. Dashboard. Retrieved from https://apps.sentinel-hub.com/sentinel-playground/?source=S2L2A&lat=40.4&lng=-3.730000000000018&zoom=12&preset=1_TRUE_COLOR&layers=B01%2CB02%2CB03&maxcc=20&gain=1.0&gamma=1.0&time=2022-10-01%7C2023-04-20&atmFilter=&showDates=false

Smedley, P. L., & Kinniburgh, D. G. (2002). A review of the source, behaviour, and distribution of arsenic in natural waters. *Applied geochemistry*, *17*(5), 517-568.

Spence, C., & Woo, M. K. (2006). Hydrology of subarctic Canadian Shield: heterogeneous headwater basins. *Journal of Hydrology*, *317*(1-2), 138-154.

Spliethoff, H. M., Mason, R. P., & Hemond, H. F. (1995). Interannual variability in the speciation and mobility of arsenic in a dimictic lake. *Environmental science & technology*, *29*(8), 2157-2161.

Sprague, D. D., & Vermaire, J. C. (2018). Legacy arsenic pollution of lakes near Cobalt, Ontario, Canada: arsenic in lake water and sediment remains elevated nearly a century after mining activity has ceased. *Water, air, & soil pollution*, *229*(3), 1-16.

Tamaki, S., & Frankenberger, W. T. (1992). Environmental biochemistry of arsenic. *Reviews of environmental contamination and toxicology*, 79-110.

Tufano, K. J., & Fendorf, S. (2008). Confounding impacts of iron reduction on arsenic retention. *Environmental Science & Technology*, *42*(13), 4777-4783.

Van Den Berghe, M. D., Jamieson, H. E., & Palmer, M. J. (2018). Arsenic mobility and characterization in lakes impacted by gold ore roasting, Yellowknife, NWT, Canada. *Environmental Pollution*, *234*, 630-641

Vitre, R. D., Belzile, N., & Tessier, A. (1991). Speciation and adsorption of arsenic on diagenetic iron oxyhydroxides. *Limnology and Oceanography*, *36*(7), 1480-1485.

Wagemann, R., Snow, N. B., Rosenberg, D. M., & Lutz, A. (1978). Arsenic in sediments, water, and aquatic biota from lakes in the vicinity of Yellowknife, Northwest

Territories, Canada. *Archives of environmental contamination and toxicology*, *7*(1), 169-191.

Wayland, M. (2003). Mackenzie River Basin: State of the Aquatic Ecosystem Report. [Fort Smith, NWT]: Mackenzie River Basin Board.

WHO, WHO Guidelines for Drinking-Water Quality. In 4th ed.;World Health Organisation: Geneva, Switzerland, 2011.

Wilkin R. T. and Ford R. G. (2006) Arsenic solid-phase partitioning in reducing sediments of a contaminated wetland. Chem. Geol. 228, 156–174.

Wolfe, S. A., Morse, P. D., Kokelj, S. V., & Gaanderse, A. J. (2017). Great slave lowland: the legacy of glacial Lake McConnell. In *Landscapes and Landforms of Western Canada* (pp. 87-96). Springer, Cham.

Wrye, L. A. (2008, September). Distinguishing between natural and anthropogenic sources of arsenic in soils from the Giant mine, Northwest Territories and the North Brookfield mine, Nova Scotia. In *Masters Abstracts International* (Vol. 47, No. 03).

YSI, X. (2022). *EXO2 multiparameter sonde*. YSI EXO2 Multiparameter Water Quality Sonde. Retrieved December 4, 2022, from https://www.ysi.com/exo2